

RECLAMATION

Managing Water in the West

Hydraulic Laboratory Report HL-2008-04

Erosion Indices of Soils Used in ARS Piping Breach Tests



U.S. Department of the Interior
Bureau of Reclamation
Technical Service Center
Hydraulics Laboratory & Materials Engineering Research Laboratory
Denver, Colorado

September 2008

REPORT DOCUMENTATION PAGE			Form Approved OMB No. 0704-0188		
<p>The public reporting burden for this collection of information is estimated to average 1 hour per response, including the time for reviewing instructions, searching existing data sources, gathering and maintaining the data needed, and completing and reviewing the collection of information. Send comments regarding this burden estimate or any other aspect of this collection of information, including suggestions for reducing the burden, to Department of Defense, Washington Headquarters Services, Directorate for Information Operations and Reports (0704-0188), 1215 Jefferson Davis Highway, Suite 1204, Arlington, VA 22202-4302. Respondents should be aware that notwithstanding any other provision of law, no person shall be subject to any penalty for failing to comply with a collection of information if it does not display a currently valid OMB control number.</p> <p>PLEASE DO NOT RETURN YOUR FORM TO THE ABOVE ADDRESS.</p>					
1. REPORT DATE (DD-MM-YYYY) 01-05-2008		2. REPORT TYPE Hydraulic Laboratory (HL)		3. DATES COVERED (From - To) Nov 2007 – April 2008	
4. TITLE AND SUBTITLE Erosion Indices of Soils Used in ARS Piping Breach Tests			5a. CONTRACT NUMBER		
			5b. GRANT NUMBER		
			5c. PROGRAM ELEMENT NUMBER		
6. AUTHOR(S) Tony L. Wahl, Zeynep Erdogan			5d. PROJECT NUMBER		
			5e. TASK NUMBER		
			5f. WORK UNIT NUMBER		
7. PERFORMING ORGANIZATION NAME(S) AND ADDRESS(ES) U.S. Dept. of the Interior, Bureau of Reclamation Technical Service Center, 86-68460 Denver, CO 80225			8. PERFORMING ORGANIZATION REPORT NUMBER HL-2008-04		
9. SPONSORING/MONITORING AGENCY NAME(S) AND ADDRESS(ES) U.S. Department of the Interior, Bureau of Reclamation Dam Safety Office, 84-44000 P.O. Box 25007 Denver, CO 80225			10. SPONSOR/MONITOR'S ACRONYM(S)		
			11. SPONSOR/MONITOR'S REPORT NUMBER(S)		
12. DISTRIBUTION/AVAILABILITY STATEMENT National Technical Information Service, 5285 Port Royal Road, Springfield, VA 22161 http://www.ntis.gov					
13. SUPPLEMENTARY NOTES					
14. ABSTRACT Three soils used in a series of embankment dam piping erosion and breach tests at the Agricultural Research Service hydraulics laboratory in Stillwater, Oklahoma were analyzed by the Bureau of Reclamation to determine their erodibility. Erosion indices were determined using the hole erosion test (HET) method and the submerged jet erosion test (JET) method. Tests were performed in the laboratory on three series of remolded specimens, the first compacted at optimum moisture content to approximately 95% of Standard Proctor maximum density (representative conditions), the second compacted to match the real soil conditions from the ARS breach tests, and the third covering a range of compaction moisture contents. Erodibility of the soils varied from specimens so weak that they could not be tested by the HET method (likely HET group 1 or 2) up to specimens in the upper end of HET group 4 (moderately slow erosion rate). For the samples compacted to match field conditions, the two test methods ranked the erodibility of the soils similarly, but erodibility rankings were reversed for the samples compacted to the representative conditions. Jet tests on the samples compacted to match field conditions were relatively consistent with field jet tests conducted in Oklahoma immediately after each breach test. Differences between detachment rate coefficients and critical shear stresses determined by the two methods were significant and consistent with ongoing research being performed to compare these test methods across a broad range of soil types.					
15. SUBJECT TERMS Erodibility, critical shear stress, erosion rate, dam failure, piping erosion.					
16. SECURITY CLASSIFICATION OF:			17. LIMITATION OF ABSTRACT	18. NUMBER OF PAGES	19a. NAME OF RESPONSIBLE PERSON
a. REPORT	b. ABSTRACT	a. THIS PAGE			Clifford A. Pugh
UU	UU	UU	SAR	142	19b. TELEPHONE NUMBER (Include area code) 303-445-2151

Hydraulic Laboratory Report HL-2008-04

Erosion Indices of Soils Used in ARS Piping Breach Tests

**Tony L. Wahl
Zeynep Erdogan**



**U.S. Department of the Interior
Bureau of Reclamation
Technical Service Center
Hydraulics Laboratory & Materials Engineering Research Laboratory
Denver, Colorado**

September 2008

Mission Statements

The mission of the Department of the Interior is to protect and provide access to our Nation's natural and cultural heritage and honor our trust responsibilities to Indian Tribes and our commitments to island communities.

The mission of the Bureau of Reclamation is to manage, develop, and protect water and related resources in an environmentally and economically sound manner in the interest of the American public.

Acknowledgments

Zeynep Erdogan performed soil properties tests and provided helpful comments as the peer reviewer of this report. Steve Reo, Casey Dowling, and Zeynep Erdogan processed the soil materials, prepared the test specimens, and performed many of the erodibility tests. Greg Hanson of the Agricultural Research Service provided soils, field test data, and helpful advice and critique of the test plan and results.

Disclaimer

The information provided in this report is believed to be appropriate and accurate for the specific purposes described herein, but users bear all responsibility for exercising sound engineering judgment in its application, especially to situations different from those studied. References to commercial products do not imply endorsement by the Bureau of Reclamation and may not be used for advertising or promotional purposes.

CONTENTS

EXECUTIVE SUMMARY	1
BACKGROUND	1
OBJECTIVES AND TEST PROGRAM	3
EROSION MODEL AND ERODIBILITY CLASSIFICATIONS	4
TEST FACILITIES AND EQUIPMENT	7
Hole Erosion Test	7
Submerged Jet Erosion Test	8
SOILS	9
SPECIMEN PREPARATION	10
RESULTS AND ANALYSIS.....	11
Samples at Representative Conditions.....	11
Samples Compacted to Match Breach-Test Conditions	14
HET vs. JET – Effect of Compaction Moisture Content.....	17
CONCLUSIONS.....	21
REFERENCES	23
APPENDIX A: CURRENT HOLE EROSION TEST PROCEDURES USED BY THE BUREAU OF RECLAMATION	24
APPENDIX B: SELECTED EROSION TEST PHOTOGRAPHS.....	31
APPENDIX C: HET AND JET TEST RECORDS	36

TABLES

Table 1. — Embankment piping erosion and breach tests performed by ARS.....	3
Table 2. — Qualitative description of rates of progression of internal erosion or piping for soils with specific erosion rate indices.....	5
Table 3. — Qualitative description of soil erodibility based on the volumetric detachment rate coefficient.	6
Table 4. — Properties of soils used in ARS embankment tests and soil samples tested at the Bureau of Reclamation.	9
Table 5. — Piping breach test soil conditions and <i>in situ</i> measurements of soil erodibility.....	10
Table 6. — HET and JET erodibility parameters for samples compacted to representative conditions.	12
Table 7. — HET and JET erodibility parameters for samples compacted to conditions approximating the ARS piping breach tests.....	14

Table 8. — Erodibility test results for P2 and P3 soils over a range of compaction moisture contents. 17

FIGURES

Figure 1. — ARS piping test P1, 9 minutes after initiation of piping failure. 2

Figure 2. — Proposed erodibility classifications for streambank soils (Hanson and Simon 2001). 6

Figure 3. — HET apparatus consisting of constant-head tank, test section, and downstream V-notch weir. 8

Figure 4. — Laboratory JET apparatus. 9

Figure 5. — Erodibility parameters of soils P2 and P3 at representative compaction conditions (optimum moisture content and 95% of maximum dry density). 13

Figure 6. — Compacted dry density and detachment rate coefficients of P2 and P3 soil specimens tested to determine erodibility at representative conditions (optimum moisture content and 95% of maximum dry density). 13

Figure 7. — Erodibility parameters measured in ARS piping breach tests compared to erodibility parameters obtained from laboratory HET and JET specimens compacted to similar conditions. 15

Figure 8. — Compacted dry density and detachment rate coefficients for specimens of P1, P2, and P3 compacted to conditions similar to the ARS piping breach tests. 16

Figure 9. — Results of erodibility tests on soil P2 at compaction moisture contents ranging from about 4% dry of optimum to 4% wet of optimum. 18

Figure 10. — Results of erodibility tests on soil P3 at compaction moisture contents ranging from about 3% dry of optimum to 5.5% wet of optimum. 19

Figure 11. — Variation of erodibility for soils P2 and P3 as a function of compaction moisture content. 20

Executive Summary

Three soils used in a series of embankment dam piping erosion and breach tests at the Agricultural Research Service's outdoor hydraulics laboratory in Stillwater, Oklahoma were analyzed by the Bureau of Reclamation to determine their erodibility. Erosion indices were determined using the hole erosion test (HET) method, which is an input to Reclamation's internal erosion and piping risk toolbox currently under development, and using the submerged jet erosion test (JET) method, for comparison with jet tests previously performed by ARS in the field immediately after each embankment breach test. Tests were performed in the laboratory on three series of remolded specimens, the first compacted at optimum moisture content to approximately 95% of Standard Proctor maximum density (*representative conditions*), the second compacted to match the real soil conditions from the ARS breach tests, and the third covering a range of compaction moisture contents. Erodibility of the soils varied from specimens so weak that they could not be tested by the HET method (likely HET group 1 or 2; extremely rapid to very rapid erosion rate) up to specimens in the upper end of HET group 4 (moderately slow erosion rate). For the samples compacted to match field conditions, the two test methods ranked the erodibility of the soils similarly, but erodibility rankings were reversed for the samples compacted to the representative conditions. Submerged jet tests on the samples compacted to match field conditions were relatively consistent with the field jet tests conducted in Oklahoma. Overall, differences between detachment rate coefficients and critical shear stresses determined by the two methods were significant and consistent with ongoing research being performed to compare these test methods over a broad range of soil types.

Background

Among numerous methods available for quantifying erodibility of cohesive soils, the hole erosion test (HET) (Wan and Fell 2004) and submerged jet erosion test (JET) (Hanson and Cook 2004) have emerged as popular techniques when studying embankment dam breach processes. The HET simulates a small scale progressive internal erosion or piping failure by causing erosive enlargement of a 6-mm diameter predrilled hole through a 116-mm long soil specimen under a constant-head condition. The JET uses a 6-mm diameter nozzle aimed at an exposed soil surface to produce scour erosion similar to that occurring during headcut erosion. The two tests both determine numerical values for a critical shear stress needed to initiate erosion and a detachment rate coefficient expressing the increase in erosion rate per unit of excess applied stress. Ongoing research at the Bureau of Reclamation is showing that although the tests attempt to determine the same parameters of the same basic erosion equation, the results are often markedly different. A number of factors are thought to be responsible for this difference, including simplifications of the stress descriptions used to analyze

both tests, different erosion mechanisms in the two tests, effects of the different geometry of the exposed surfaces in each test, and differences in the sensitivity of each test to variations of soil fabric or structure. The Bureau of Reclamation (Reclamation) has adopted the HET as one means of classifying soils in embankment dams for evaluating risks of internal erosion and piping failures. The procedures used to evaluate these risks have been collectively described as the “piping risk toolbox”.

In 2006 and 2007, the Hydraulic Engineering Research Unit of the USDA-Agricultural Research Service (ARS) performed 3 large-scale physical model tests of the piping-initiated breach of homogeneous cohesive embankment dams at their outdoor laboratory near Stillwater, Oklahoma. Preliminary data from the first of these tests was reported by Hunt et al. (2007); a second and third test took place in late 2007 (personal communication, Greg Hanson and Sherry Hunt), with results not yet published, and a fourth test is planned for 2008. The embankments were all of homogeneous construction, 4 ft high with a 6 ft wide crest and 3:1 (h:v) upstream and downstream slopes. Piping erosion was produced by embedding a 1.5-inch diameter pipe in each embankment and pulling it out through the downstream side of the embankment with a tractor to begin each test. The reservoir upstream from the embankments was supplied with a continuous flow of water during the tests and its water surface elevation was held nearly constant during the test by allowing excess flow to exit over a long-crested weir spillway. Figure 1 shows the first of these tests underway. Note in this figure that piping was initiated at the elevation of the lowest set of markers visible on the downstream slope; headcutting down to the base of the embankment is occurring simultaneously with enlargement of the piping hole. Table 1 summarizes the results of the embankment piping breach tests run through 2007.



Figure 1. — ARS piping test P1, 9 minutes after initiation of piping failure.

Table 1. — Embankment piping erosion and breach tests performed by ARS.

Test and Soil Designation	Soil Type	Time to Collapse of Soil Bridge over Enlarged Pipe
P1	Silty Sand, SM (non-plastic)	0.23 hr
P2	Silty Clay, CL-ML LL=21, PI=7	17.2 hr
P3	Lean Clay, CL LL=28, PI=13	20.5 hr

To characterize erodibility of the soils, submerged jet erosion tests (Hanson and Cook 2004) were performed in the field immediately after completion of each embankment breach test. Laboratory jet tests were also performed by ARS on the three soils used in the tests over a range of moisture contents and compaction efforts. At the time of these tests, there was not a firmly established correlation between results of submerged jet tests and hole erosion tests. Recent research at the Bureau of Reclamation (Wahl et al. 2008) has been exploring the relation between them.

Objectives and Test Program

The ARS embankment breach tests present an opportunity to improve our understanding of piping-induced embankment failure and specifically could serve as case studies to support the piping risk toolbox under development at Reclamation. To facilitate the use of the breach tests for these purposes, Reclamation performed a series of laboratory HETs on samples of the ARS soils. Each of the three soils was tested at two specific conditions:

1. Optimum moisture content and 95% of maximum dry density, as established by a Standard Proctor compaction test, and
2. Moisture content and dry density approximating the compacted test embankments.

The first series of tests allowed the determination of the Representative HET Erosion Rate Index, \tilde{I}_{HET} , for each soil, as defined by Wan and Fell (2004). This allows the normalized ranking of the soils relative to other embankment soils tested by Wan and Fell (2004) using the HET. The second series of tests established I_{HET} values for the soils at conditions approximating those of the tested embankments. These tests will facilitate the inclusion of the ARS piping breach tests into the database of case studies used to develop Reclamation's piping risk toolbox.

For each series of tests, companion jet tests were performed on parallel specimens prepared with similar moisture content and compaction effort. These tests allowed a verification check against the laboratory and field jet tests performed by ARS. The data from these paired HET and JET specimens are also being included in Reclamation's ongoing research effort to study the relation between erosion indices determined by the HET and JET methods across a variety of soil types and compaction conditions.

Following the completion of these two series of tests, a third set of tests was performed in which the P2 and P3 soils were tested using the HET and JET over a range of compaction moisture contents at Standard Proctor compaction effort.

Erosion Model and Erodibility Classifications

Both erosion tests used in this study are designed to determine the parameters of a simple soil detachment equation of the form:

$$\dot{m} = C_e(\tau - \tau_c) \quad \text{or} \quad \dot{\epsilon} = k_d(\tau - \tau_c)$$

where τ and τ_c are the applied shear stress and critical shear stress, respectively, \dot{m} is the rate of erosion expressed as a mass per unit area per unit of applied stress, $\dot{\epsilon}$ is the rate of erosion expressed on a volumetric basis, and C_e and k_d are rate coefficients. The equation applies only for $\tau > \tau_c$; otherwise, the erosion rate is zero. The mass-based equation has typically been used to analyze data collected in the hole erosion test, while the volumetric equation has been used for the jet test. The two equations can be made equivalent by recognizing that $C_e = k_d \rho_d$, where ρ_d = dry density of the soil. The volumetric form of the equation is preferred for the jet test because the test is often performed in the field in situations where the in-place density of the tested material is not known. The hole erosion test is only performed in a laboratory setting, using either remolded or undisturbed soil samples, so density information is usually readily available, making a mass-based calculation feasible. A volumetric erosion model is also preferred for field use, since most applications are concerned with the volumetric rate of material removal, either to predict depths or lateral extent of erosion, or rates of enlargement of internal erosion channels.

Values of C_e obtained from the HET are usually reported in S.I. units of $\text{kg/s/m}^2/\text{Pa}$, which simplifies to seconds per meter (s/m). C_e varies over several orders of magnitude in soils of engineering interest. For convenience, Wan and Fell (2004) proposed classifying soils according to an Erosion Rate Index, I_{HET} , defined as

$$I_{HET} = -\log_{10} C_e$$

with C_e in units of s/m. Values of this index can range from less than 1 to above 6, with larger values indicating decreasing erosion rate. The fractional part of the index value is often dropped and the test result reported as a simple integer group number. Soils with group numbers less than 2 are usually so erodible that they cannot be effectively tested in the HET device. Table 2 shows proposed descriptive terms associated with each value of the I_{HET} index.

Table 2. — Qualitative description of rates of progression of internal erosion or piping for soils with specific erosion rate indices.

HET Group Number	Erosion Rate Index, I_{HET}	Description
1	< 2	Extremely rapid
2	2 – 3	Very rapid
3	3 – 4	Moderately rapid
4	4 – 5	Moderately slow
5	5 – 6	Very slow
6	> 6	Extremely slow

Because erodibility varies significantly as a function of the compaction moisture content and dry density, Wan and Fell (2004) further proposed that the value of I_{HET} for soils compacted to 95% of maximum dry density (Standard Proctor) at optimum moisture content should be called the Representative Erosion Rate Index, designated \tilde{I}_{HET} . Wan and Fell (2004) performed numerous HETs at varied compaction and moisture conditions and used multi-variable regression techniques to estimate values of \tilde{I}_{HET} for 13 different soils. Soils that could not be eroded in their HET apparatus (maximum head of 1200 mm) were presumed to be in group 6.

S.I. units of the k_d coefficient determined from the submerged jet erosion test are $\text{m}^3/\text{s}/\text{m}^2/\text{Pa}$ which reduces to $\text{m}^3/(\text{N}\cdot\text{s})$. Another S.I. unit combination commonly used for this parameter is $\text{cm}^3/(\text{N}\cdot\text{s})$. When working in U.S. customary units, k_d is usually expressed in $\text{ft}/\text{hr}/\text{psf}$ [$1 \text{ cm}^3/(\text{N}\cdot\text{s}) = 0.5655 \text{ ft}/\text{hr}/\text{psf} = 10^{-6} \text{ m}^3/(\text{N}\cdot\text{s})$]. Hanson and Simon (2001) have proposed a qualitative classification of the erodibility of soils, similar to that suggested by Wan and Fell (2004) for the HET. Their classification scheme identifies five erodibility groupings, illustrated in Figure 2. It uses both the k_d and τ_c value of the soil, in contrast to Wan and Fell's approach of using just the rate coefficient. Hanson and Simon (2001) used the JET to study erodibility of cohesive streambeds in loess formations in the midwestern USA and proposed a best-fit relation between the critical shear stress and the detachment rate coefficient:

$$k_d = 0.2\tau_c^{-0.5}$$

with values of τ_c specified in Pa and values of k_d specified in $\text{cm}^3/(\text{N}\cdot\text{s})$.

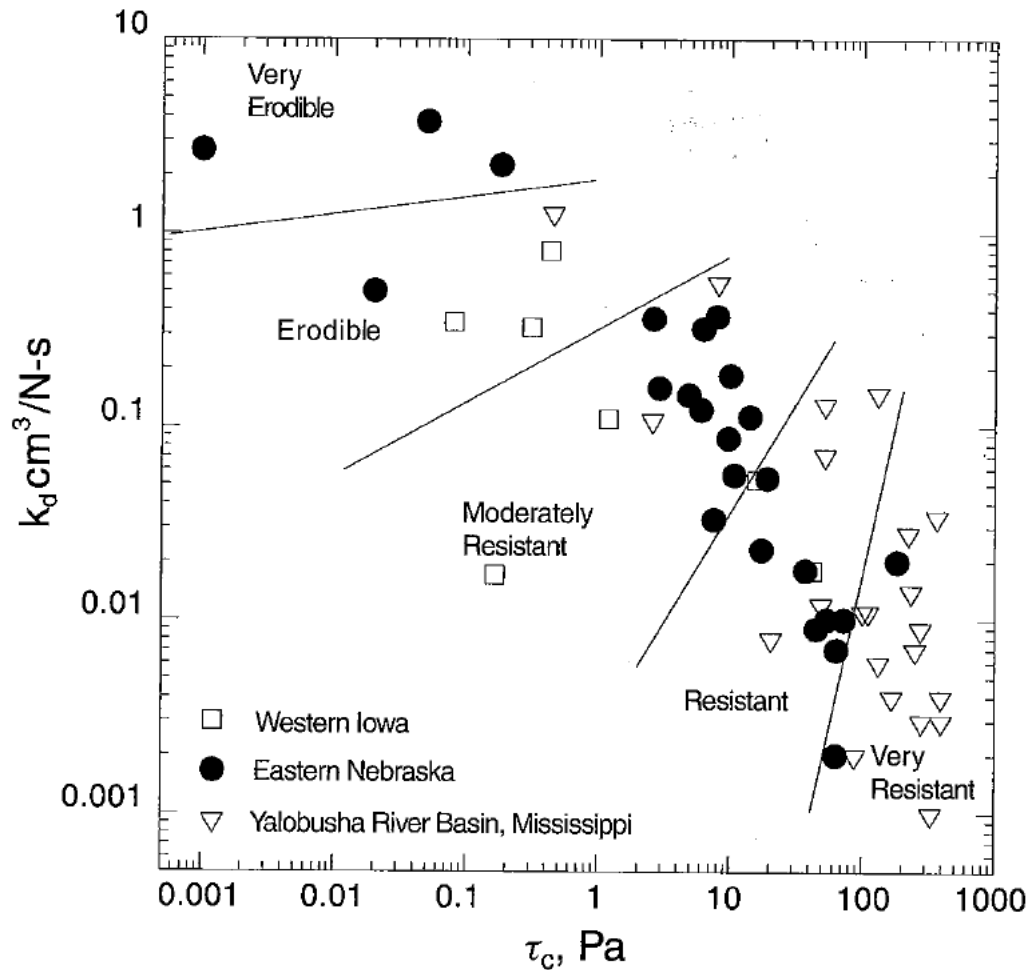


Figure 2. — Proposed erodibility classifications for streambank soils (Hanson and Simon 2001).

Hanson (personal communication) has also suggested a 6-tier classification system shown in Table 3 which is based only on the k_d value expressed in units of ft/hr/psf. The conversion to $\text{cm}^3/(\text{N}\cdot\text{s})$ is of the order of 2, and since the classifications are based on order of magnitude ranges of k_d , one could argue that a classification system using similar numerical divisions would also be appropriate for k_d values expressed in $\text{cm}^3/(\text{N}\cdot\text{s})$.

Table 3. — Qualitative description of soil erodibility based on the volumetric detachment rate coefficient.

k_d , ft/hr/psf	Description
> 10	Extremely erodible
1 – 10	Very erodible
0.1 – 1	Moderately erodible
0.01 – 0.1	Moderately resistant
0.001 – 0.01	Very resistant
< 0.001	Extremely resistant

Test Facilities and Equipment

Hole Erosion Test

The Hole Erosion Test was originally developed in Australia (Wan and Fell 2002 and 2004). The test is performed in the laboratory using an undisturbed tube sample or a soil specimen compacted into a Standard Proctor mold. A 6.35-mm (1/4-inch) diameter hole is pre-drilled through the centerline axis, and the specimen is then installed into a test apparatus in which water flows through the hole under a constant hydraulic head that is increased incrementally until progressive erosion is produced. Once erosion is observed, the test is continued at a constant hydraulic head for a period long enough to observe a definite acceleration of the flow rate, which is indicative of a progressive erosion condition. Tests can last from 15 minutes to 2 hours. Measurements of the increasing flow rate during the test and the initial and final diameter of the erosion hole are used to compute applied hydraulic stress and hole diameters at intermediate times, from which the erosion rate can be deduced. Plotting the computed values of stress versus erosion rate produces a chart that allows graphical determination of the critical shear stress and erosion rate coefficient. Spreadsheets are used at the Bureau of Reclamation to facilitate analysis of the data. The final diameter is typically estimated visually immediately after a test, and then confirmed by caliper measurements made on a plaster casting of the final hole.

The Bureau of Reclamation also uses a supplementary data analysis technique based on a model for piping erosion proposed by Bonelli et al. (2006). This technique does not require measurement of the final hole diameter and is sometimes well-suited to tests in which erosion behavior is somewhat erratic due to temporary clogging of the erosion hole. The method uses a curve-fitting approach to match the test data to a theoretical model for the exponential increase of dimensionless discharge as a function of dimensionless test time. Details of all of the HET data analysis procedures are provided in Appendix A.

Figure 3 shows one of two HET devices installed in the Bureau of Reclamation laboratory in Denver, Colorado. Flow rate through the specimen is measured by a 10° V-notch weir on the downstream side of the apparatus. The weir is calibrated in place by volumetric methods (stopwatch and graduated cylinder). Measurement of differential head across the specimen and head on the weir is automated using pressure transducers and a computerized data acquisition system that records data at 5 second intervals throughout a test. The HET apparatus shown in Figure 3 is capable of operating at heads up to 1600 mm. Reclamation has also recently constructed a high-head HET apparatus that is functionally equivalent to the apparatus in Figure 3, but allows testing at heads up to about 5400 mm.

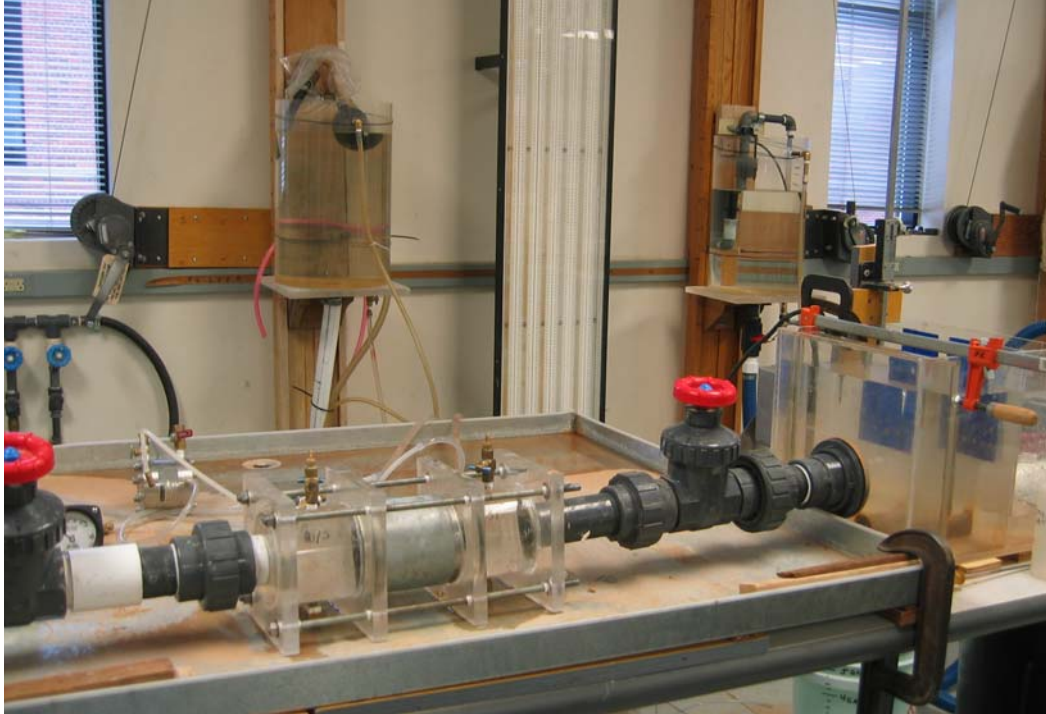


Figure 3. — HET apparatus consisting of constant-head tank, test section, and downstream V-notch weir.

Submerged Jet Erosion Test

The submerged jet erosion test was developed at the Agricultural Research Service Hydraulic Engineering Research Unit, Stillwater, Oklahoma (Hanson and Cook 2004). This test can be performed *in situ*, or in the laboratory using tube samples or remolded samples in compaction molds (Hanson and Hunt 2007). The test is described in ASTM Standard D5852.

The JET apparatus is designed to erode the soil surface with a submerged jet, which is produced by a 6.35-mm ($\frac{1}{4}$ -inch) diameter nozzle initially positioned between 6 and 30 nozzle diameters from the soil surface. The starting nozzle position and test head may be adjusted to vary the stress applied to the soil sample, although once a test head is selected it is usually held constant for the duration of a test. Scour of the soil surface beneath the jet is measured over time using a point gage that passes through the nozzle, temporarily stopping the flow. No post-test handling or processing of the specimen is needed. The data analysis procedure is described in Hanson and Cook (2004) and has been automated with a Microsoft Excel spreadsheet. Figure 4 shows Reclamation's submerged jet test equipment.

Soils

Soils for the ARS piping breach tests were obtained from borrow areas and stockpiles on the ARS laboratory grounds. All of the soils are native to the Stillwater, Oklahoma area. Soils were analyzed after the breach tests at the USDA-NRCS soil mechanics laboratory in Fort Worth, Texas.

Approximately 80-100 pounds of soils P1, P2, and P3 were shipped to Denver, Colorado in November 2007 for use in the first two series of tests. There are a few notable differences between the soils used at the ARS lab and the samples tested at Reclamation (see Table 4). For the P2 soil, the PI of the Reclamation sample was 9, compared to 3 for the ARS breach test sample, which changes the soil classification from a Sandy Silt, ML, to a Lean Clay with Sand, (CL)s. For the P3 soil, the Reclamation sample also has a significantly higher PI.



Figure 4. — Laboratory JET apparatus.

A second shipment of soils P2 and P3 was provided in July 2008 to complete the third set of tests (HETs and JETs at varying compaction moisture content and fixed compaction effort). The properties of these soils were similar to those in the first shipment.

Table 4. — Properties of soils used in ARS embankment tests and soil samples tested at the Bureau of Reclamation.

	Soil	USCS	Grain size distribution			Atterberg limits			Compaction Properties (Standard Proctor)	
			% sand > 0.075 mm	% silt 0.005-0.075 mm	% clay < 0.005 mm	LL	PL	PI	Optimum moisture content (%)	Maximum dry density (g/cm ³)
ARS breach test soils	P1	SM	74	19	8	--	NP	NP	11.0	1.813
	P2	ML	32	47	21	23	20	3	11.5	1.888
	P3	(CL)s	21	44	35	29	14	15	12.9	1.799
Samples at BOR lab Nov 2007	P1	SM	76	19	5	--	NP	NP	12.5	1.802
	P2	s(CL)	31	50	19	25	16	9	12.2	1.894
	P3	(CL)s	20	50	30	36	12	24	14.2	1.817
Samples at BOR lab July 2008	P2	s(CL)	31	50	19	25	16	9	11.8	1.900
	P3	(CL)s	20	50	30	36	12	24	12.3	1.906

Grain size distributions and Atterberg limits were determined through laboratory testing performed at Reclamation. Compaction properties of the soils received in November 2007 were established from data provided by ARS, with some reanalysis at Reclamation; for soil P1 some additional compaction testing was also performed at Reclamation. These optimum moisture content and maximum dry density values were used to determine the compaction conditions for the specimens to be tested at optimum moisture content and 95% of maximum density. Compaction properties for the P2 and P3 soils received in July 2008 were determined over the course of the third series of tests. The optimum moisture content for the July 2008 sample of soil P3 was somewhat lower and the maximum dry density somewhat higher than expected.

Table 5 provides the properties of the compacted test embankments, including the results of *in situ* submerged jet tests performed after each embankment was breached.

Table 5. — Piping breach test soil conditions and *in situ* measurements of soil erodibility.

Test	Conditions of Tested Embankments		Erodibility - JET	
	Moisture content %	Dry density γ_d g/cm ³	k_d cm ³ /(N·s)	τ_c Pa
P1	11.49	1.696	150.	0.0
P2	12.67	1.746	2.0	2.5
P3 (upper lifts)*	15.06	1.776	1.2	4.6
P3 (lowest 3 lifts)	16.45	1.785	0.17	22.

* Note: P3 embankment was observed to fail through upper lifts

Specimen Preparation

Soils were prepared for compaction into Standard Proctor molds in accordance with standard procedure USBR 5210 (Reclamation 1990). Soils were air dried and pulverized to pass a U.S. Standard No. 4 sieve, then oven dried to establish zero moisture content. Computed masses of soil and water were then mixed and stored in plastic bags in the laboratory's 75% humidity room for required amounts of time according to soil type (>4 hours for P1, >24 hours for P2 and P3).

Following this conditioning period, soils were compacted into Standard Proctor molds in three equal lifts using manual compaction by a 5.5 lb hammer dropped from a 1 ft height. The number of blows was constant for each layer, but varied by specimen depending on the desired final dry density. Following compaction, the top layer was trimmed flush with the end of the mold and the compacted mass of the specimen was determined. The compaction moisture content was determined from a specimen of excess soil set aside during compaction.

Compacted specimens were cured overnight or longer before erodibility testing was performed. Tests performed immediately after compaction showed soils to

be more erodible. Hole erosion test specimens were tested with the last compacted layer placed upstream. Jet erosion specimens were tested with the bottom surface of the first compacted layer subjected to erosion (i.e., specimen inverted), since trimming of the top of the specimen is likely to disturb the last layer.

Following the completion of hole erosion tests, specimens were photographed, oven dried and weighed, and plaster casts of the enlarged holes were made. The length of the portion of a casting that was of relatively uniform diameter was determined, and the diameter of each casting was measured with calipers at five locations evenly distributed along the length of the uniform-diameter portion of the casting. By this method, excessively large scour holes at the entrance or exit of the specimens were considered in the data analysis to cause a shortening of the hole length (which increases the hydraulic gradient on the remaining length of the hole) that was assumed to occur linearly through time.

Analysis of the hole erosion test data used the procedures described in Appendix A. Most tests were analyzed by both described methods and the results given here are averages of the two methods. For each test, a *subjectivity index* was assigned, indicating the degree to which erosion occurred during the test in a manner consistent with the underlying analysis assumptions, and the degree to which subjective judgment was needed to analyze the data. Higher values of the subjectivity index indicate greater uncertainty in the test results. A complete description of the criteria used to assign these ratings is given in Appendix A.

Results and Analysis

Samples at Representative Conditions

Table 6 provides results of the tests performed on specimens compacted to approximately representative conditions (optimum moisture content and 95% of maximum dry density). Results are only shown for soils P2 and P3, as we were unable to successfully perform an HET on the P1 soil at this compaction condition, or at the compaction conditions matching the ARS P1 breach test. In two attempted tests, the P1 specimens collapsed immediately when the test apparatus was filled with water. Figure 5 shows the results graphically, in comparison to the best-fit line and jet test erodibility classifications proposed by Hanson and Simon (2001). Note that the HETs yielded critical stresses about 2 to 3 orders of magnitude higher than the corresponding jet tests, and detachment rate coefficients about 1 to 2 orders of magnitude lower. Both P2 and P3 soils have I_{HET} values that place them in group 4, designated as “moderately slow” erosion rate by Wan and Fell (2004). Figure 6 shows the moisture contents, dry densities, and detachment rate coefficients for each of the tests.

Table 6. — HET and JET erodibility parameters for samples compacted to representative conditions.

Soil	Compacted samples				$I_{-log(C_e)}$	τ_c (Pa)	C_e (s/m)	k_d cm ³ /(N-s)	HET Subjectivity Index
	Compaction energy (kJ/m ³)	Moisture content (%)	Dry density, (g/cm ³)	Relative density, (%)					
P2	HET Results								
	213	11.9	1.758	92.8%	4.33	200	4.68E-05	0.0266	½
	213	12.4	1.783	94.1%	4.37	103	4.27E-05	0.0239	½
	JET Results								
	213	12.4	1.766	93.2%	3.09	0.232	8.12E-04	0.46	-
	237	12.8	1.811	95.6%	3.43	0.946	3.75E-04	0.21	-
P3	HET Results								
	213	14.2	1.739	95.7%	4.77	206	1.70E-05	0.0098	½
	213	14.2	1.706	93.9%	4.71	402	1.95E-05	0.0114	2
	JET Results								
	213	14.0	1.694	93.2%	2.53	0.177	2.98E-03	1.76	-
	237	14.0	1.745	96.0%	2.67	0.217	2.14E-03	1.23	-

The two HET samples of soil P2 bracketed the desired optimum moisture content of 12.2%, but were 1 and 3 percent lighter than the desired 95% relative density. The I_{HET} index was about 4.3 to 4.4. HET samples of soil P3 were compacted at the desired moisture content of 14.2% and bracketed the desired relative density. The I_{HET} index for these two samples was 4.7 to 4.8. These results are consistent with the ARS JET data and the breach times observed in the piping breach tests.

The JET samples of P2 and P3 provided surprising results in this series of tests. All previous ARS data showed soil P3 to be more erosion resistant than P2, generally by about one order of magnitude when similarly compacted (Hanson and Hunt 2007), but the jet tests we performed showed P2 to be more erosion resistant, both in terms of critical shear stress and the detachment rate coefficient. This may be due to the differences already noted between the ARS soils and the samples tested at Reclamation. The difference may also be related to the fact that we used a significantly reduced compaction effort (7, 9, or 10 blows per layer, rather than the standard 25 blows per layer) in the attempt to achieve 95% relative density. Hanson and Hunt (2007) showed that the optimum moisture content for these soils increases as compaction effort is reduced, especially for soil P3. Because we were compacting at the optimum moisture corresponding to standard compaction effort (25 blows per layer), we were effectively compacting at a moisture content that is drier than optimum *for the applied compaction effort*. Hanson and Hunt (2007) further showed that the erodibility of these soils is very sensitive to moisture content on the dry side of optimum, increasing dramatically as moisture content is reduced. This is likely due to a relative coarsening of the soil structure at drier moisture contents, where the soil mass does not fully mold together and some aggregates remain independent of other groupings of tightly molded materials. The jet test seems to be more capable of exploiting this soil structure and may thus be more sensitive to changing structure than the HET. This might explain why the relative erodibilities of the two soils are ranked oppositely by the HET and JET at this compaction condition.

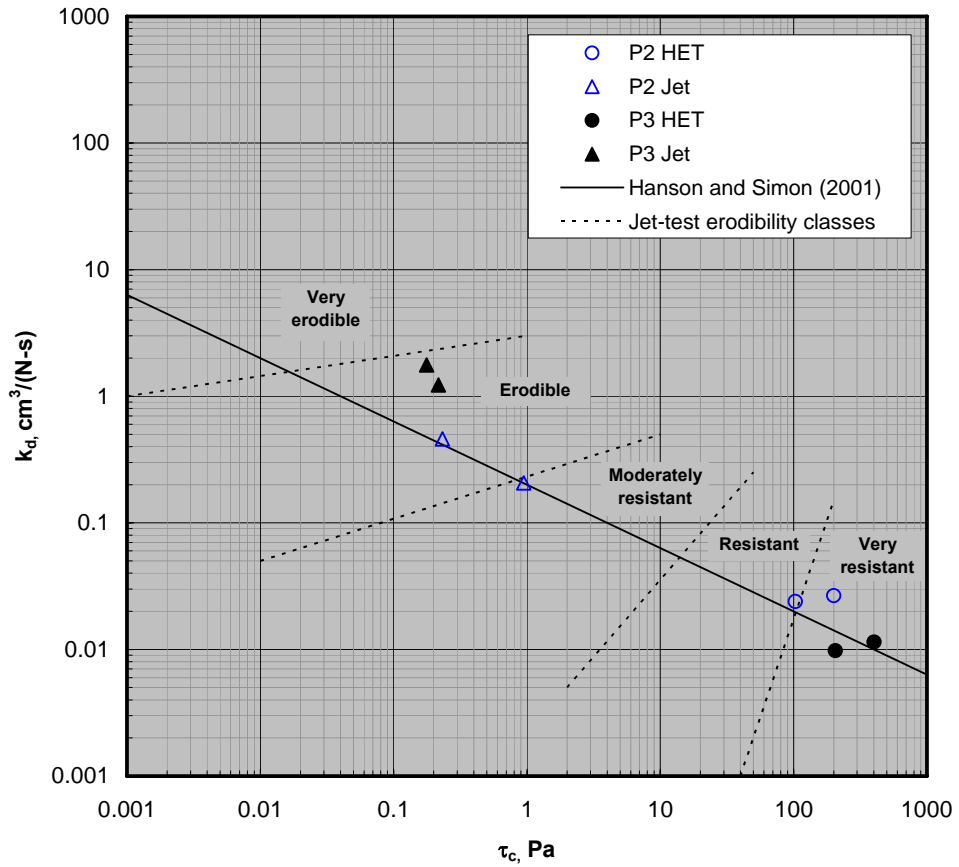


Figure 5. — Erodibility parameters of soils P2 and P3 at representative compaction conditions (optimum moisture content and 95% of maximum dry density).

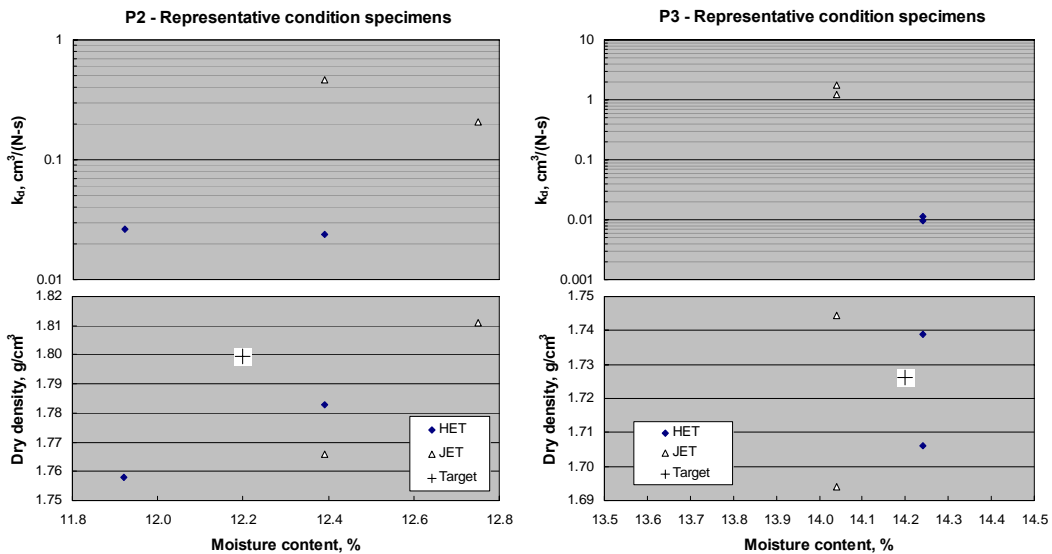


Figure 6. — Compacted dry density and detachment rate coefficients of P2 and P3 soil specimens tested to determine erodibility at representative conditions (optimum moisture content and 95% of maximum dry density).

Samples Compacted to Match Breach-Test Conditions

Table 7 shows the results of the tests performed at compaction conditions similar to the ARS piping breach tests. These tests produced more consistent results. Both the HET and JET results rank the erosion rates of the three soils in the same order as one would expect from the ARS piping breach tests. The fact that soil P1 was too weak to test in the HET suggests that it is probably in HET group 1 or 2. Soil P2 is in the upper part of group 3 to lower group 4, while soil P3 is in the upper half of group 4. The one HET on soil P2 that indicated it to be in HET group 3 was performed on a specimen compacted about 0.5% drier than the corresponding field test.

Jet test results show similar relative erodibility differences between the soils and compare reasonably to the field jet tests performed by ARS after the piping breach tests. Figure 7 shows the results in comparison with the best-fit line and erodibility classifications proposed by Hanson and Simon (2001) for jet test results, and Figure 8 shows the moisture contents, dry densities, and detachment rate coefficients for each HET and JET (JET results only for soil P1). Again, HET results exhibit critical shear stresses about two orders of magnitude greater than corresponding JET results, and detachment rate coefficients about 1 order of magnitude lower. Both the HET and JET results reasonably follow the best-fit line, while the field data tend to deviate somewhat above it. The laboratory and field JET results are in similar erodibility classes, even though the field JET results are above the best-fit line. Critical shear stress values obtained from the HET show little difference between the soils, with both having critical shear stresses that are in the same order of magnitude.

Table 7. — HET and JET erodibility parameters for samples compacted to conditions approximating the ARS piping breach tests.

Soil	Compacted samples				I -log(C _e)	τ _c (Pa)	C _e (s/m)	k _d cm ³ /(N-s)	HET Subjectivity Index
	Compaction energy (kJ/m ³)	Moisture content (%)	Dry density, (g/cm ³)	Relative density (%)					
P1	JET Results								
	166	11.0	1.692	93.3%	0.33	0.000087	4.63E-01	274.	-
	166	11.0	1.692	93.3%	0.28	0.00031	5.23E-01	309.	-
ARS P1 field jet test(s)	192 - 287	11.5	1.696		0.59	0.0	2.54E-01	150.	-
P2	HET Results								
	166	12.4	1.749	92.6%	4.20	231.	6.38E-05	0.037	½
	166	12.0	1.731	91.7%	3.42	357.	3.80E-04	0.220	½
	JET Results								
	166	12.5	1.732	91.7%	3.17	0.911	6.77E-04	0.391	-
ARS P2 field jet test(s)	192 - 287	12.7	1.746		2.46	2.5	3.49E-03	2.	-
P3	HET Results								
	213	15.1	1.768	98.3%	4.90	346.	1.26E-05	0.007	0
	213	16.2	1.744	96.9%	4.46	203.	3.47E-05	0.020	½
	JET Results								
	213	15.3	1.765	98.1%	3.48	1.616	3.28E-04	0.186	-
ARS P3 field jet test(s) - lower 3 lifts	192 - 287	16.5	1.785		3.52	22.	3.03E-04	0.17	-
ARS P3 field jet test(s) - upper lifts	192 - 287	15.1	1.776		2.67	4.6	2.13E-03	1.2	-

A comparison of the HET and JET results for all of these tests shows significant differences. In general, the detachment rate coefficients determined by the HET are about one order of magnitude lower than those determined by the JET method, and the critical shear stress values are two or more orders of magnitude higher. This is consistent with results of an ongoing research effort at Reclamation that is examining the relation between the HET and JET erosion indices for a variety of soils. The fact that all of the HET and JET data roughly follow the best-fit line proposed by Hanson and Simon (2001) suggests that both tests are measuring an intrinsic erodibility property of soils, but with a significant bias between them. The source of this bias is probably a combination of factors, including simplifications of the stress descriptions used to analyze both tests, different erosion mechanisms in the two tests, effects of the different geometry of the exposed surfaces in each test, and differences in the sensitivity of each test to variations of soil fabric or structure.

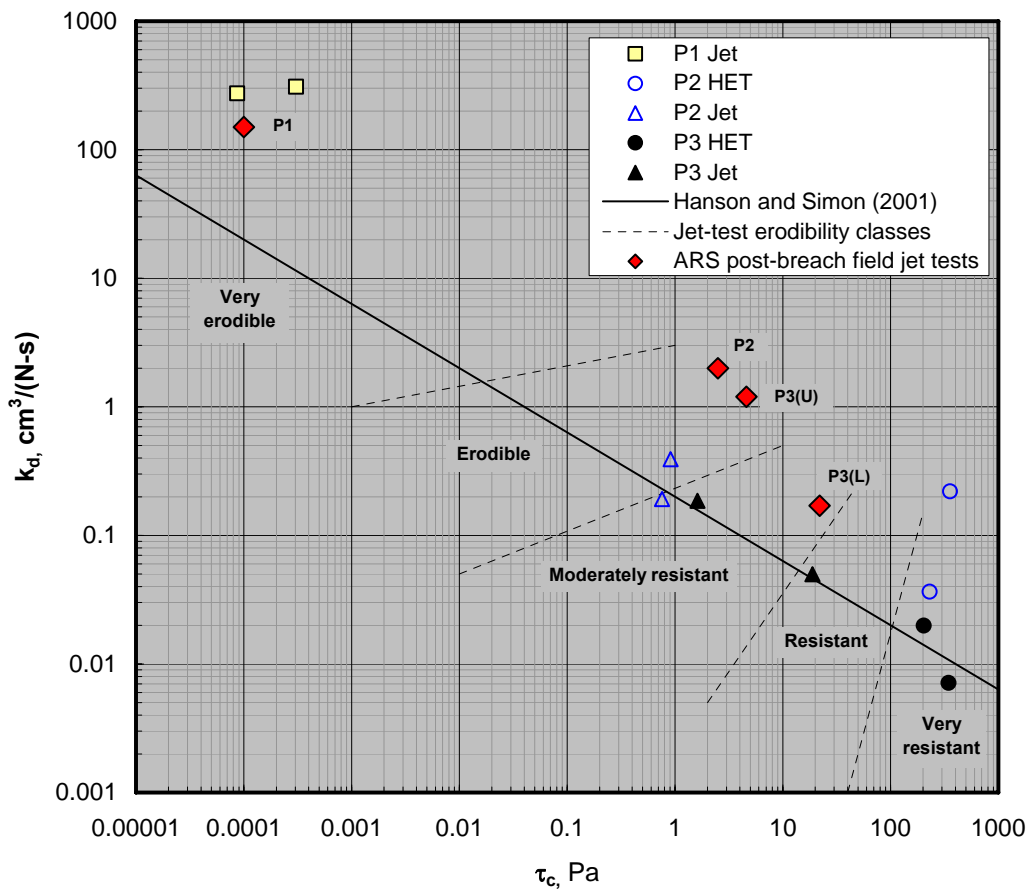


Figure 7. — Erodibility parameters measured in ARS piping breach tests compared to erodibility parameters obtained from laboratory HET and JET specimens compacted to similar conditions.

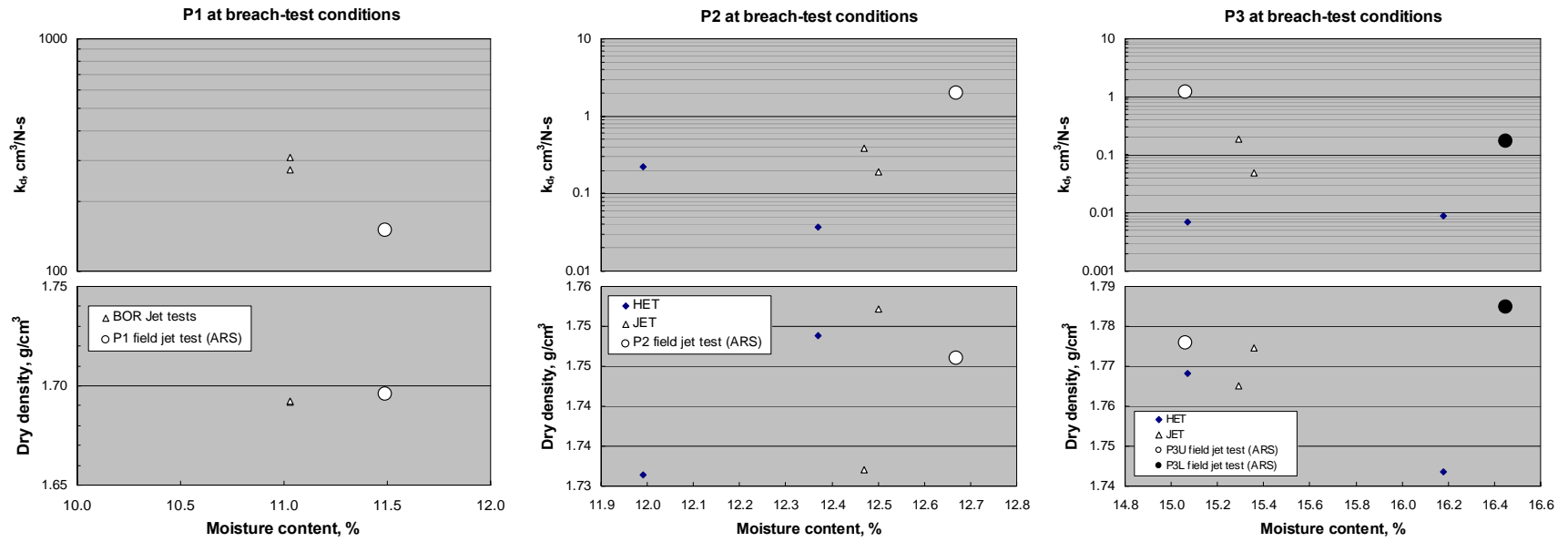


Figure 8. — Compacted dry density and detachment rate coefficients for specimens of P1, P2, and P3 compacted to conditions similar to the ARS piping breach tests.

HET vs. JET – Effect of Compaction Moisture Content

The third series of tests consisted of HET and JET tests on soils P2 and P3 at a range of moisture contents, using Standard Proctor compaction. Three soil layers were compacted into 4-inch diameter, 1/30 ft³ molds, with 25 blows per layer from a 5.5 lb hammer dropped 12 inches. Five moisture contents were targeted: the presumed optimum, -4%, -2%, +2%, and +4% from optimum. Actual optimum moisture content for each soil was determined after-the-fact. HET and JET specimens were prepared individually, so there is no direct comparison of specific tests, since the actual moisture content of each specimen varied.

Table 8 shows the test results, including the subjectivity indices for the HETs (see Appendix A). There were three tests with a subjectivity index of 2, indicating poor confidence in the test result, and three additional tests of soil P3 (not shown in the table) were excluded entirely (subjectivity index 3; analyses could not be completed). All of the jet tests were fully successful. Figures 9, 10, and 11 show the results graphically, first for the individual soils (Figs. 9 and 10), and then for both soils together (Fig. 11). The tests confirm that in general the P3 soil is less erodible than P2, but the erodibility of the P3 soil is more sensitive to moisture content differences on the dry side of optimum.

Table 8. — Erodibility test results for P2 and P3 soils over a range of compaction moisture contents.

Soil	Test Type	Compaction Conditions		Results		
		Moisture Content	Dry Density	τ_c	k_d	HET Subjectivity Index
		%	g/cm ³			
P2	HET	7.51	1.795	65.	0.217	2
		9.36	1.853	958.	0.0578	2
		11.56	1.895	856.	0.0311	0
		13.59	1.872	242.	0.0547	1
		15.65	1.795	133.	0.0372	1
	JET	7.55	1.785	0.062	1.39	-
		9.27	1.847	0.168	0.688	-
		11.57	1.929	7.58	0.0410	-
		13.43	1.872	0.081	0.188	-
		15.49	1.794	0.558	0.203	-
P3	HET	11.73	1.877	622	0.00420	0
		12.56	1.913	510	0.00266	1
		13.75	1.884	378	0.00253	2
		13.96	1.884	731	0.0122	1
		14.45	1.875	968	0.00524	0
		15.82	1.827	656	0.0131	1
		17.55	1.768	385	0.0205	1
	JET	10.18	1.848	0.456	0.508	-
		11.48	1.918	20.4	0.0329	-
		13.78	1.888	43.8	0.0234	-
		14.02	1.892	49.8	0.0493	-
		14.06	1.897	60.7	0.0198	-
		14.49	1.869	28.6	0.0124	-
		15.67	1.839	23.2	0.0303	-
17.82	1.773	15.1	0.0568	-		

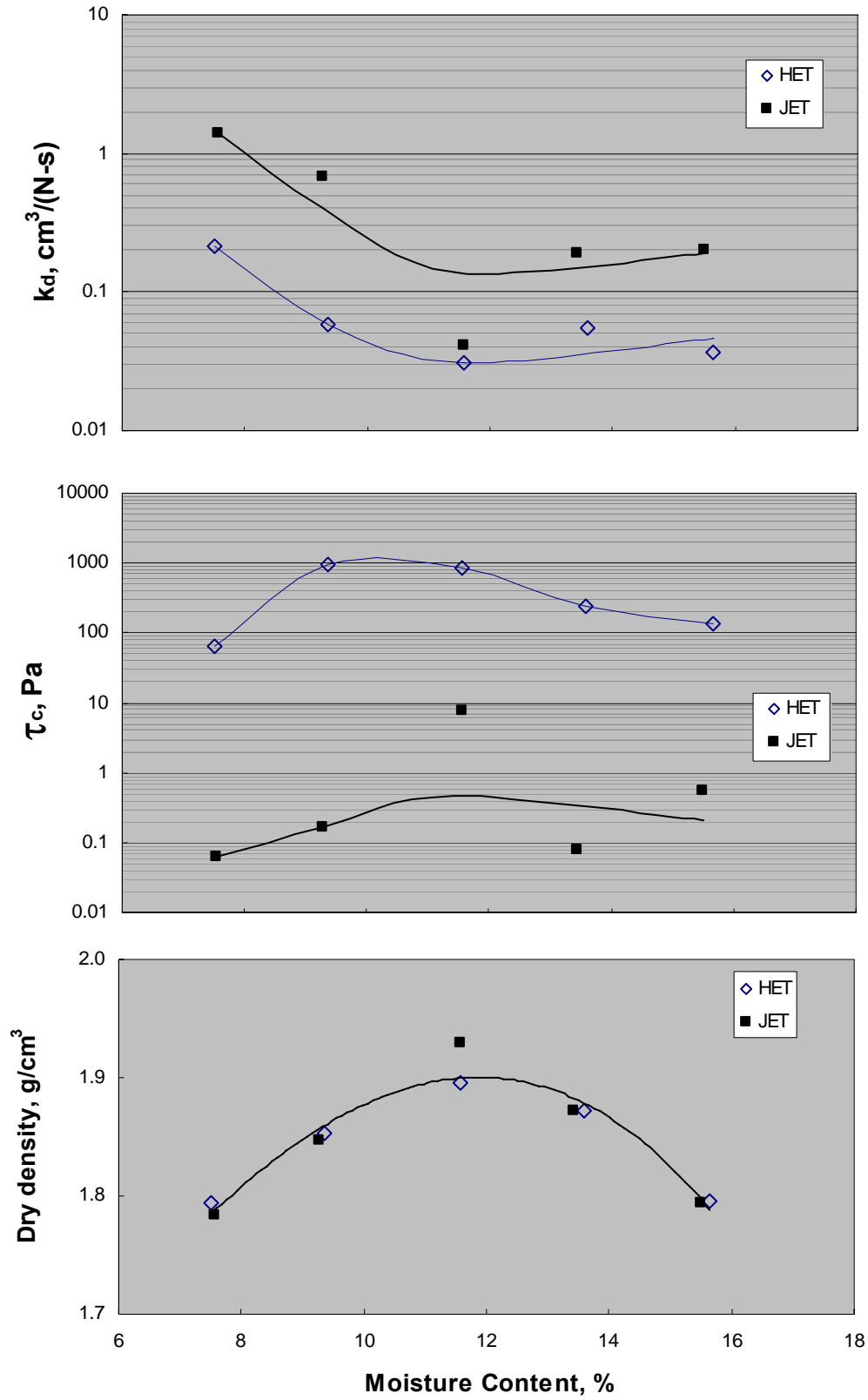


Figure 9. — Results of erodibility tests on soil P2 at compaction moisture contents ranging from about 4% dry of optimum to 4% wet of optimum.

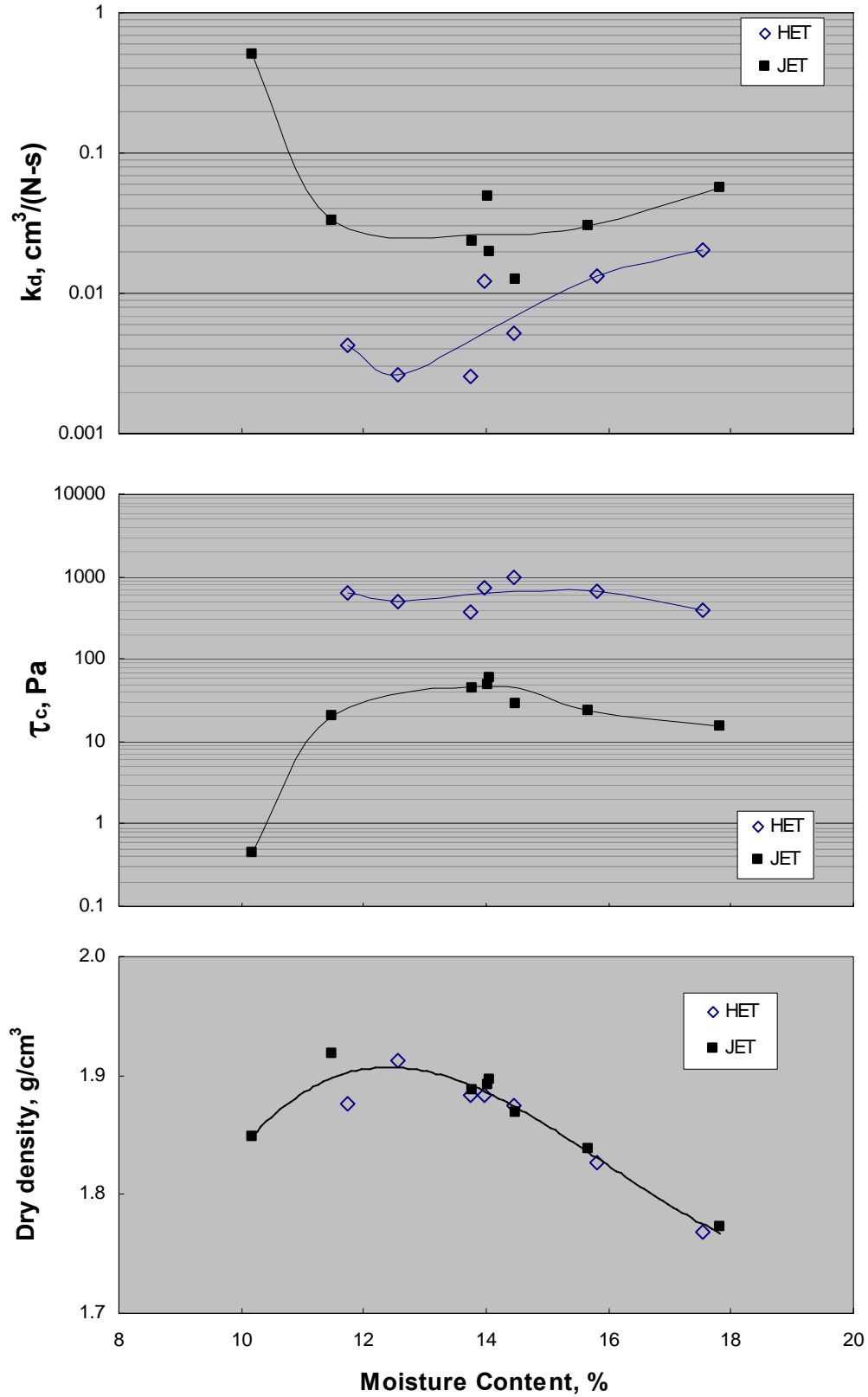


Figure 10. — Results of erodibility tests on soil P3 at compaction moisture contents ranging from about 3% dry of optimum to 5.5% wet of optimum.

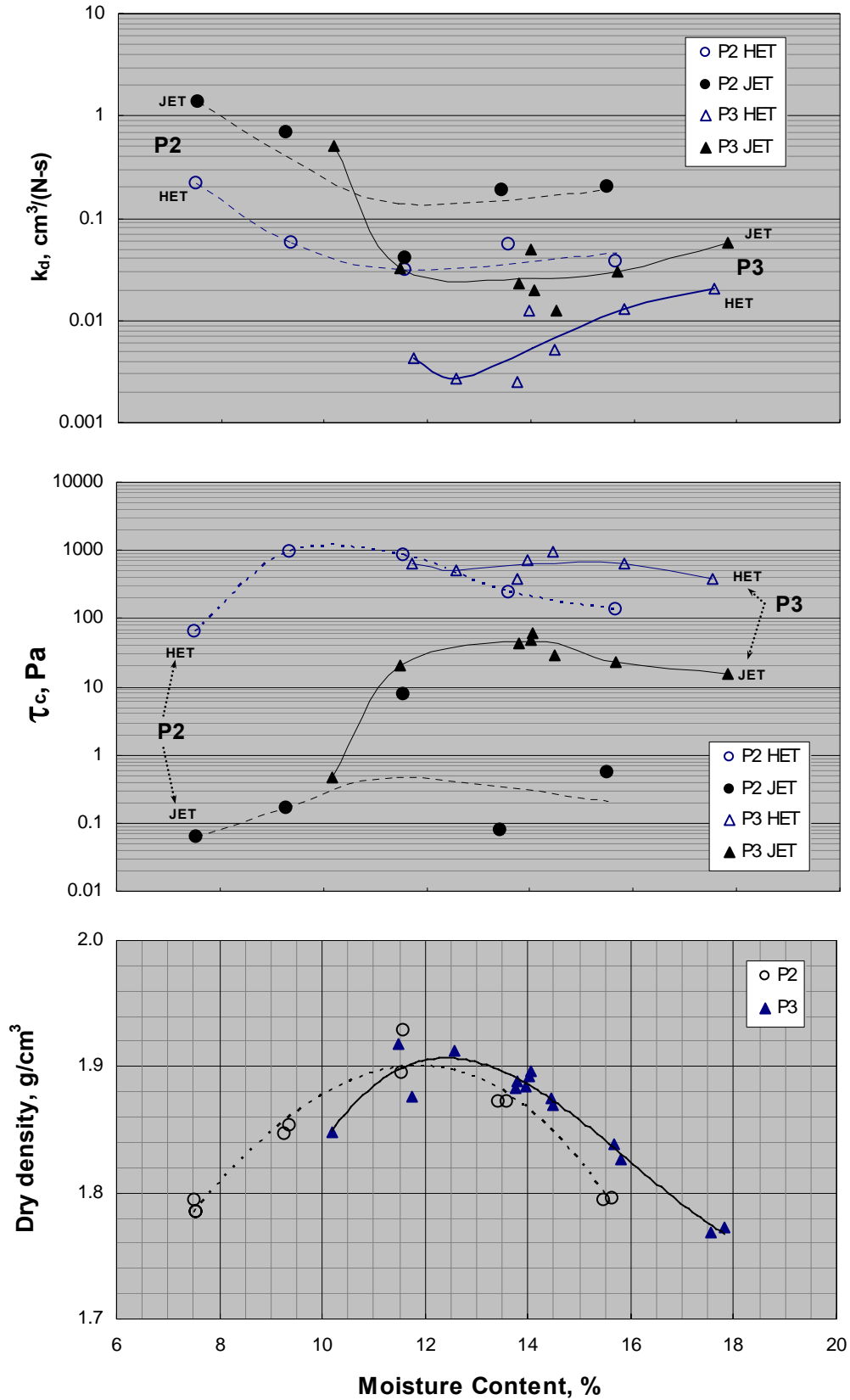


Figure 11. — Variation of erodibility for soils P2 and P3 as a function of compaction moisture content.

Differences between HET and JET results for soil P2 were relatively consistent across the range of tested moisture contents. The JET yielded detachment rate coefficients about 0.75 to 1 order of magnitude greater than those obtained from the HET. Critical shear stresses were about 2 to 3 orders of magnitude lower in the JET than in the HET.

Differences between the tests for soil P3 appear to be somewhat sensitive to the compaction moisture content. The detachment rate coefficients were only about 0.5 orders of magnitude different on the wet side of optimum, and about 1 order of magnitude different on the dry side, although there was not a successful HET test at the 4% dry condition to completely illustrate the effect. Critical shear stresses were consistently about 1.5 orders of magnitude different in the range for which a comparison could be made. The sensitivity of the JET results (both the detachment rate coefficient and the critical shear stress) to changes in moisture content on the dry side was greater for soil P3 than for P2. The unsuccessful HET performed on soil P3 at the nominally 4% dry condition experienced excessive local scour at the entrance and exit and erratic variations in flow during the test, making analysis impossible; this probably indicates a material with high erodibility, so the HET may have been as sensitive as the JET to the effect of dry compaction of this soil. Unfortunately, performing a successful test becomes difficult with the HET as the soil becomes more erodible.

Conclusions

Hole erosion tests and jet erosion tests performed on soils used in ARS embankment piping breach tests showed that the relative erodibility of the soils is generally consistent with the results of the breach tests. Soil P1 is so erodible that it could not be effectively tested in the HET, and as a result is believed to be in HET group 1 or 2 (extremely rapid to very rapid erosion rate). Soil P2 exhibited erosion that placed it in HET group 3 or 4 (moderately fast to moderately slow erosion rate), and all specimens of P3 were in HET group 4 (moderately slow erosion rate). Jet tests of these soils compacted to conditions approximating the ARS piping breach test conditions also exhibited similar erodibility relative to one another, but detachment rate coefficients and critical shear stresses were significantly different from those obtained by the HET method.

Tests of specimens compacted at optimum moisture content and 95% of maximum dry density produced surprising results, with the HET and JET indicating different erodibility rankings for soils P2 and P3. In reality, the moisture content was optimum for standard compaction effort but dry of optimum for the reduced effort needed to achieve 95% density. The results suggest that the JET may be more sensitive than the HET to differences in soil structure that occur when soils are compacted at drier than optimum conditions. A set of tests that evaluated HET and JET performance on samples compacted at a range of

moisture contents showed that the erodibility as determined by the JET increases rapidly for samples compacted dry-of-optimum; data for similar HET samples were inconclusive because a successful HET was not obtained at the driest compaction condition.

In general, detachment rate coefficients determined by the HET method are about one to two orders of magnitude lower than those determined by the JET method for similarly prepared specimens, and critical shear stress values are two to three orders of magnitude higher. The results for these soils are consistent with results of a broader, ongoing research program at Reclamation that is examining the relation between the HET and JET erosion indices for a variety of soils. Although there is a systematic difference between absolute results of each test, the relation between critical shear stresses and erosion rate coefficients seems to be similar for both tests. The source of the differences between the tests is probably a combination of factors, including simplifications of the stress descriptions used to analyze both tests, different erosion mechanisms in the two tests, effects of the different geometry of the exposed surfaces in each test, and differences in the sensitivity of each test to variations of soil fabric or structure.

References

- ASTM. 2007. Standard D5852. Standard test method for erodibility determination of soil in the field or in the laboratory by the jet index method. *Annual Book of ASTM Standards*, Section 4: Construction, Vol. 04.08. Philadelphia, Penn.: American Society for Testing and Materials.
- Bonelli, S., Brivois, O., Borghi, R., and Benahmed, N., 2006. On the modeling of piping erosion. *Comptes Rendus Mecanique* 334, Elsevier SAS, pp. 555-559.
- Hanson, G.J., and Simon, A., 2001. Erodibility of cohesive streambeds in the loess area of the midwestern USA. *Hydrological Processes*, Vol. 15, pp. 23-38.
- Hanson, G.J., and Cook, K.R., 2004. Apparatus, test procedures, and analytical methods to measure soil erodibility *in situ*. *Applied Engineering in Agriculture*, Vol. 20, No. 4, pp. 455-462.
- Hanson, G.J., and Hunt, S.L., 2007. Lessons learned using laboratory jet method to measure soil erodibility of compacted soils. *Applied Engineering in Agriculture*, Vol. 23, No. 3, pp. 305-312.
- Hunt, S.L., Hanson, G.J., Temple, D.L., and Tejral, R., 2007. Earthen embankment internal erosion research. In *Dam Safety 2007*. Proceedings of the 24th Annual Meeting of the Association of State Dam Safety Officials, Austin, TX September 9-12, 2007.
- Reclamation, 1990. USBR 5210 - Preparing Compacted Soil Specimens for Laboratory Use. Earth Manual, Part 2, U.S. Dept. of the Interior, Bureau of Reclamation, Denver, CO.
- Wahl, T.L., Regazzoni, P.-L., and Erdogan, Z., 2008. Determining erosion indices of cohesive soils with the hole erosion test and jet erosion test. U.S. Department of the Interior, Dam Safety Office.
- Wan, C.F., and Fell, R., 2002. *Investigation of internal erosion and piping of soils in embankment dams by the slot erosion test and the hole erosion test*, UNICIV Report No. R-412, The University of New South Wales, Sydney, Australia.
- Wan, C.F., and Fell, R., 2004. Investigation of rate of erosion of soils in embankment dams. *Journal of Geotechnical and Geoenvironmental Engineering*, Vol. 130, No. 4, pp. 373-380.

Appendix A: Current Hole Erosion Test Procedures Used by the Bureau of Reclamation

The hole erosion test (Wan and Fell 2004) is one of several methods for evaluating the erodibility of cohesive soils. The HET utilizes an internal flow, similar to that occurring during piping erosion of embankment dams. A 6-mm or ¼-inch diameter hole is pre-drilled through a soil specimen and flow is passed through that hole under constant head. The head is increased incrementally until the threshold stress to initiate erosion is exceeded. Once erosion is initiated, the flow rate will accelerate over time, since enlargement of the hole leads to further increases in shear stress and higher rates of erosion. One must reach this “progressive erosion” condition in order to have a successful test.

An ASTM standard for the hole erosion test does not yet exist; in its absence, tests are performed and analyzed using methods consistent with those described by Wan and Fell (2004). Recently, the Bureau of Reclamation and others have also investigated other methods for analyzing the data collected during HETs, focusing on the use of a piping erosion model developed by Bonelli et al. (2006). The data reported here were analyzed using the Wan and Fell (2004) procedures, although they were also checked for consistency using the Bonelli method when applicable. The data analysis procedures are described below.

Test Facilities and Procedures

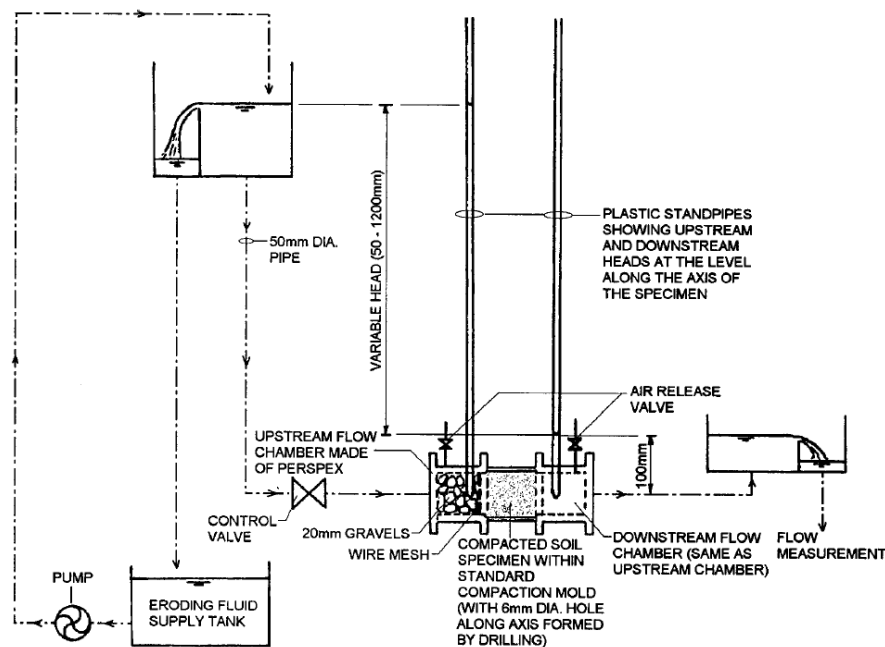


Figure A-1. Schematic diagram of hole erosion test facilities (Wan and Fell 2004).

The hole erosion test facilities at the Bureau of Reclamation are similar to those used by Wan and Fell (2004), except that the maximum head values in our two facilities are approximately 1600 mm and 5400 mm. Flow measurement is accomplished using 10° V-notch weirs, and data collection is automated using a computerized data acquisition system that records differential head and flow rate at 5 second intervals. The upstream and downstream chambers are similar to those shown in the schematic diagram. With erosion-resistant soils we have found no need for the 20 mm gravel in the upstream chamber. When testing very erosive soils we have found it helpful to place a plastic geotextile mesh fabric in the upstream chamber and protect the upstream and downstream faces of the compacted soil specimen with end plates. We have a range of end plates available, with orifice openings varying from 10 mm to 25 mm. The orifice size is selected based on the expected erodibility of the sample, with smaller orifices generally used to provide more protection to the faces of weaker specimens. The test operator must consider the orifice size and plan to end the test before the hole enlarges enough to allow the orifice openings to limit the flow rate.

The basic test procedure is as follows:

1. Following specimen preparation and compaction, specimens are sealed in plastic bags to prevent moisture loss and cured overnight before testing.
2. After curing, a ¼-inch diameter hole is drilled through the specimen using a drill press and wood auger bit to minimize compaction of the side walls of the hole. Drilling is performed at the slowest possible speed and the bit is advanced slowly and cleaned repeatedly during drilling.
3. The hole is cleaned using a 0.22-inch diameter rifle brush.
4. Specimens are installed into the apparatus with the original top surface (last compacted layer) upstream. If the soil is expected to be highly erodible or susceptible to scour of the upstream and downstream faces, protective end plates are also installed. A plastic geofabric mesh filter is also installed in the upstream chamber to reduce turbulence when specimens are expected to be highly erodible.
5. The test facility is filled slowly with water and all air is bled from piezometer tubes connected to pressure sensors.
6. The water supply head tank is positioned to the desired starting head level. For specimens of unknown erodibility, tests are usually started at 50 mm of head.
7. The downstream weir box tank is filled with water to the level of the horizontal weir that maintains nearly-constant downstream head, and some additional water is then added to produce flow through the V-notch weir at a rate that approximates the expected starting flow rate. This is done in an attempt to have the test start with the weir box system in a state of flow rate equilibrium.
8. The data acquisition system is started and the inlet valve upstream from the test specimen is opened.
9. The flow rate is monitored to determine whether it is increasing or becoming steady. If the flow rate stabilizes at a given head, then the head

tank is raised to increase the head. We generally double the head each time, or if we feel that the erosion threshold is near, we will increase the head in somewhat smaller increments.

10. When the flow rate begins to accelerate, the test head is maintained until at least several minutes of accelerating flow is observed. The operator should be aware of the approximate maximum flow increase that can occur if end plates have been installed. For example, if 10 mm end plates have been installed, the ratio of flow rates with a 10 mm hole diameter to the flow through the original 6 mm diameter hole is approximately $(10/6)^2 \approx 3$. Thus, one should stop the test well before the flow rate has tripled from its value at the start of accelerating flow. If the test is allowed to continue too long, the orifice plate opening will begin to limit the flow rate, which will hinder the data analysis.
11. After the test is stopped, the upstream and downstream chambers are drained and the specimen is removed from the test facility. An initial visual estimate of the final hole diameter is made, and the specimen is weighed.
12. Specimens are oven-dried, weighed, and then a hydrostone casting is made of the erosion hole.
13. Hole diameters are determined from the casting, typically at 5 positions spaced approximately equally along the length. The length of the portion of the casting that is of relatively uniform diameter is also recorded. (Large scour holes at the upstream or downstream end are considered to reduce the effective length of the hole, which is taken into account in the data analysis.)

Wan and Fell Analysis Procedure

The deterministic data analysis method described by Wan and Fell (2004) attempts to compute the hole diameter at each time step at which data have been recorded. The computed time series of hole diameters can then be used to estimate the erosion rate and applied shear stress. Microsoft Excel spreadsheets are used to make the computations and present the data graphically.

The analysis begins by considering a cylinder of eroding fluid passing through the pre-drilled hole in a soil specimen. Assuming that over a short interval of time the flow is at steady state, the equation for force equilibrium is:

$$\tau \cdot P_w \cdot L = \rho_w \cdot g \cdot \Delta h \cdot \frac{\pi d^2}{4}$$

where:

τ = shear stress along the sides of the hole

P_w = perimeter of the hole

L = length of the hole

ρ_w = fluid density

g = acceleration due to gravity

Δh = head difference across the hole from upstream to downstream

d = diameter of the hole

For a laminar flow condition, the shear stress is expected to be proportional to the mean velocity of the flow

$$\tau = f_L \bar{v}$$

where

f_L = friction factor, S.I. units of kg/s/m

\bar{v} = mean velocity of the flow, $Q/(\pi d^2/4)$

Q = flow rate

Combining these equations and solving for the friction factor yields:

$$f_L = \frac{\rho_w g \Delta h \pi d^3}{Q L 16}$$

This equation can be used to solve for the friction factor at the start and end of the test, when the hole diameter, length, head differential and flow rate are all known. Research has shown that the friction factor varies in proportion to the hole diameter, but the hole diameters during the test are not known until the analysis is complete, so the friction factor is instead assumed to vary during the test in proportion to the value of $(Q/\Delta h)^{1/3}$ for laminar flow, and $(Q^2/\Delta h)^{1/5}$ for turbulent flow. These quantities are surrogates for the hole diameter. The length of the erosion hole is assumed to vary linearly with time during the test (although it stays constant in many tests). The quantity $(Q^2/\Delta h)^{1/5}$ is also plotted on the data acquisition computer during a test to help the operator know when accelerating enlargement of the hole diameter is occurring. Most tests take place with turbulent flow conditions. The onset of turbulence is assumed to occur when the Reynolds number of flow through the hole exceeds 2000 ($Re = Vd/\nu$, where V is the flow velocity, d is the hole diameter, and ν is the kinematic viscosity).

Denoting friction factors and hole lengths at intermediate times during the test by the subscript t , the same equations can be solved for the hole diameter to allow it to be computed throughout the test from measured values of the flow rate.

$$d = \left(f_{L_t} \frac{Q_t}{\rho_w g} \frac{L_t}{\Delta h_t} \frac{16}{\pi} \right)^{1/3}$$

If the flow is turbulent, the shear stress is proportional the square of the mean velocity and the following equations apply:

$$\tau = f_T \bar{v}^2$$

$$f_T = \frac{\rho_w g \Delta h \pi^2 d^5}{Q^2 L 64}$$

$$d = \left(f_T \frac{Q^2 L 64}{\rho_w g \Delta h \pi^2} \right)^{1/5}$$

Bonelli Analysis Procedure

Bonelli et al. (2006) proposed a universal model for piping erosion, applicable to analysis of the hole erosion test. They showed that the change in dimensionless hole radius is an exponential function of the dimensionless test time and the initial and critical shear stresses

$$\frac{R(t)}{R_0} = 1 + \left(1 - \frac{\tau_c}{\tau_0} \right) \left(e^{t/t_{er}} - 1 \right)$$

where $R(t)$ =radius at any time t and R_0 =the initial radius at time zero, τ_c =critical shear stress, τ_0 =shear stress at time zero, t =test time, and t_{er} =a characteristic erosion time scale for each test

$$t_{er} = \frac{2L}{k_d \gamma_w \Delta h} = \frac{2L \gamma_d}{C_e \gamma_w \Delta h}$$

where L =length of the hole, γ_w =unit weight of water ($\rho_w g$), Δh =head differential across the hole, γ_d =dry unit weight of soil, C_e =erosion rate coefficient (mass/time/area/stress), and k_d is a volumetric detachment rate coefficient (volume/time/area/stress).

The model assumes turbulent flow conditions and neglects any variation of the friction factor, the test head, or the length of the eroded hole. The method also presumes that the test data are collected entirely during the period of accelerating erosion. Bonelli et al. (2006) showed that the proposed model fit the observed hole radius data computed from 17 HETs performed by Wan and Fell (2002) using 9 different soils. Bonelli and Brivois (2007) have offered further development of the model.

Recognizing that dimensionless discharge, Q^* , is proportional to the 2.5 power of the dimensionless radius (again neglecting effects of any change in the friction factor during a test), one can write

$$Q^* = \frac{Q(t)}{Q_0} = \left(\frac{R(t)}{R_0} \right)^{5/2} = \left[1 + \left(1 - \frac{\tau_c}{\tau_0} \right) \left(e^{t/t_{er}} - 1 \right) \right]^{5/2}$$

Since flow rates are measured throughout a test and the initial shear stress is known from the starting hole diameter and flow rate, this model has only two unknown parameters, the erosion time scale, t_{er} , and the critical shear stress, τ_c . Using a non-linear optimization tool such as the Excel Solver, one can optimize these two parameters to obtain a best fit of the observed dimensionless values of discharge to predicted values computed for each dimensionless test time, t/t_{er} . The coefficient of soil erosion or the detachment rate coefficient can then be determined from the fitted value of the time scale factor, t_{er} . The significant advantages of this analysis method are the fact that the final hole diameter does not need to be measured, and the curve-fitting procedure minimizes the influence of short-term anomalies in erosion behavior during a test.

It should be emphasized that the formulation of the Bonelli model requires the fitted value of the critical shear stress τ_c to be less than the initial stress, τ_0 , otherwise the quantity $(1-\tau_c/\tau_0)$ is negative. This means that tests must be conducted at a stress level that exceeds the critical stress and produces immediate progressive erosion, or one must customize the analysis to only examine the portion of the test in which the shear stress exceeds τ_c . If a test begins at a stress level that is slightly lower than the value needed to initiate progressive erosion, but the stress then increases due to cleanout erosion of material disturbed during hole drilling, the only way to accurately determine the critical stress would be to estimate the increase in hole diameter and shear stress that takes place leading up to the progressive erosion phase, then start the Bonelli analysis at that point in time. This requires the combined use of both the Wan and Fell and Bonelli analysis procedures.

HET Subjectivity Index

Hole erosion tests do not always proceed according to plan. The ideal erosion mode is a uniform enlargement of the pre-drilled hole along its full length, producing accelerating flow over the duration of the test, once erosion is initiated. Other erosion modes, such as localized scour at the entrance and exit of the hole can yield data that are difficult or impossible to analyze. To help quantify the potential uncertainty of test results, the table below provides numerical indices for the degree to which subjective judgments were required by the analyst during the processing of HET data.

Subjectivity indices for HETs – These characteristics are offered as guidelines; not every characteristic will be present in any particular case.	
0	Start of progressive erosion is definite and progressive erosion and accelerating flow are maintained continuously until end of test. The Wan & Fell (2004) and Bonelli et al. (2006) analysis methods yield nearly identical results. The k_d and τ_c values obtained from the two methods differ by less than 1/10 order of magnitude.
1/2	Similar to grade 0, except that the two analysis methods yield only similar (not “nearly identical”) results.
1	Progressive erosion and accelerating flow are not continuously maintained. To get a reasonable result, the analysis must be restricted to a subset of the data following the initiation of erosion. Some judgment is required, but the analyst has good confidence in those judgments. Both analysis methods yield similar results.
2	Unintended modes of erosion significantly affect the test (e.g., scour at entrance or exit causing hole shortening without significant enlargement, sloughing of roof of pipe, clogging of pipe). Period(s) of progressive erosion and accelerating flow are not continuously maintained and are relatively short. Significantly different test results can be obtained by analyzing different segments of the data, and it is not readily apparent which segment should be used. Only one analysis method yields a result that seems reasonable. Analyst has poor confidence in test result. Analysis indicates $\tau_c \leq 0$, even though there was no erosion observed at low heads (and hence there should be a positive shear stress needed to initiate erosion).
3	There is no period of progressive erosion that produces continuous hole enlargement with accelerating flow. No reasonable test result can be obtained from either analysis method.

References

Bonelli, S., Brivois, O., Borghi, R., and Benahmed, N., 2006. On the modeling of piping erosion. *Comptes Rendus Mecanique* 334, Elsevier SAS, pp. 555-559.

Bonelli, S., and Brivois, O., 2007. The scaling law in the hole erosion test with a constant pressure drop. *International Journal for Numerical and Analytical Methods in Geomechanics*, 24 pp. Published online in Wiley InterScience (www.interscience.wiley.com). DOI: 10.1002/nag.683

Wan, C.F., and Fell, R., 2004. Investigation of rate of erosion of soils in embankment dams. *Journal of Geotechnical and Geoenvironmental Engineering*, Vol. 130, No. 4, pp. 373-380.

Appendix B: Selected Erosion Test Photographs



Figure B-1. Result of attempted hole erosion test of soil P1. Soil specimen collapsed immediately upon submersion in water and initiation of flow.

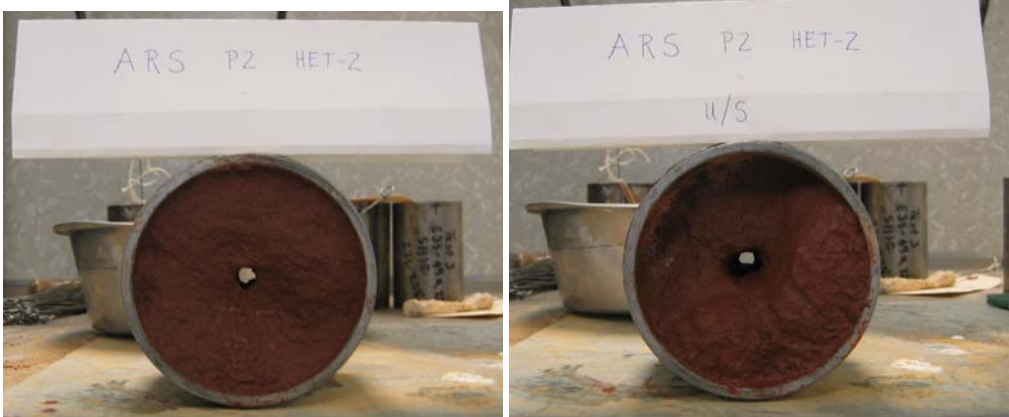


Figure B-2. Upstream and downstream views of post-test condition of specimen P2 HET-2.



Figure B-3. Upstream and downstream views of post-test condition of specimen P2 HET-3.



Figure B-4. Upstream and downstream views of post-test condition of specimen P2 HET-6.

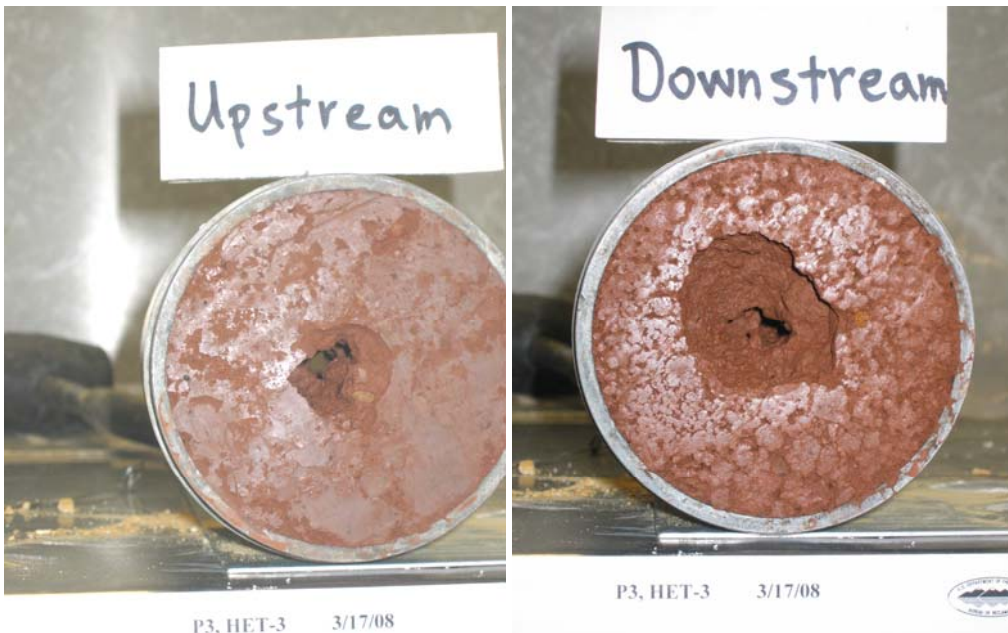


Figure B-5. Upstream and downstream views of post-test condition of specimen P3 HET-3. This specimen was compacted to representative conditions.



Figure B-6. Upstream and downstream views of post-test condition of specimen P3 HET-5. This specimen was compacted to conditions similar to the ARS piping breach test.



Figure B-7. Several representative castings of eroded holes through specimens of soil P2.



Figure B-8. Several representative castings of eroded holes through specimens of soil P3.



Figure B-9. Post-test photographs of two submerged jet tests of soil P2.

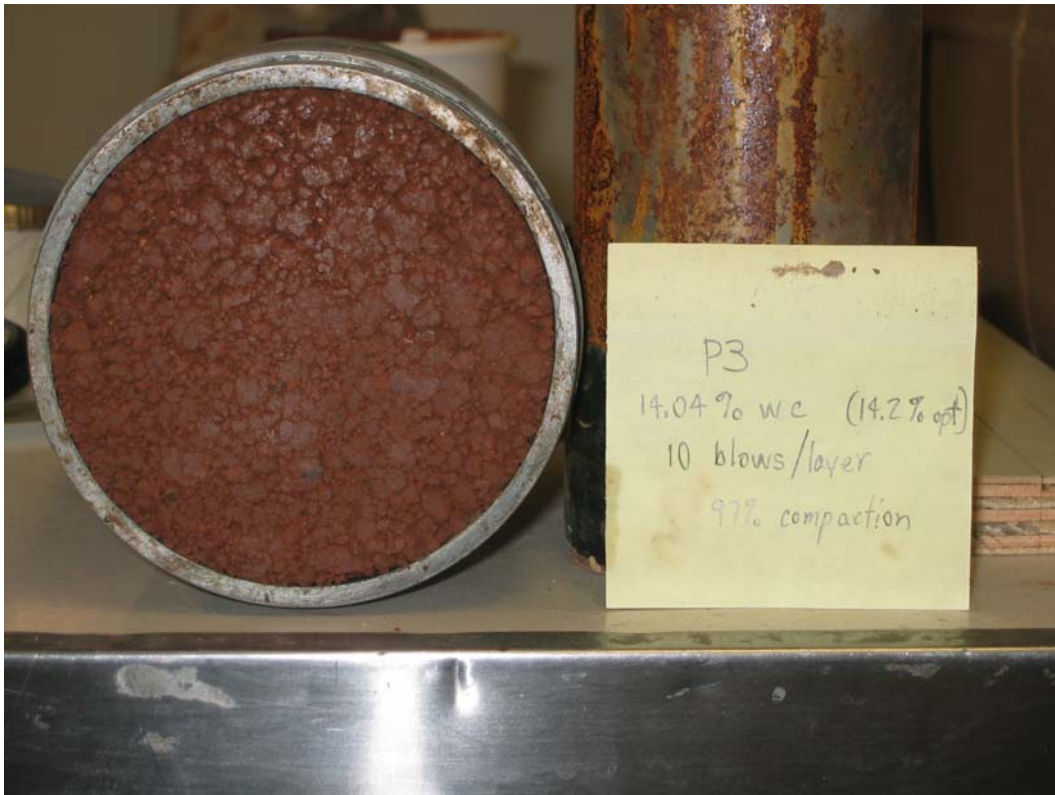


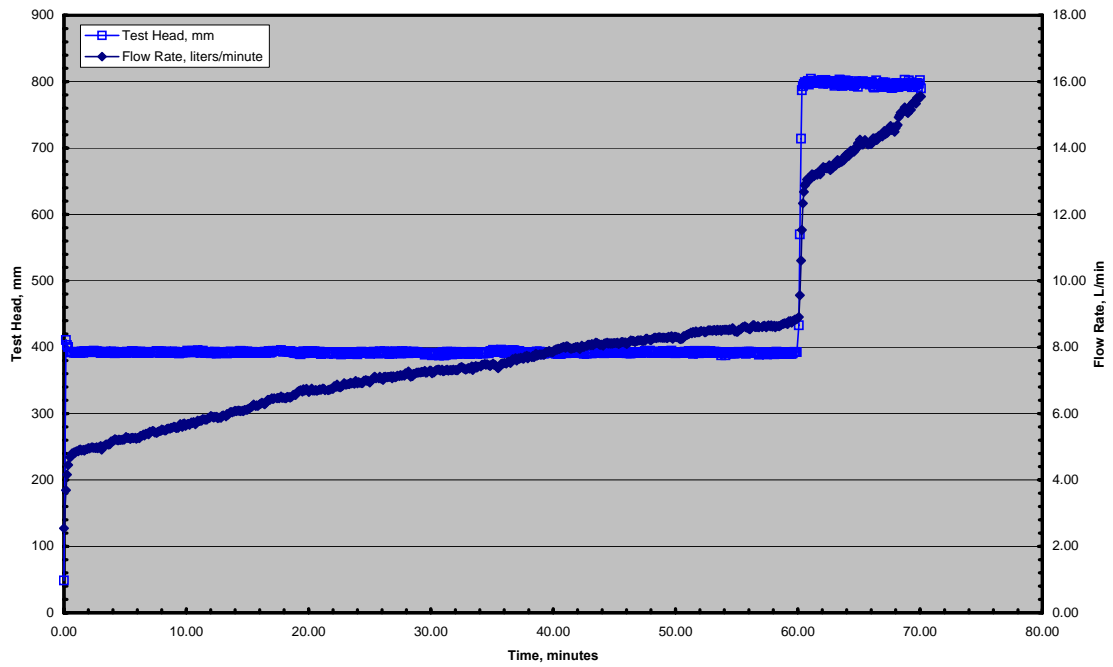
Figure B-10. Pre and post jet-test photographs of a specimen of soil P3 compacted to representative conditions.

Appendix C: HET and JET Test Records

ARS

Soil P2 - optimum w.c., 95% compaction Test 2 01-22-2008

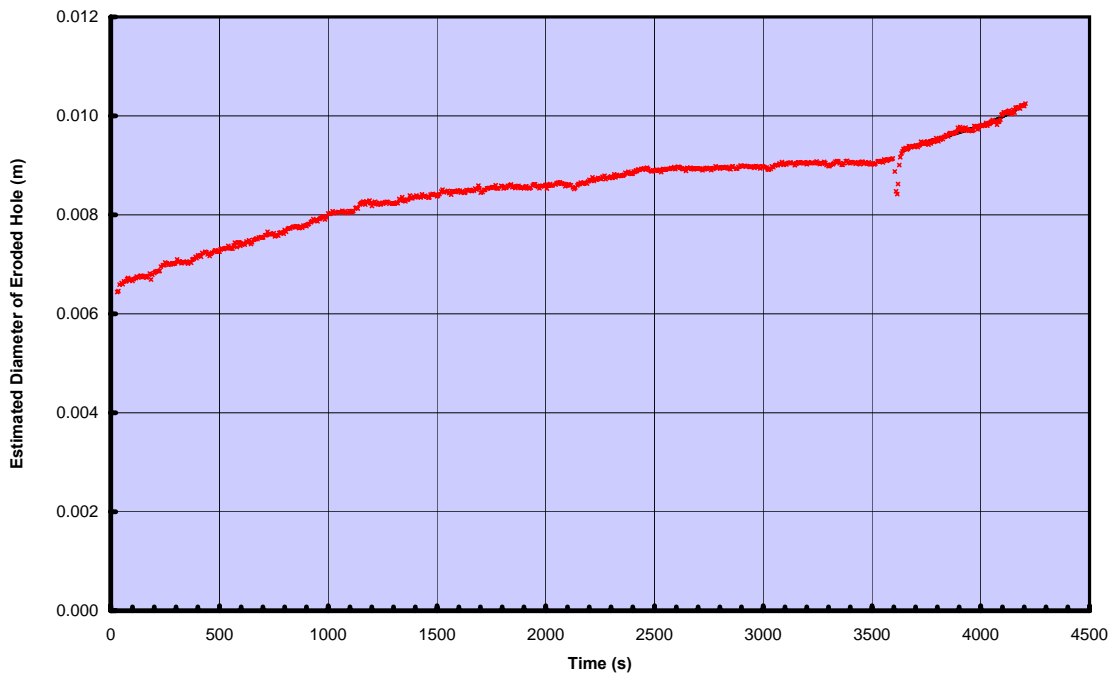
HET Test Record



ARS

Soil P2 - optimum w.c., 95% compaction Test 2 01-22-2008

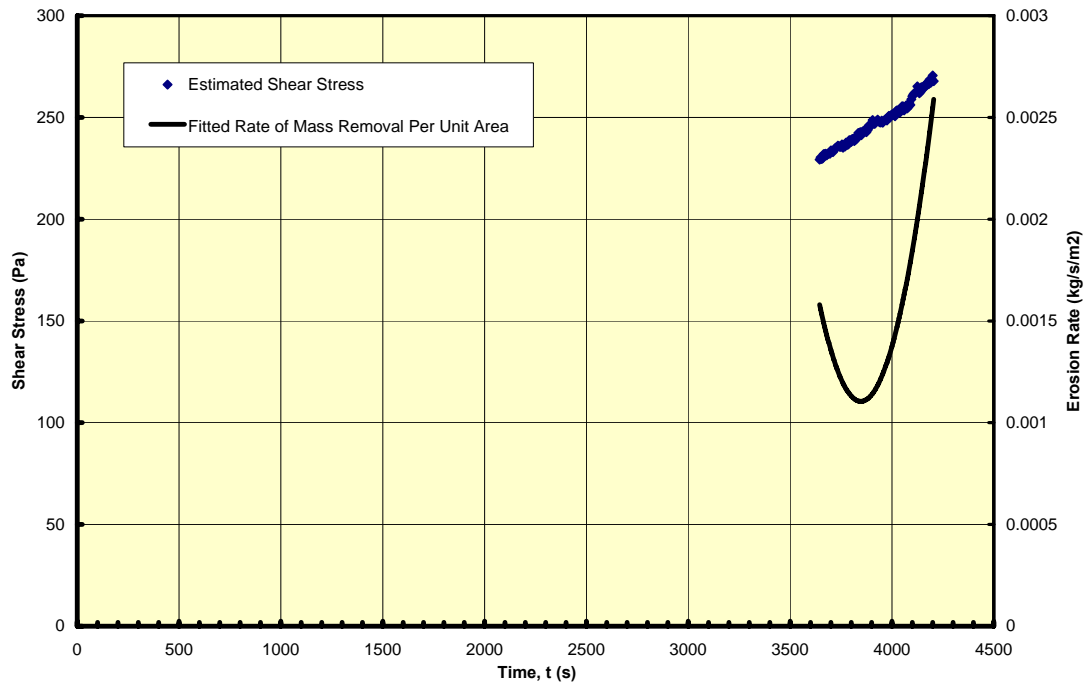
COMPUTED DIAMETER OF ERODED HOLE



ARS

Soil P2 - optimum w.c., 95% compaction Test 2 01-22-2008

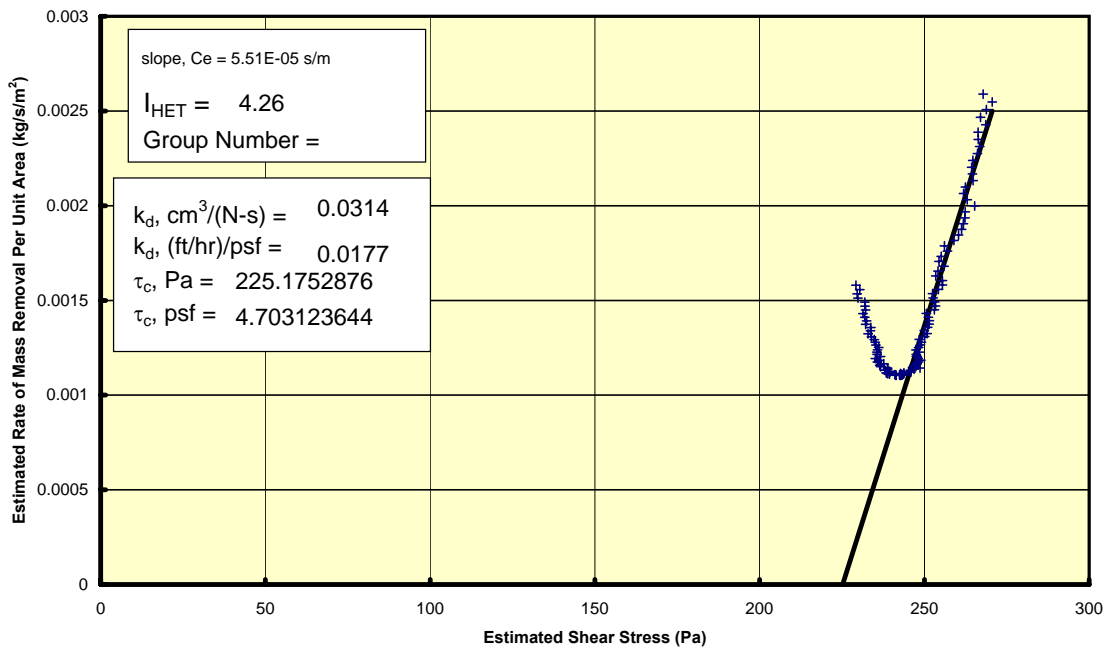
EROSION RATE AND SHEAR STRESS VS. TIME



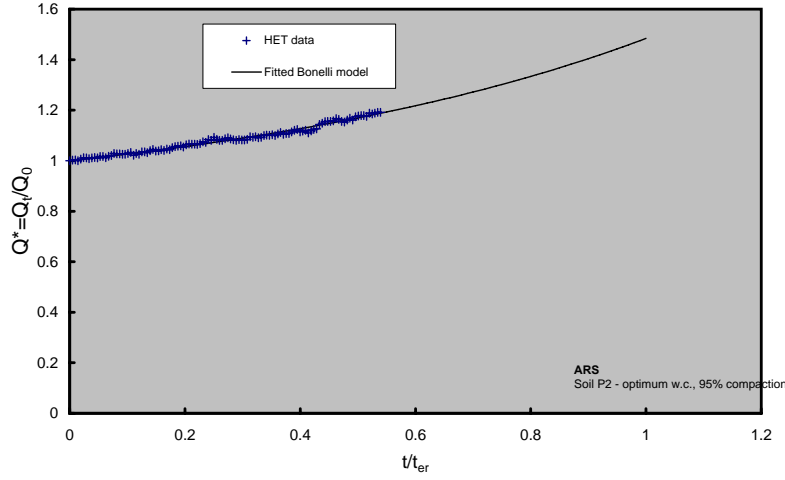
ARS

Soil P2 - optimum w.c., 95% compaction Test 2 01-22-2008

EROSION RATE VS. SHEAR STRESS



HET dimensionless flow vs. dimensionless time
(Bonelli et al. 2006)



Project ARS
 Feature Soil P2 - optimum w.c., 95% compact
 Test 2
 Date 1/22/2008

RESULTS SUMMARY

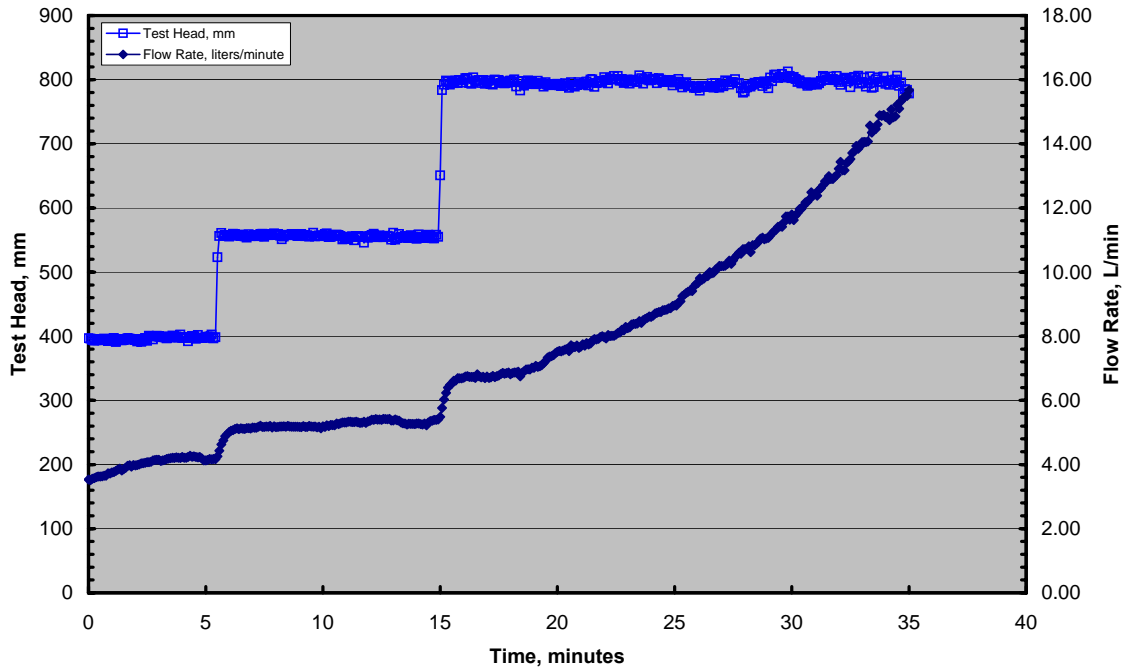
C_e	4.10E-05 ((kg/s)/m ²)/Pa = s/m	
l_{HET}	4.39	Group 4
τ_c	173.6 Pa	
k_d	2.331E-08 m/s/Pa = m ³ /(N-s)	
k_d	0.0233 cm ³ /(N-s)	
k_d	0.0132 (ft/hr)/psf	
τ_c	3.63 psf	

on

ERODS - ARS Soils

Soil P2, HET-3 Test 3 03-20-2008

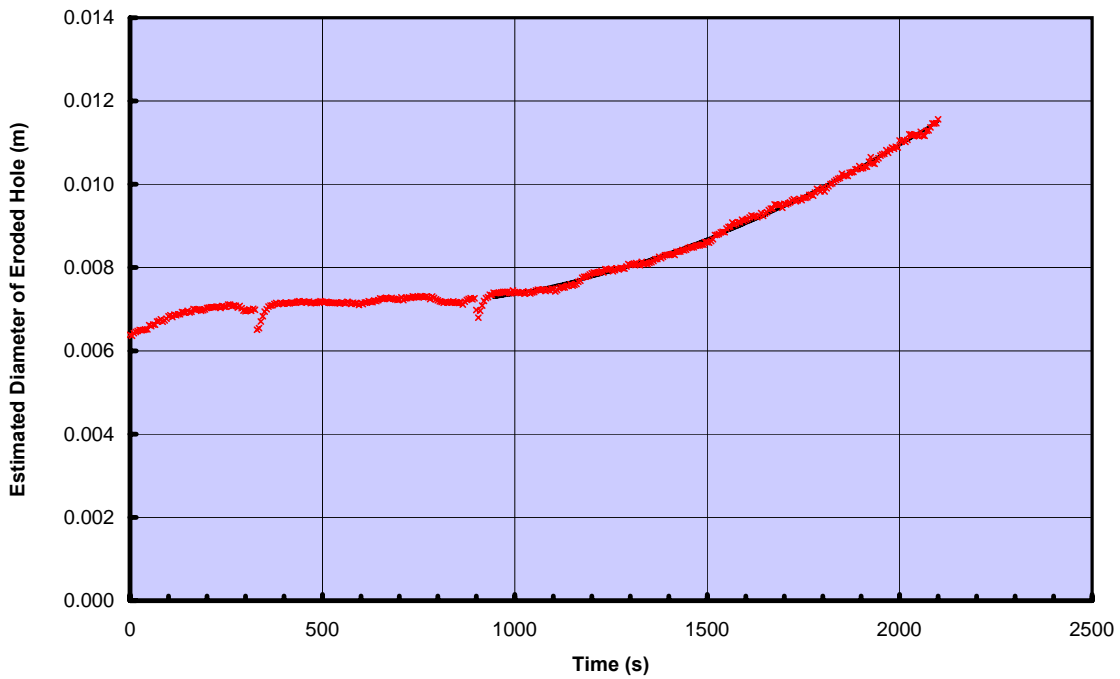
HET Test Record



ERODS - ARS Soils

Soil P2, HET-3 Test 3 03-20-2008

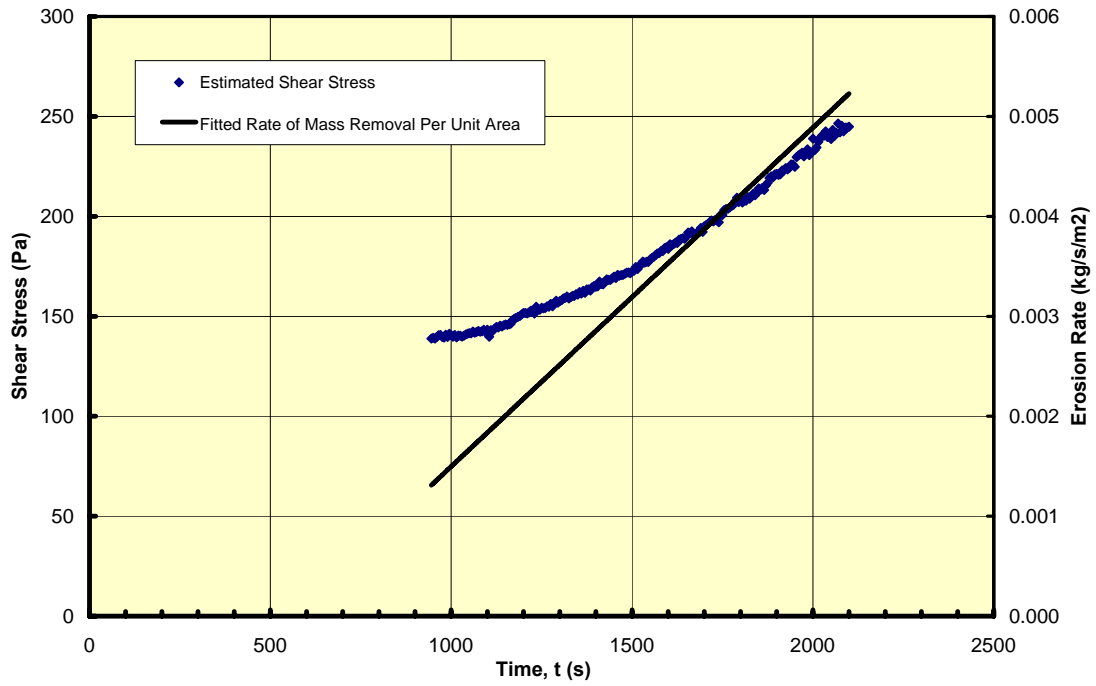
COMPUTED DIAMETER OF ERODED HOLE



ERODS - ARS Soils

Soil P2, HET-3 Test 3 03-20-2008

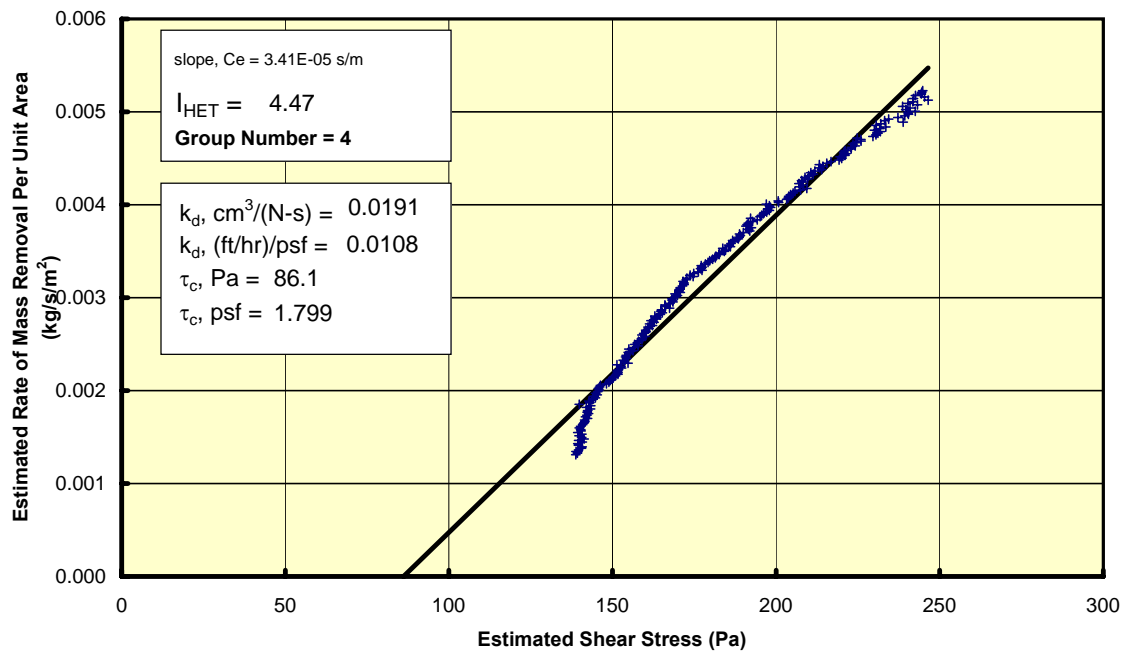
EROSION RATE AND SHEAR STRESS VS. TIME



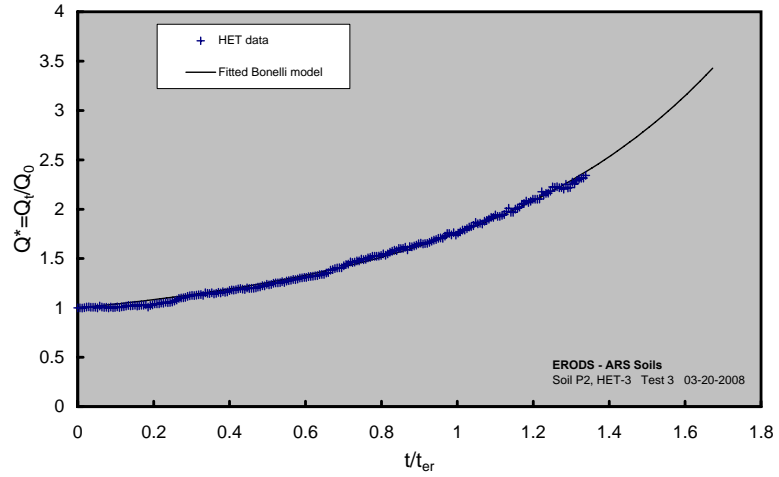
ERODS - ARS Soils

Soil P2, HET-3 Test 3 03-20-2008

EROSION RATE VS. SHEAR STRESS



HET dimensionless flow vs. dimensionless time
(Bonelli et al. 2006)



Project ERODS - ARS Soils
Feature Soil P2, HET-3
Test 3
Date 3/20/2008

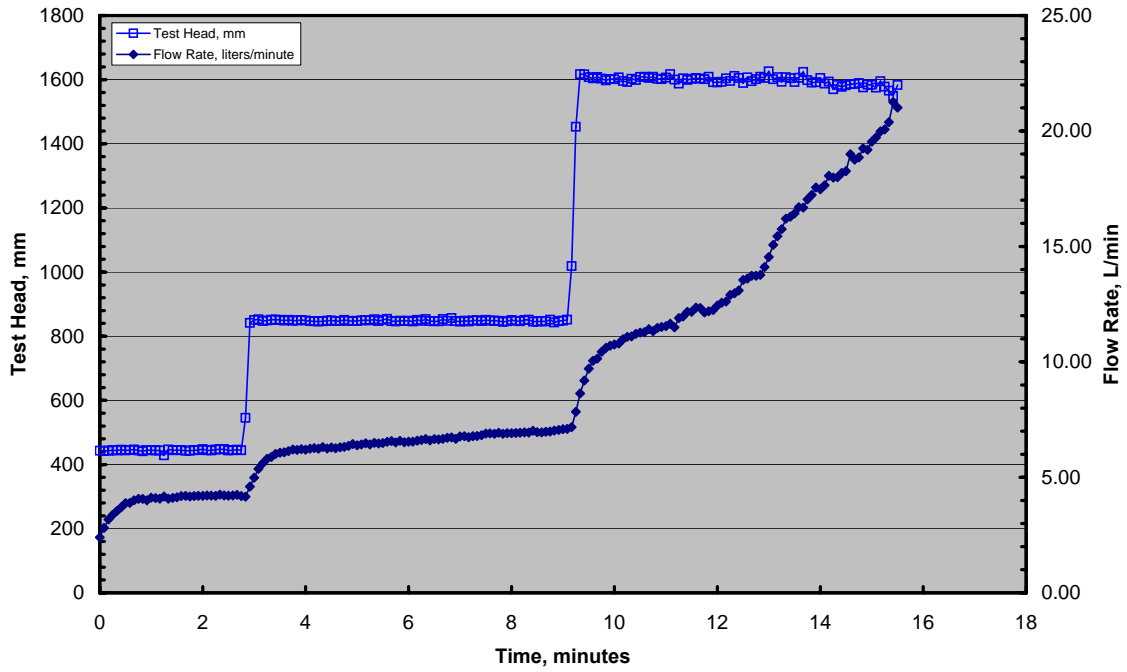
RESULTS SUMMARY

C_e	5.43E-05 ((kg/s)/m ²)/Pa = s/m	
l_{HET}	4.27	Group 4
τ_c	119.9 Pa	
k_d	3.047E-08 m/s/Pa = m ³ /(N-s)	
k_d	0.0305 cm ³ /(N-s)	
k_d	0.0172 (ft/hr)/psf	
τ_c	2.50 psf	

ARS

HET Test Record

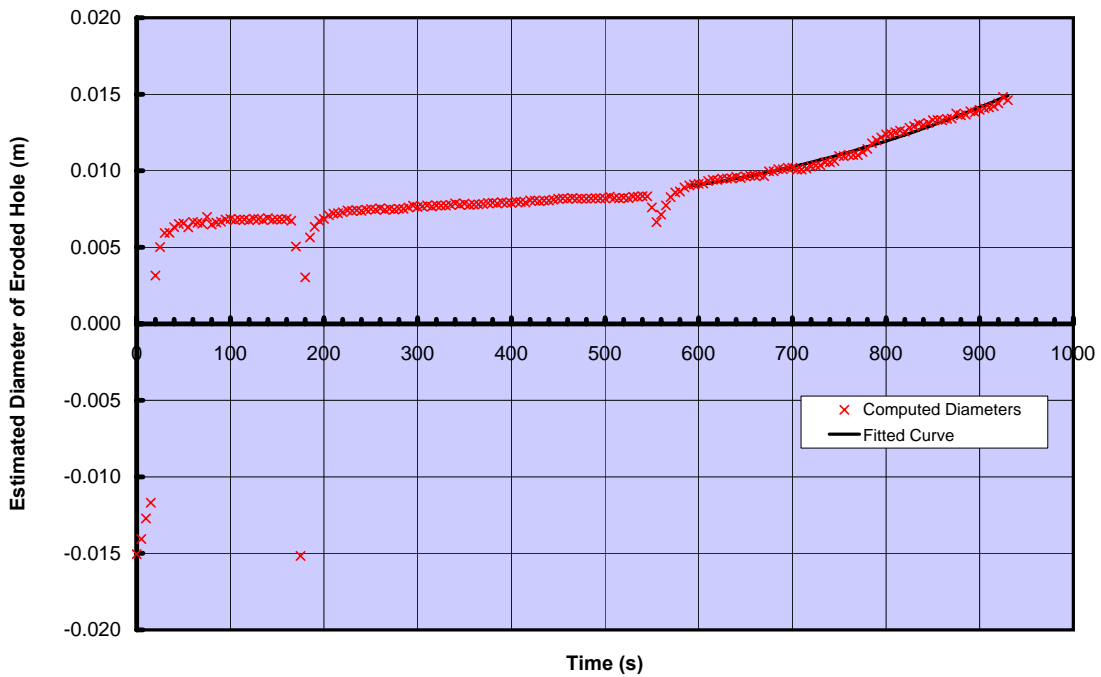
P2 at breach test conditions Test P2- HET 4 CL



ARS

COMPUTED DIAMETER OF ERODED HOLE

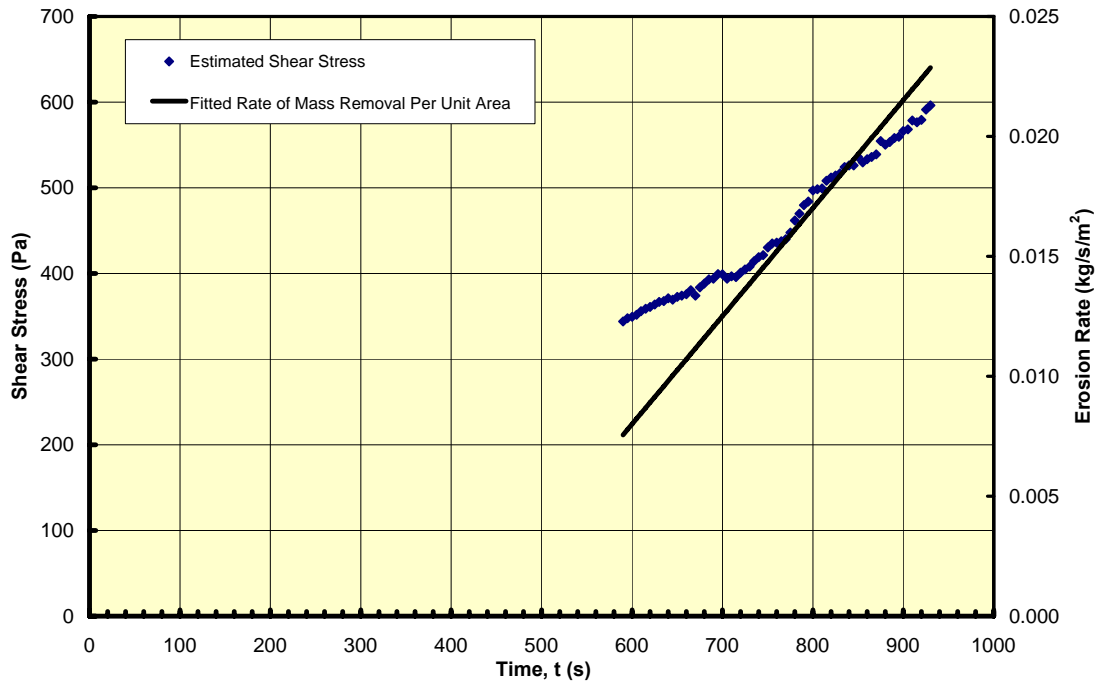
P2 at breach test conditions Test P2- HET 4 CL



ARS

EROSION RATE AND SHEAR STRESS VS. TIME

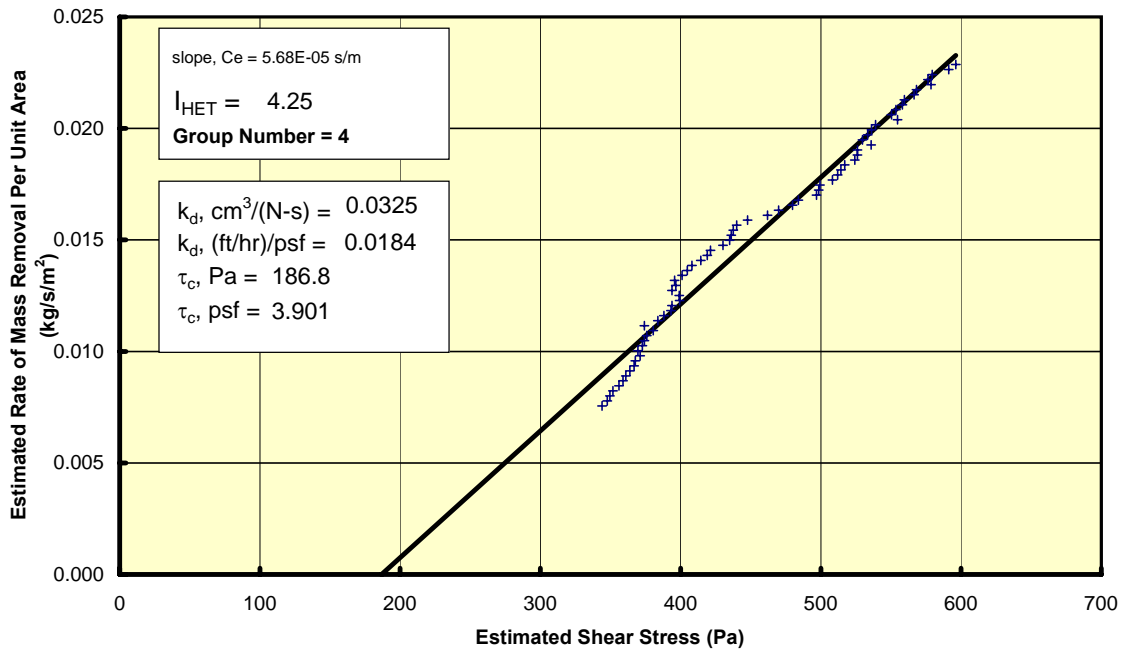
P2 at breach test conditions Test P2- HET 4 CL



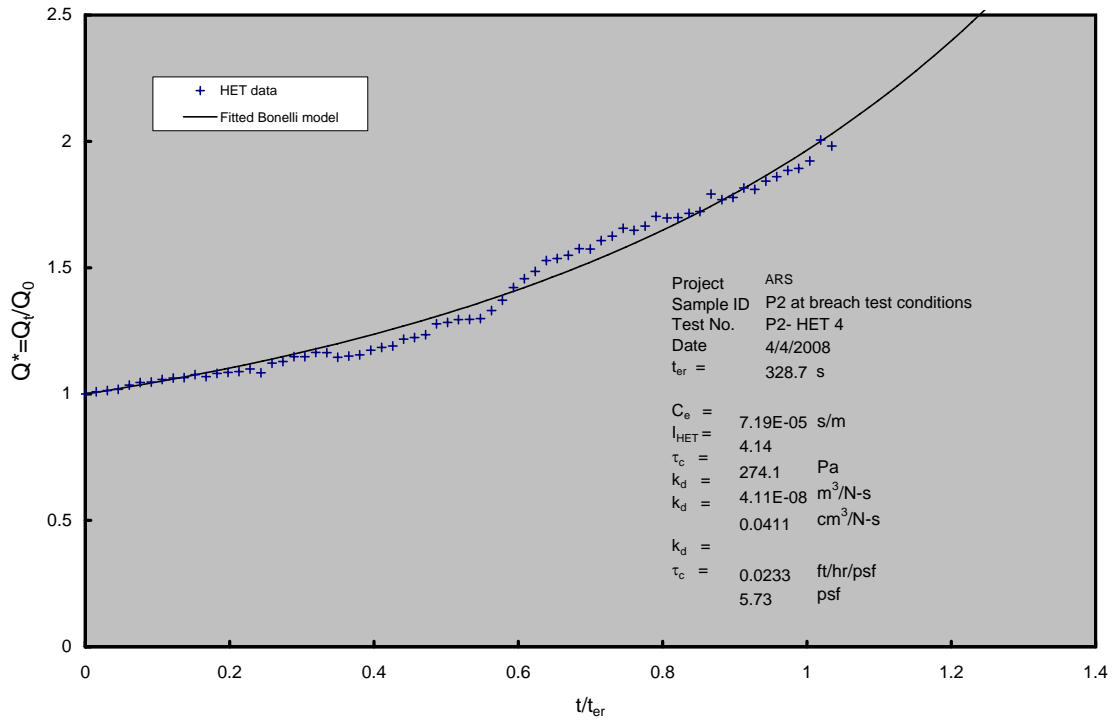
EROSION RATE VS. SHEAR STRESS

ARS

P2 at breach test conditions Test P2- HET 4 CL



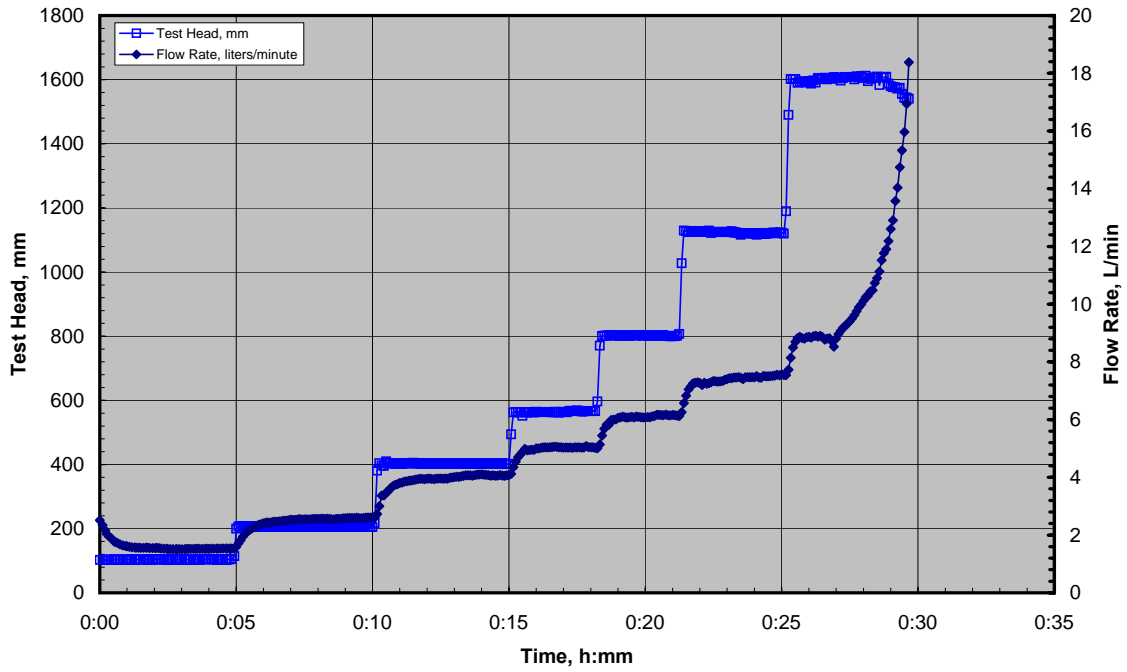
Bonelli Model - Dimensionless flow vs. Dimensionless Time



ERODS

HET Test Record

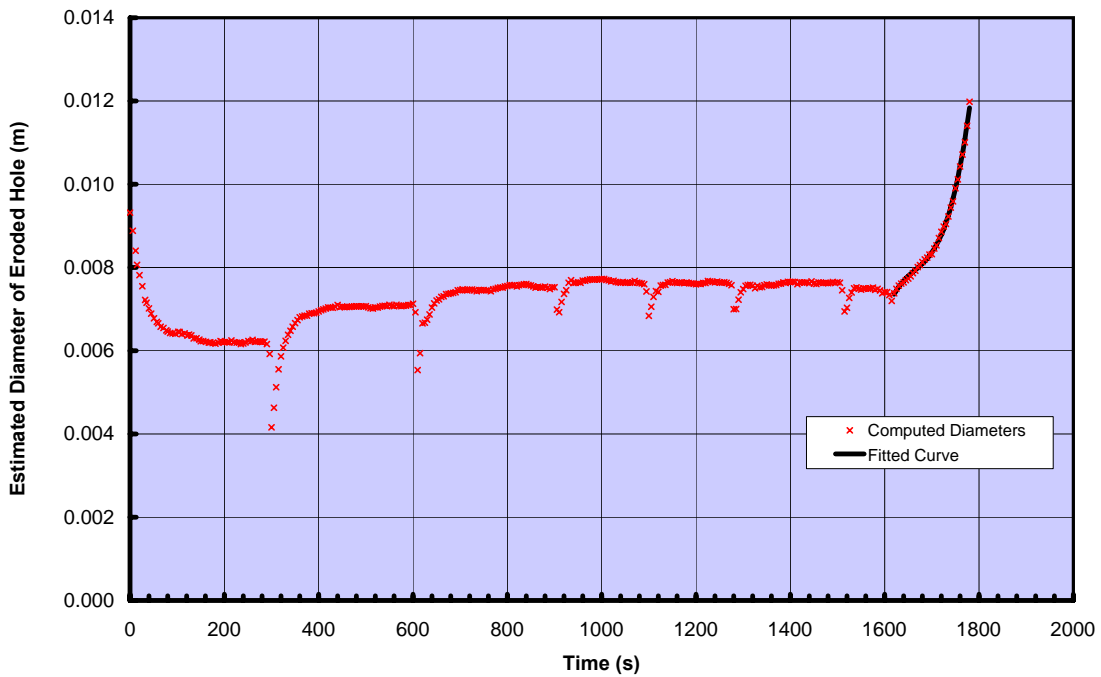
P2 at ARS breach-test conditions Test ARS-P2-HET 6 CL



ERODS

ESTIMATED DIAMETER OF ERODED HOLE

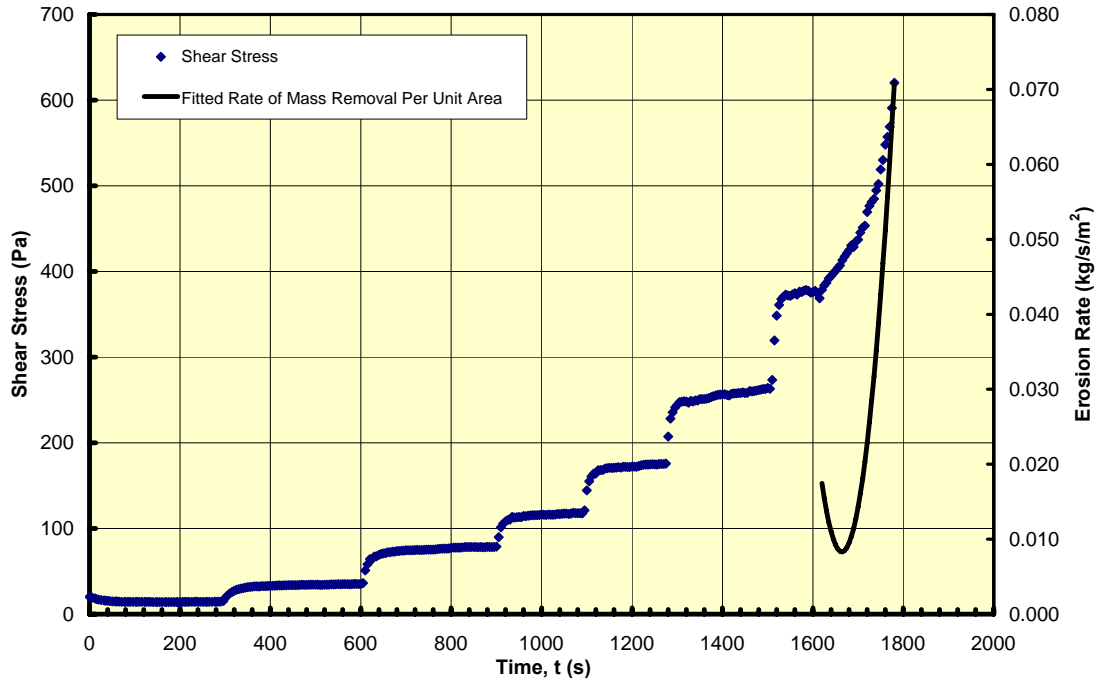
P2 at ARS breach-test conditions Test ARS-P2-HET 6 CL



ERODS

EROSION RATE AND SHEAR STRESS VS. TIME

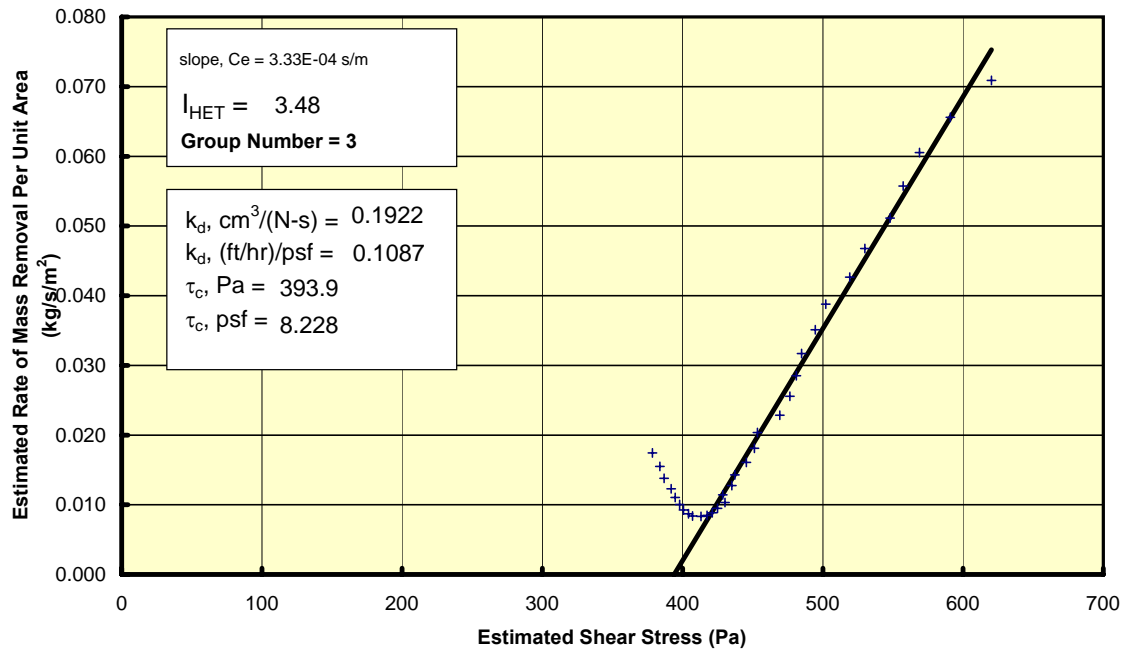
P2 at ARS breach-test conditions Test ARS-P2-HET 6 CL



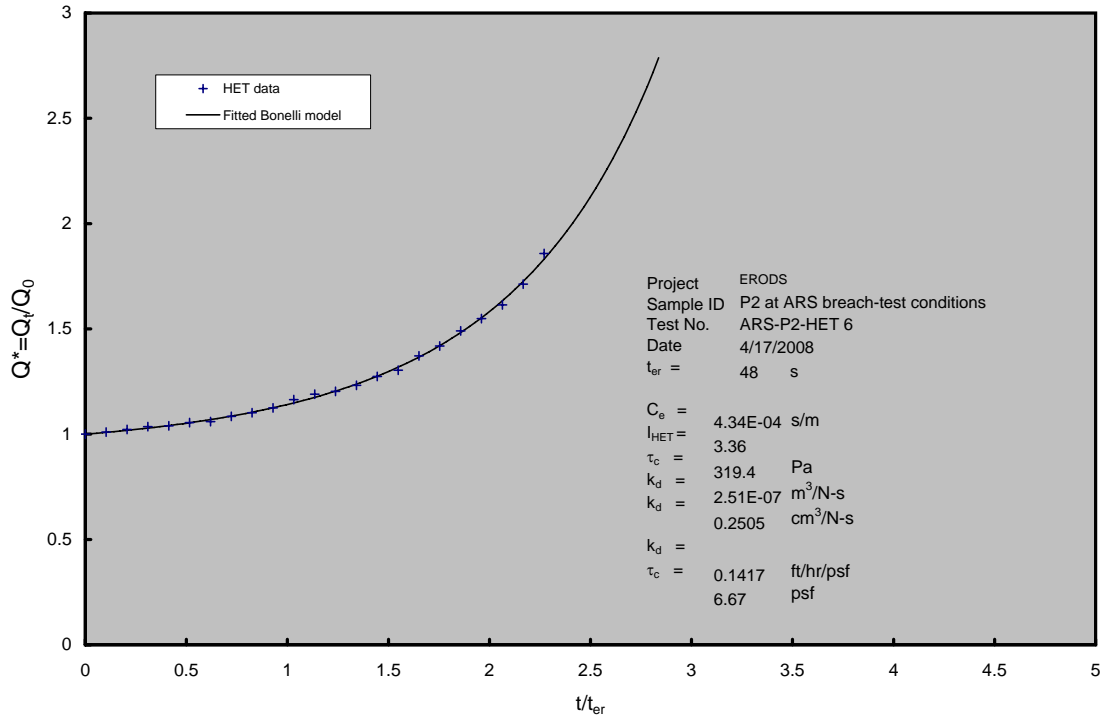
EROSION RATE VS. SHEAR STRESS

ERODS

P2 at ARS breach-test conditions Test ARS-P2-HET 6 CL



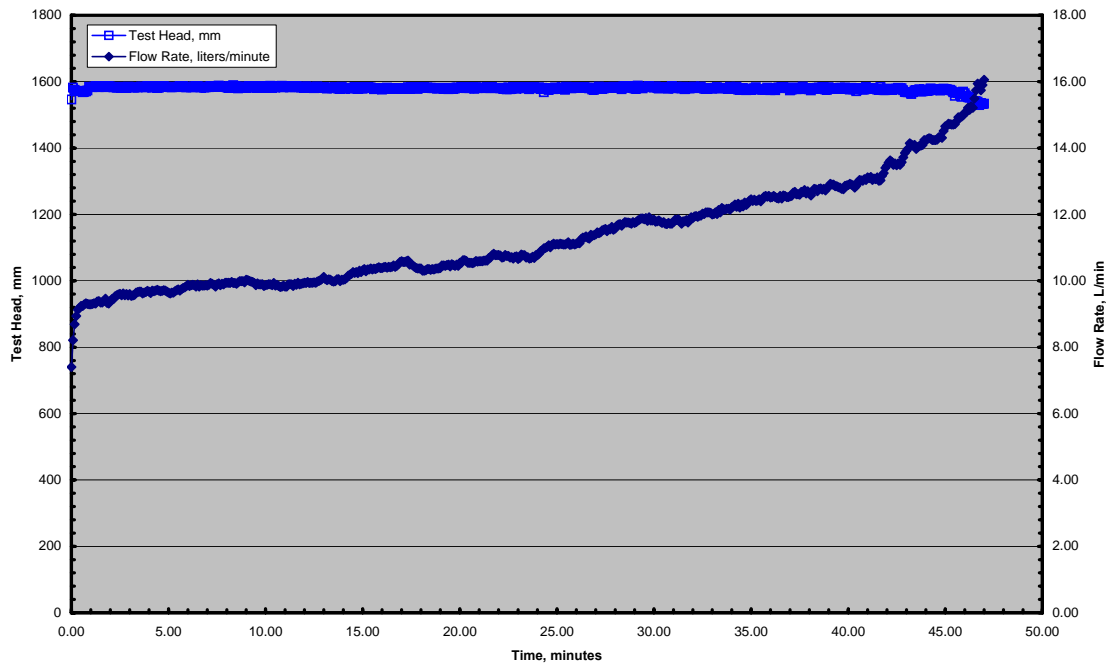
Bonelli Model - Dimensionless Flow vs. Dimensionless Time



ARS

Soil P3 Test P3 HET-2 01-22-2008

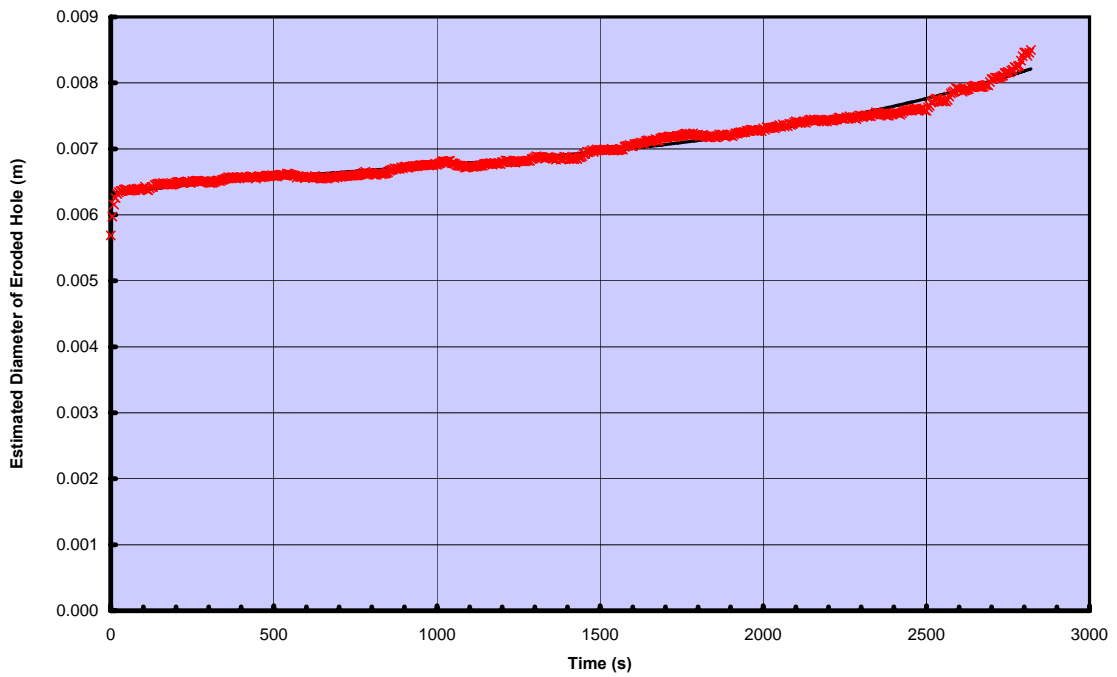
HET Test Record



ARS

Soil P3 Test P3 HET-2 01-22-2008

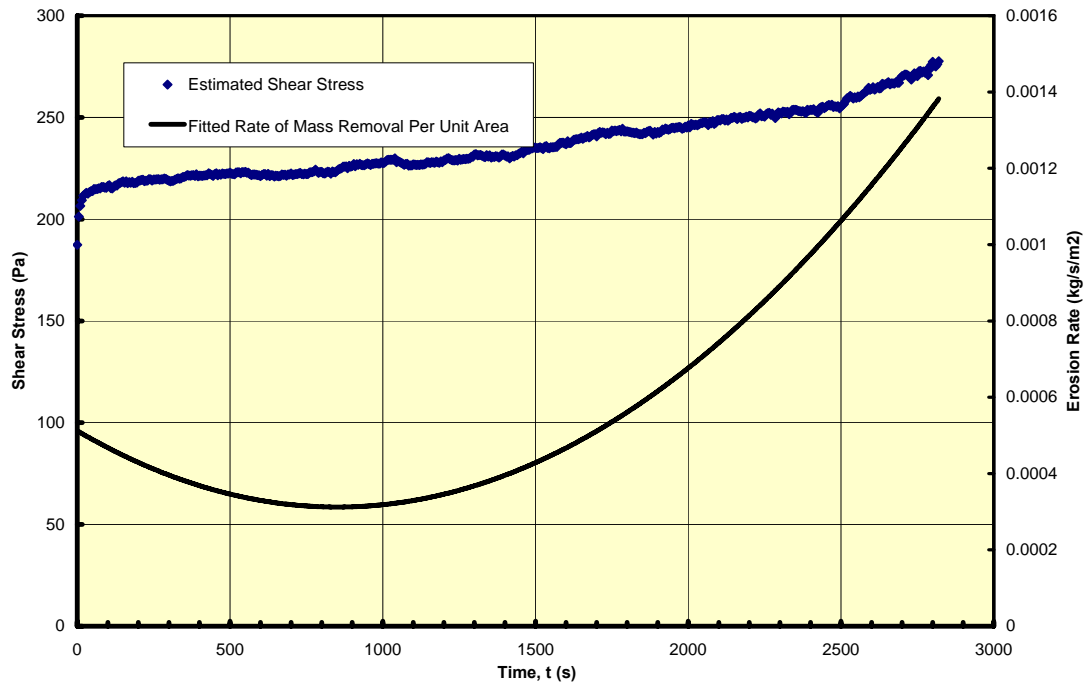
COMPUTED DIAMETER OF ERODED HOLE



ARS

Soil P3 Test P3 HET-2 01-22-2008

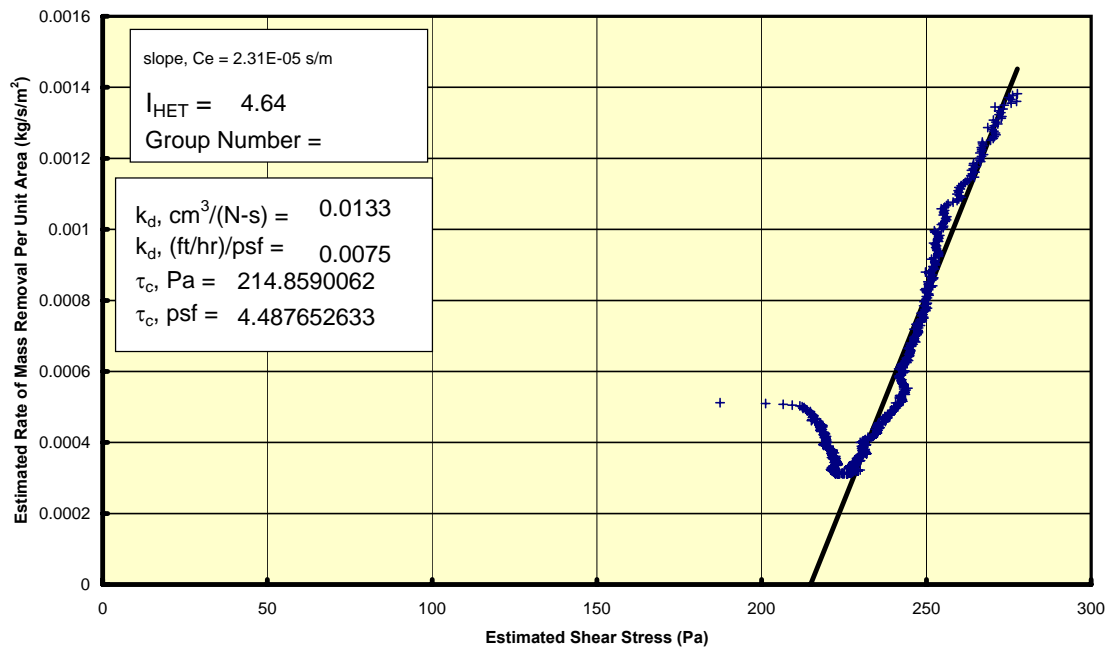
EROSION RATE AND SHEAR STRESS VS. TIME



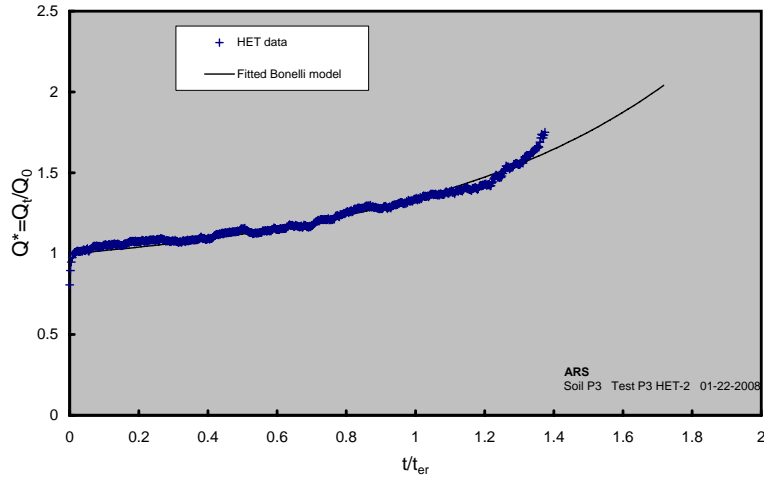
ARS

Soil P3 Test P3 HET-2 01-22-2008

EROSION RATE VS. SHEAR STRESS



HET dimensionless flow vs. dimensionless time
(Bonelli et al. 2006)



Project ARS
Feature Soil P3
Test P3 HET-2
Date 1/22/2008

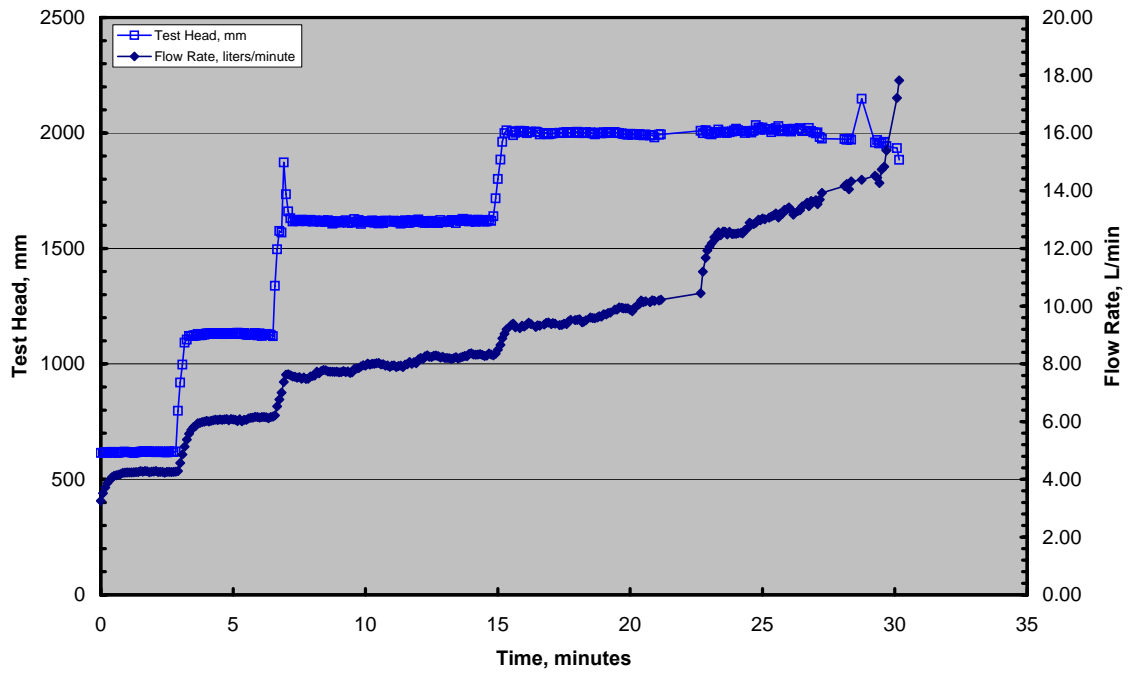
RESULTS SUMMARY

C_e	1.26E-05 ((kg/s)/m ²)/Pa = s/m	
l_{HET}	4.90	Group 4
τ_c	198.2 Pa	
k_d	7.243E-09 m/s/Pa = m ³ /(N-s)	
k_d	0.0072 cm ³ /(N-s)	
k_d	0.0041 (ft/hr)/psf	
τ_c	4.14 psf	

ARS

P3 Test 3 03-17-2008

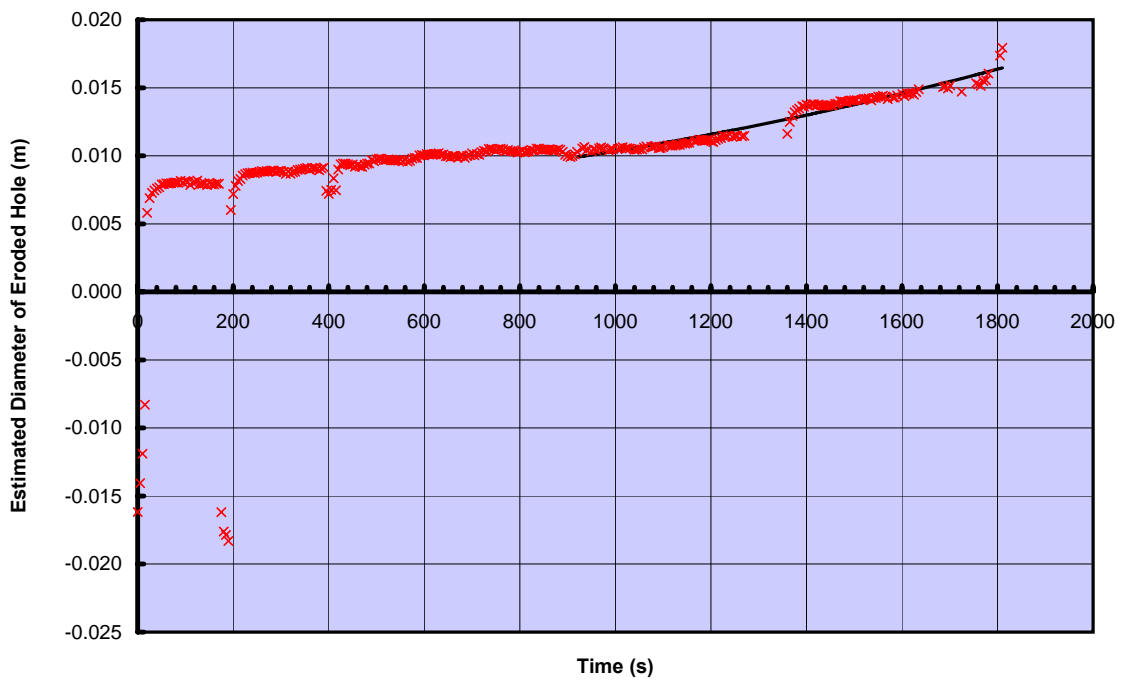
HET Test Record



ARS

P3 Test 3 03-17-2008

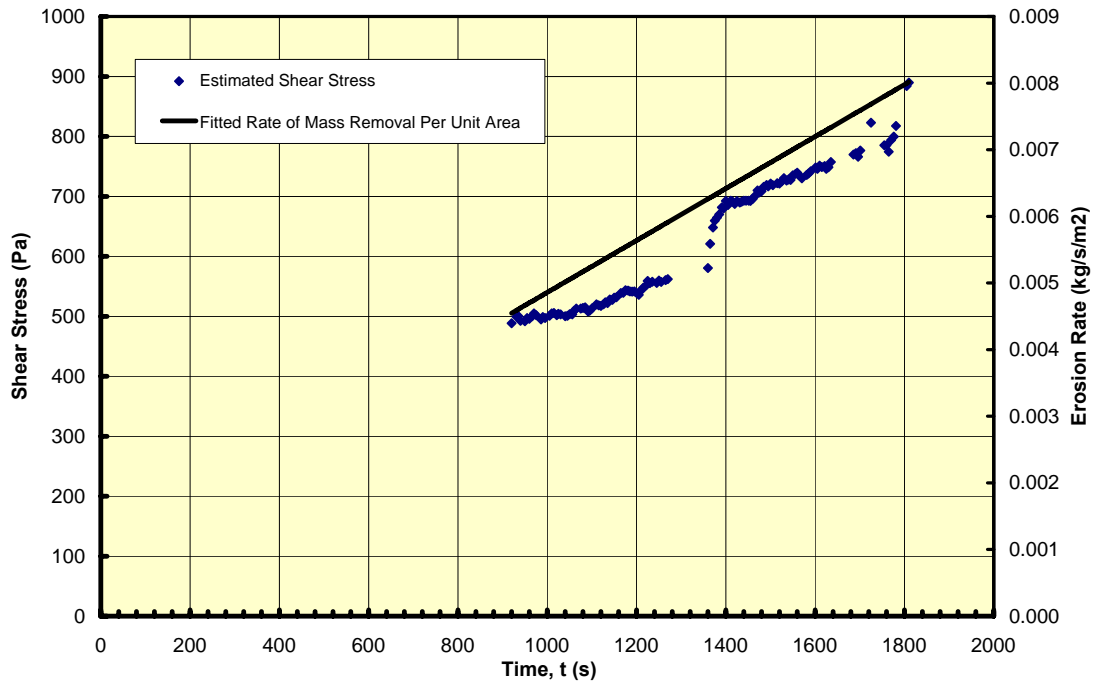
COMPUTED DIAMETER OF ERODED HOLE



ARS

P3 Test 3 03-17-2008

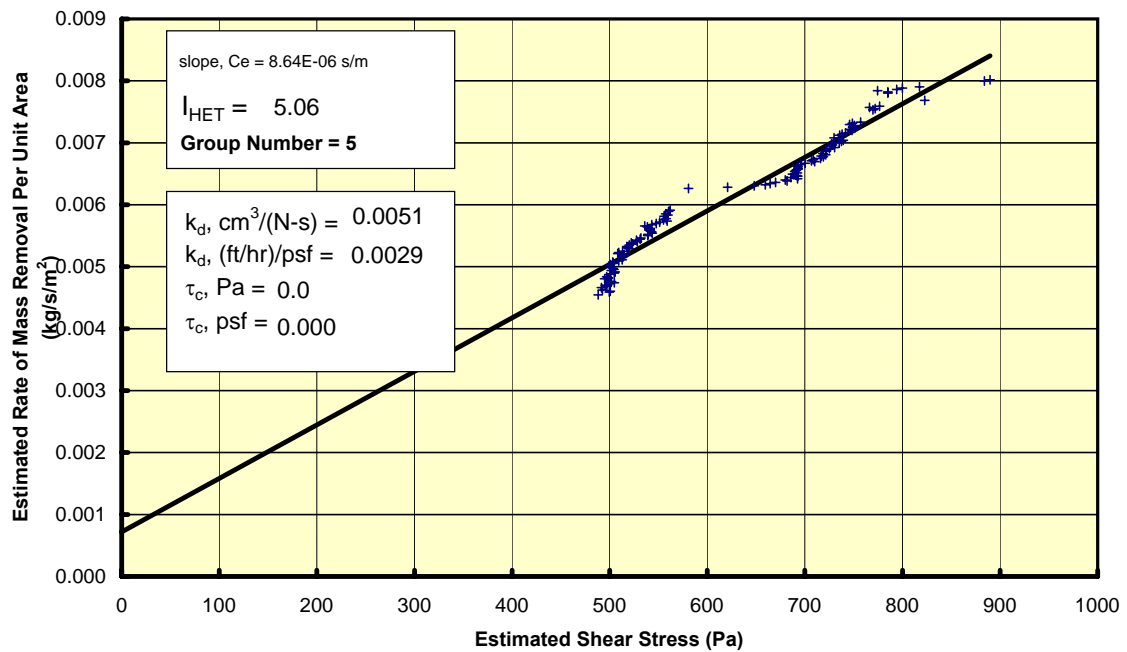
EROSION RATE AND SHEAR STRESS VS. TIME



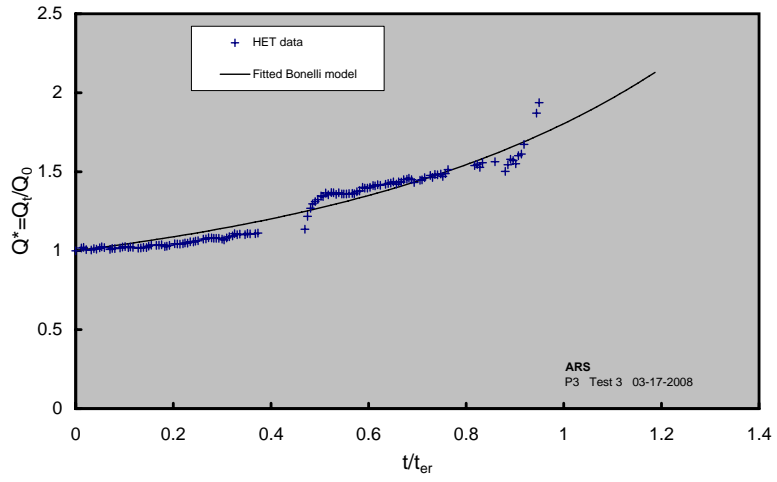
ARS

P3 Test 3 03-17-2008

EROSION RATE VS. SHEAR STRESS



HET dimensionless flow vs. dimensionless time
(Bonelli et al. 2006)



Project ARS
Feature P3
Test 3
Date 3/17/2008

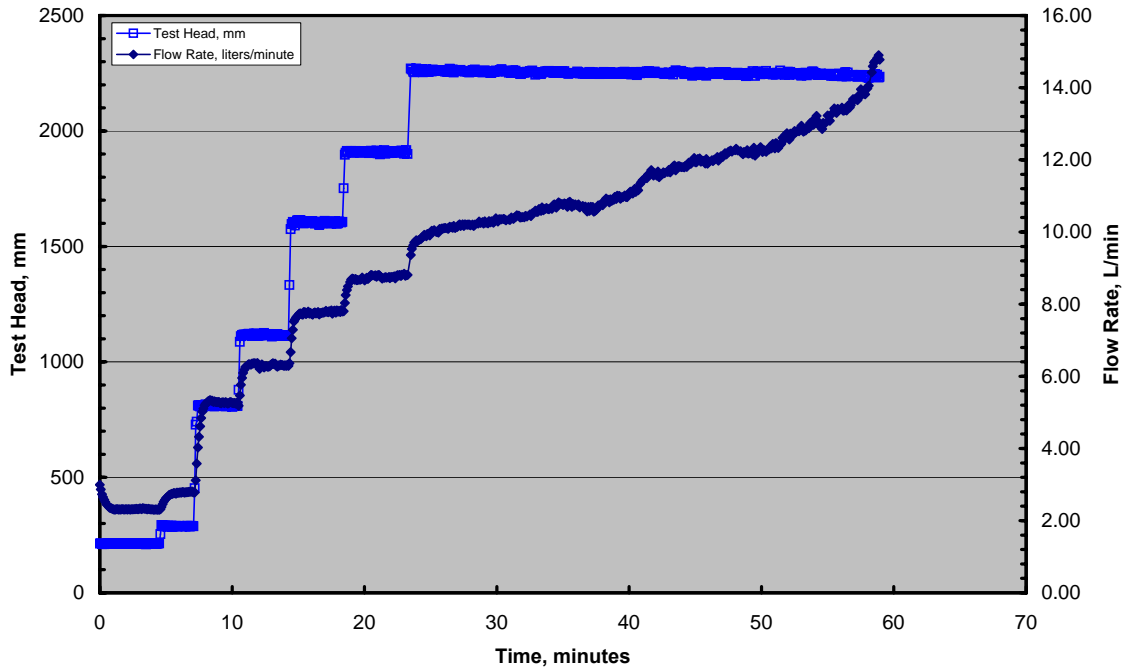
RESULTS SUMMARY

C_e	1.93E-05 ((kg/s)/m ²)/Pa = s/m	
l_{HET}	4.71	Group 4
τ_c	402.0 Pa	
k_d	1.133E-08 m/s/Pa = m ³ /(N-s)	
k_d	0.0113 cm ³ /(N-s)	
k_d	0.0064 (ft/hr)/psf	
τ_c	8.40 psf	

ARS

HET Test Record

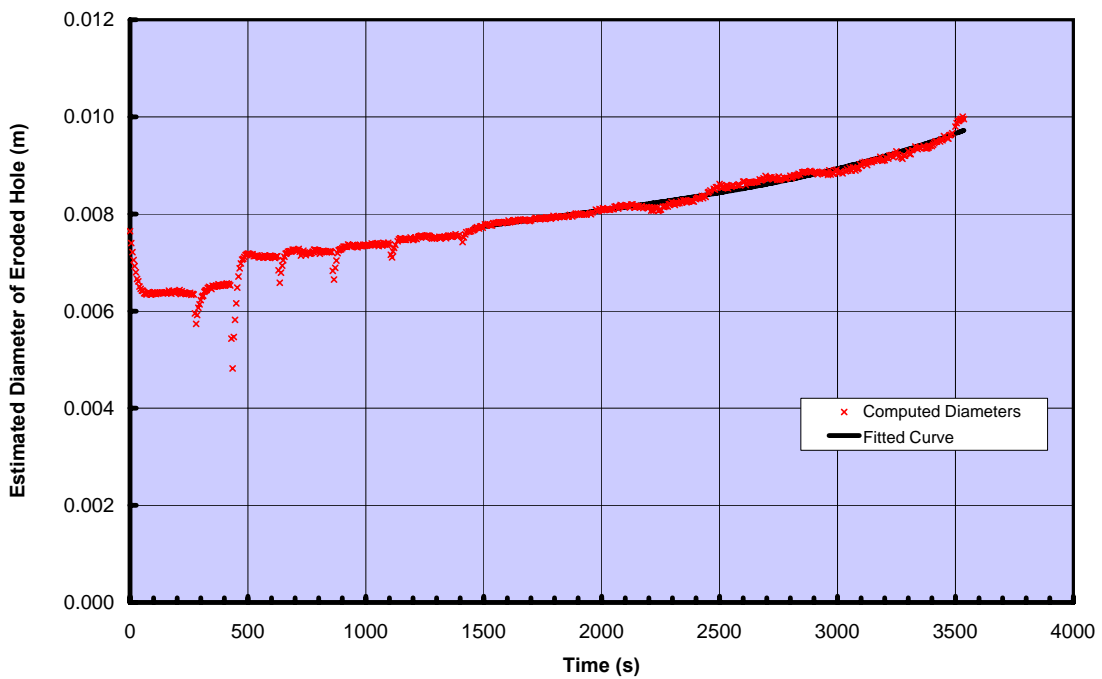
P3 at breach test conditions (targeting 111 pcf, 15.4% m.c.) Test P3 - HET 4 CL



ARS

COMPUTED DIAMETER OF ERODED HOLE

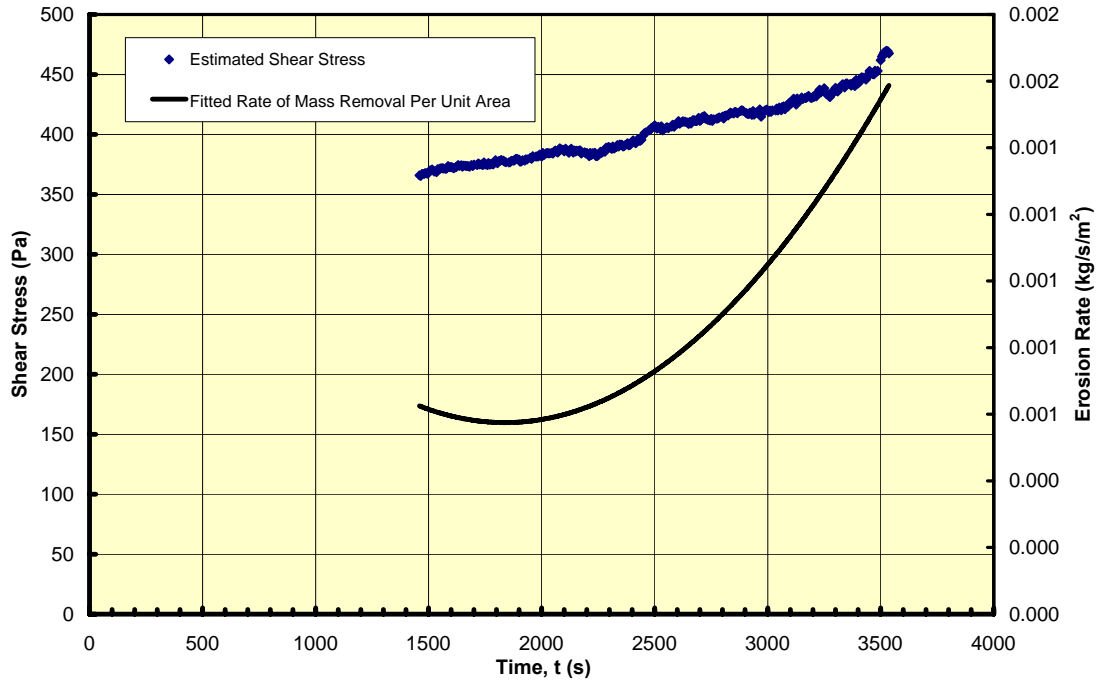
P3 at breach test conditions (targeting 111 pcf, 15.4% m.c.) Test P3 - HET 4 CL



ARS

EROSION RATE AND SHEAR STRESS VS. TIME

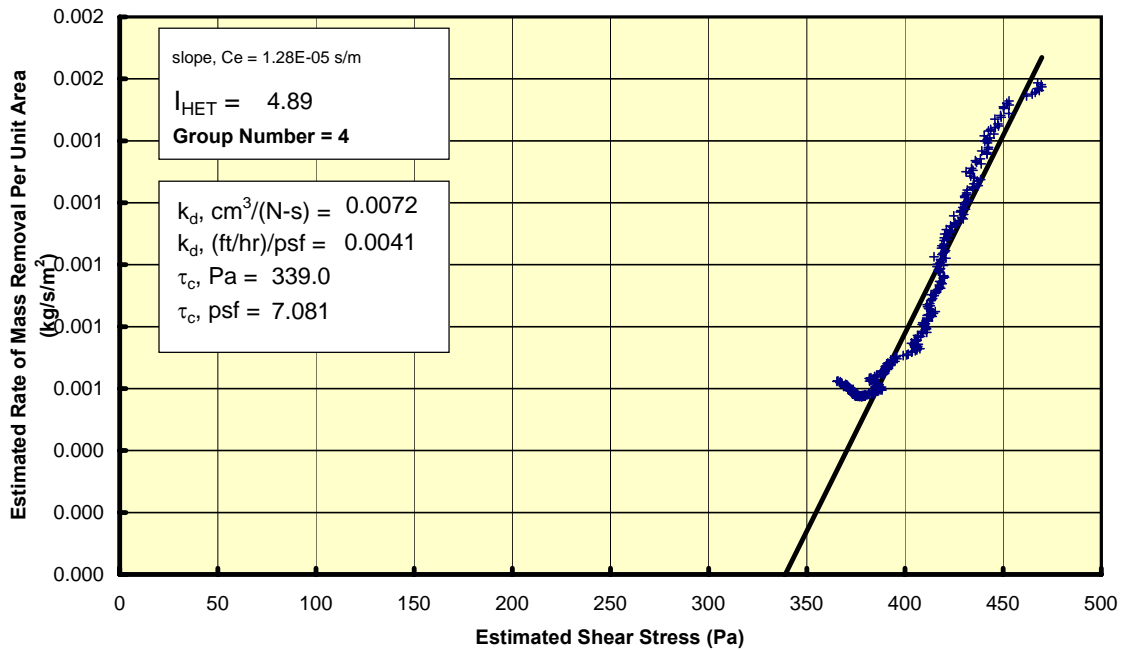
P3 at breach test conditions (targeting 111 pcf, 15.4% m.c.) Test P3 - HET 4 CL



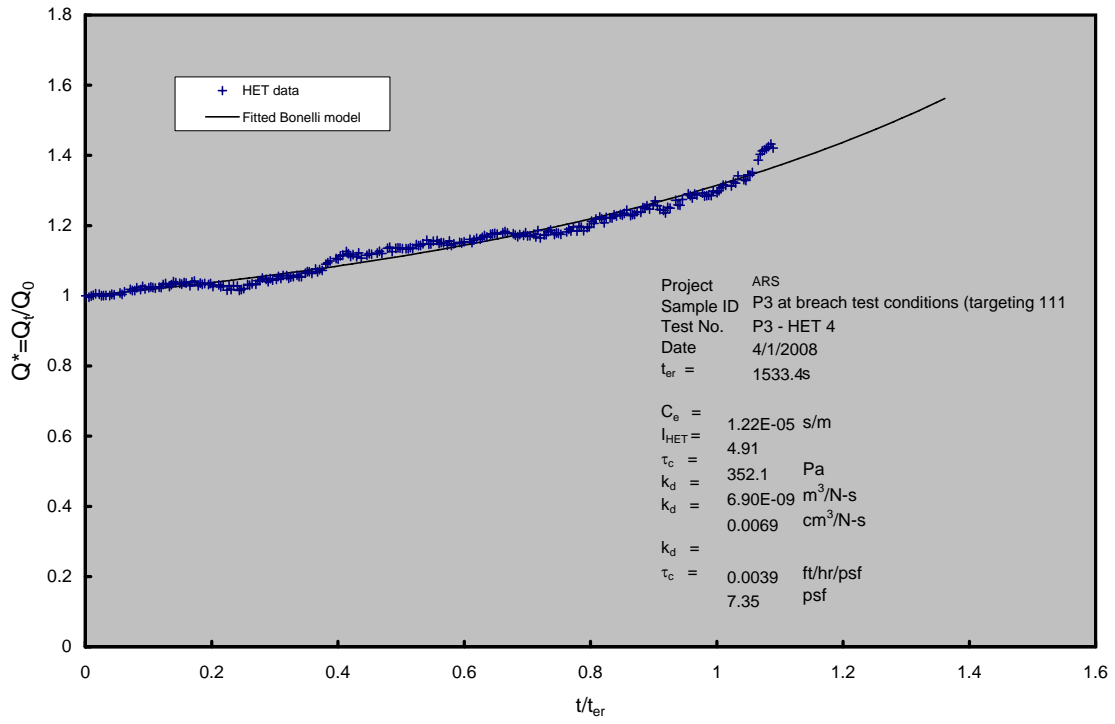
ARS

EROSION RATE VS. SHEAR STRESS

P3 at breach test conditions (targeting 111 pcf, 15.4% m.c.) Test P3 - HET 4 CL



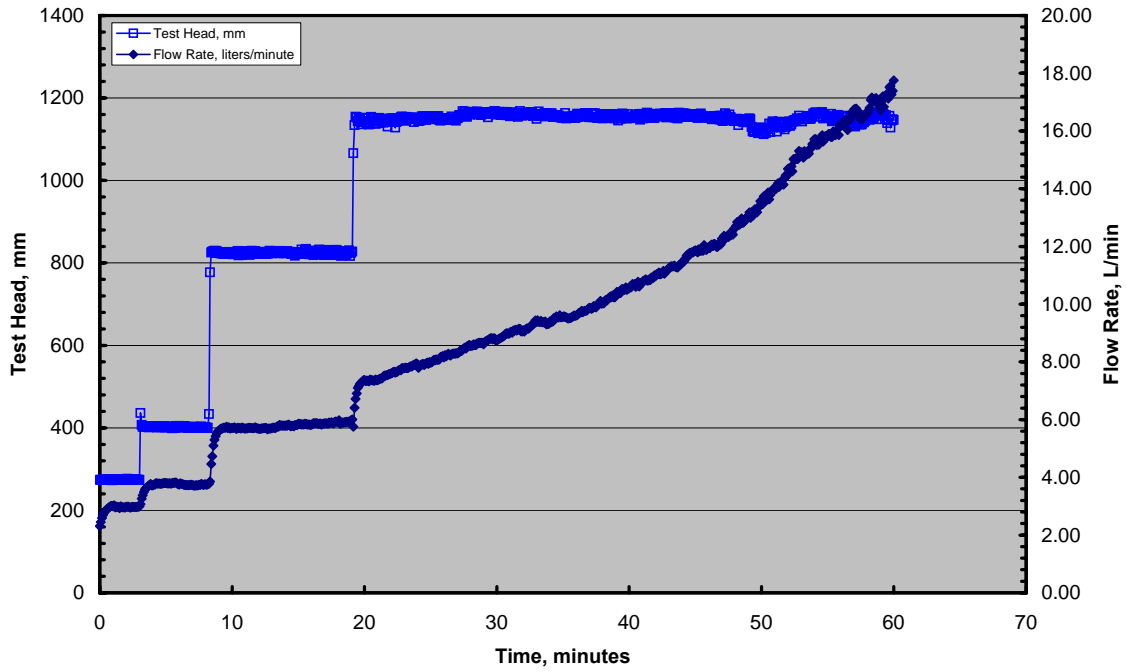
Bonelli Model - Dimensionless flow vs. Dimensionless Time



ERODS - ARS

HET Test Record

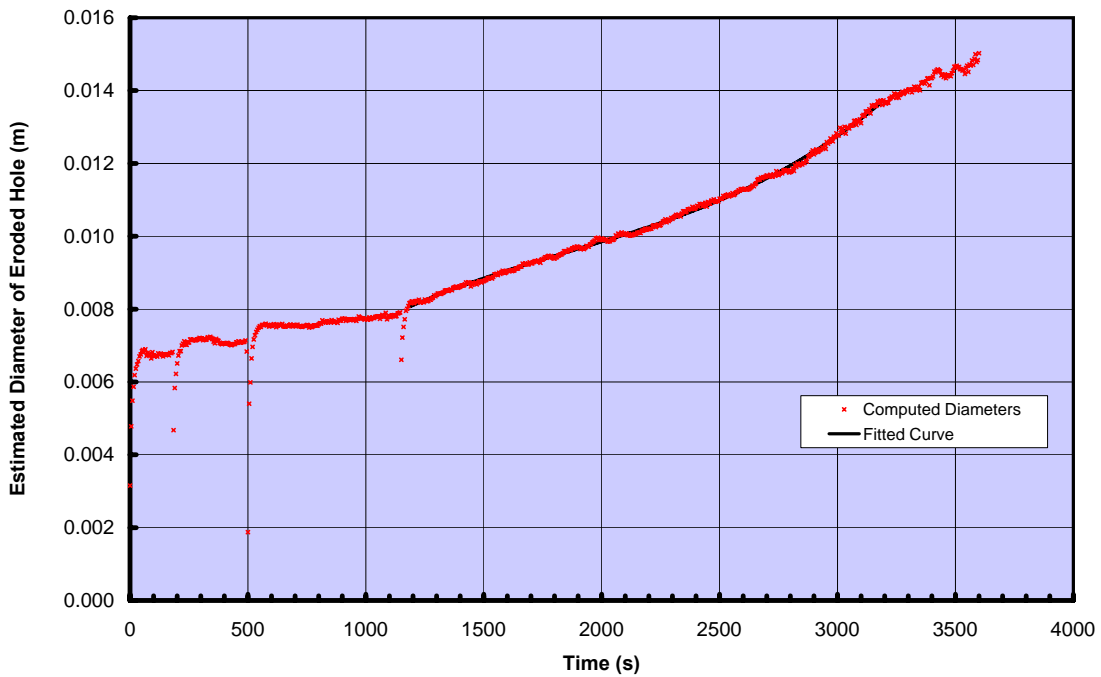
ARS P3 at breach-test conditions Test ARS-P3-HET 5 Lean Clay - CL



ERODS - ARS

COMPUTED DIAMETER OF ERODED HOLE

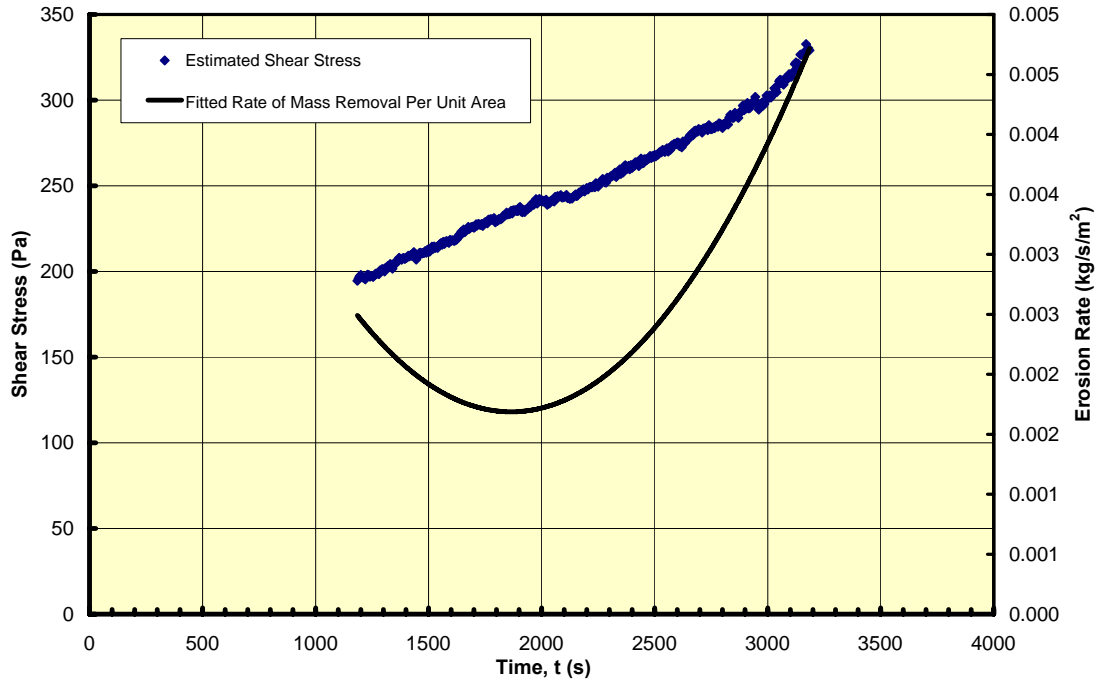
ARS P3 at breach-test conditions Test ARS-P3-HET 5 Lean Clay - CL



ERODS - ARS

EROSION RATE AND SHEAR STRESS VS. TIME

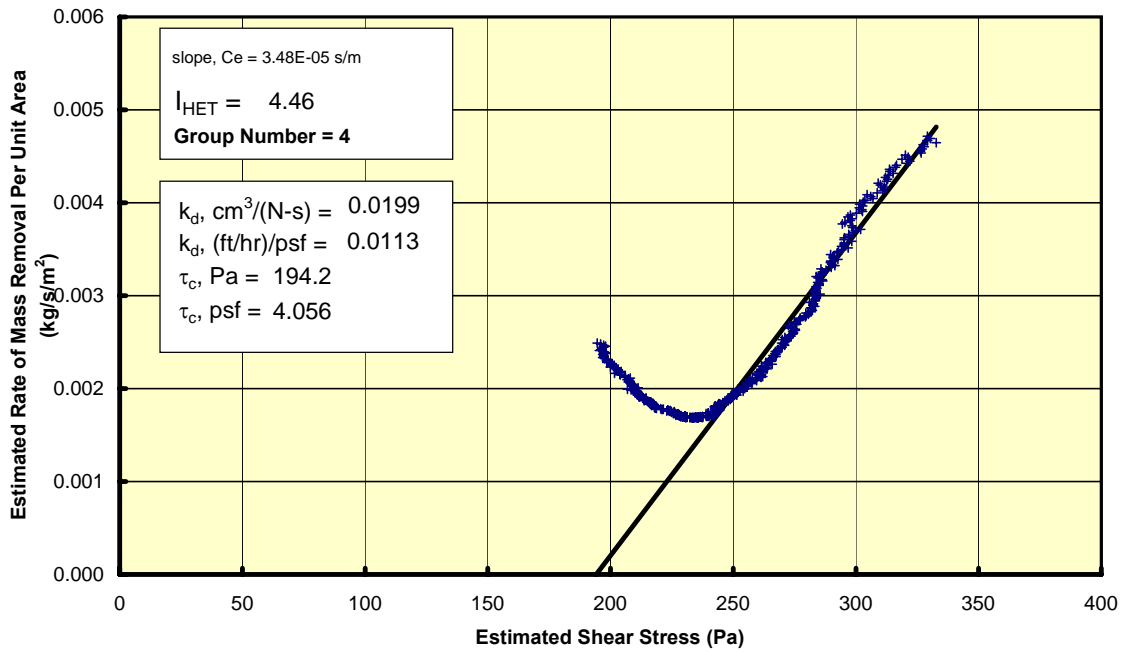
ARS P3 at breach-test conditions Test ARS-P3-HET 5 Lean Clay - CL



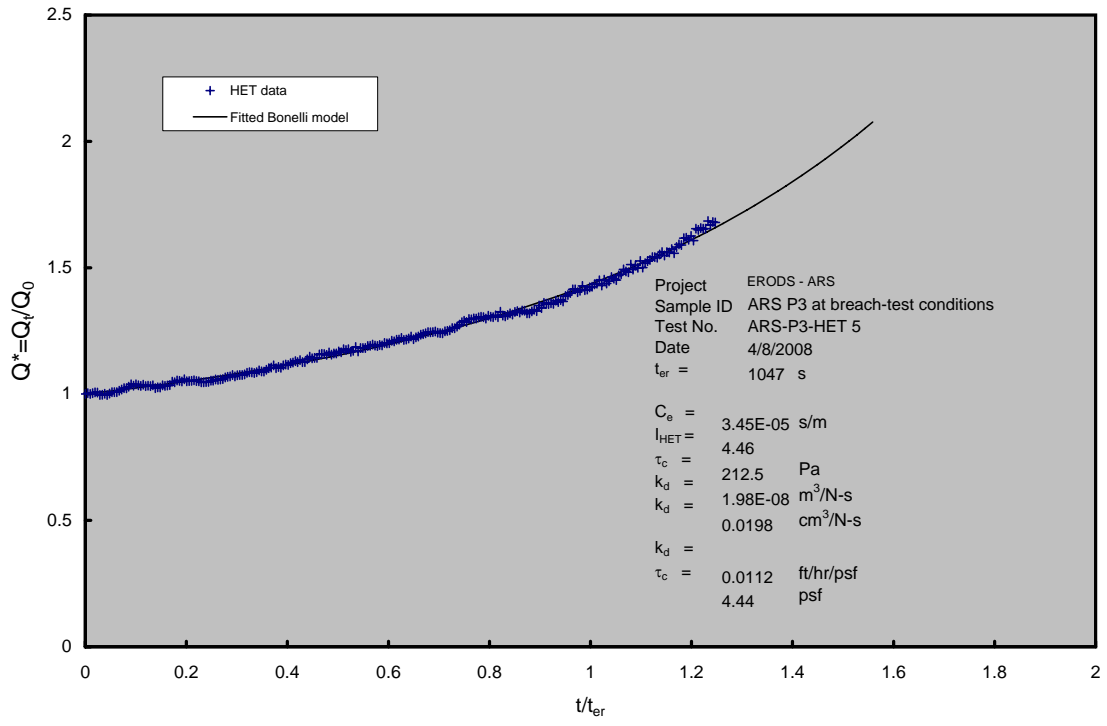
ERODS - ARS

EROSION RATE VS. SHEAR STRESS

ARS P3 at breach-test conditions Test ARS-P3-HET 5 Lean Clay - CL



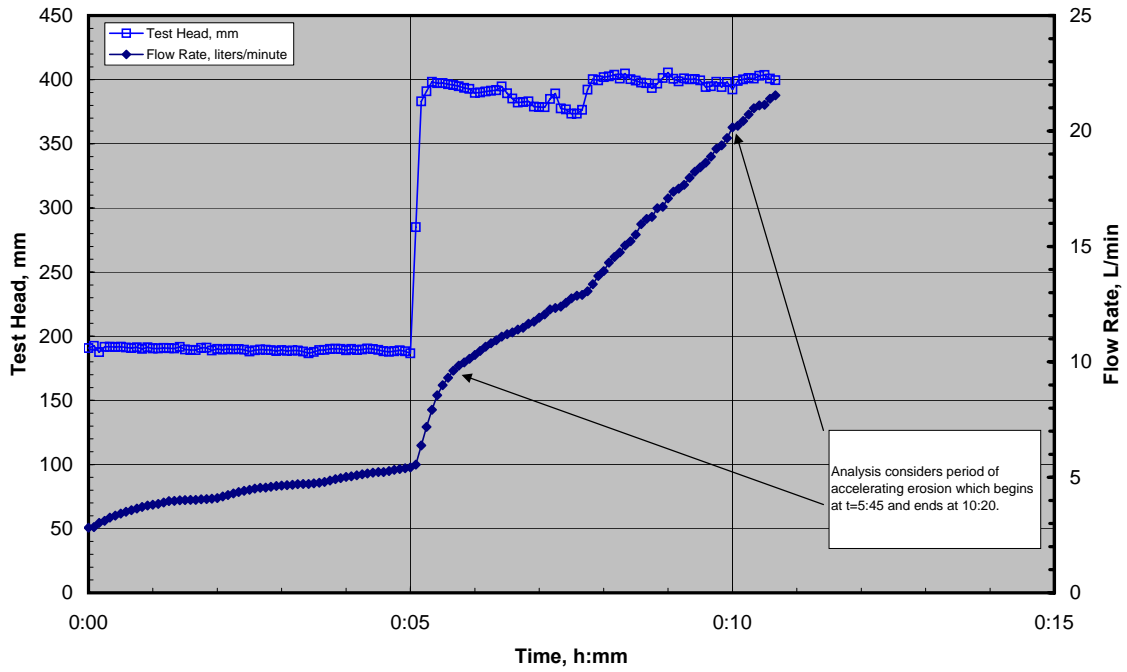
Bonelli Model - Dimensionless flow vs. Dimensionless Time



ERODS Phase 2

HET Test Record

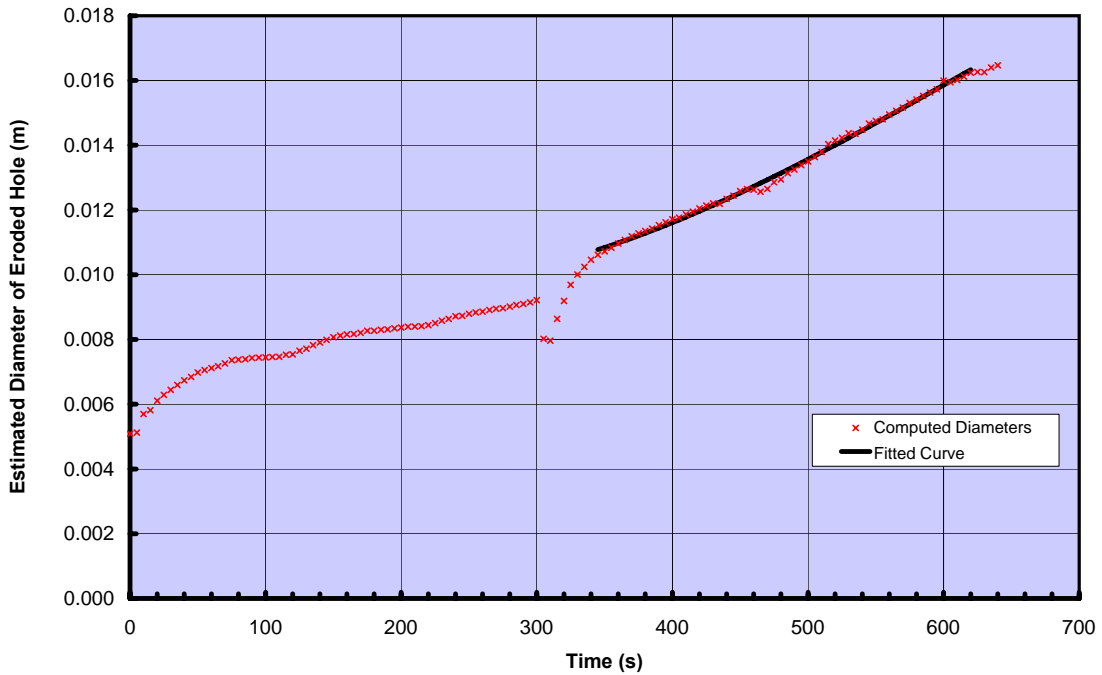
ARS-P2-HET, -4% Test ARS-P2-HET, -4% 09-15-2008



ERODS Phase 2

ESTIMATED DIAMETER OF ERODED HOLE

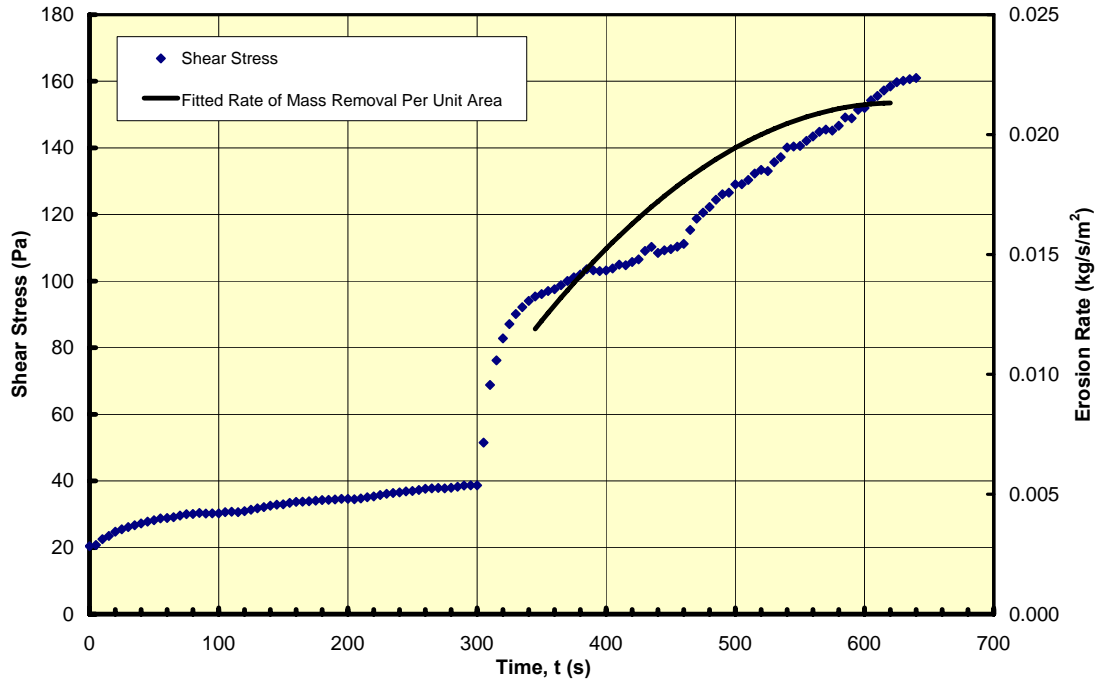
ARS-P2-HET, -4% Test ARS-P2-HET, -4% 09-15-2008



ERODS Phase 2

EROSION RATE AND SHEAR STRESS VS. TIME

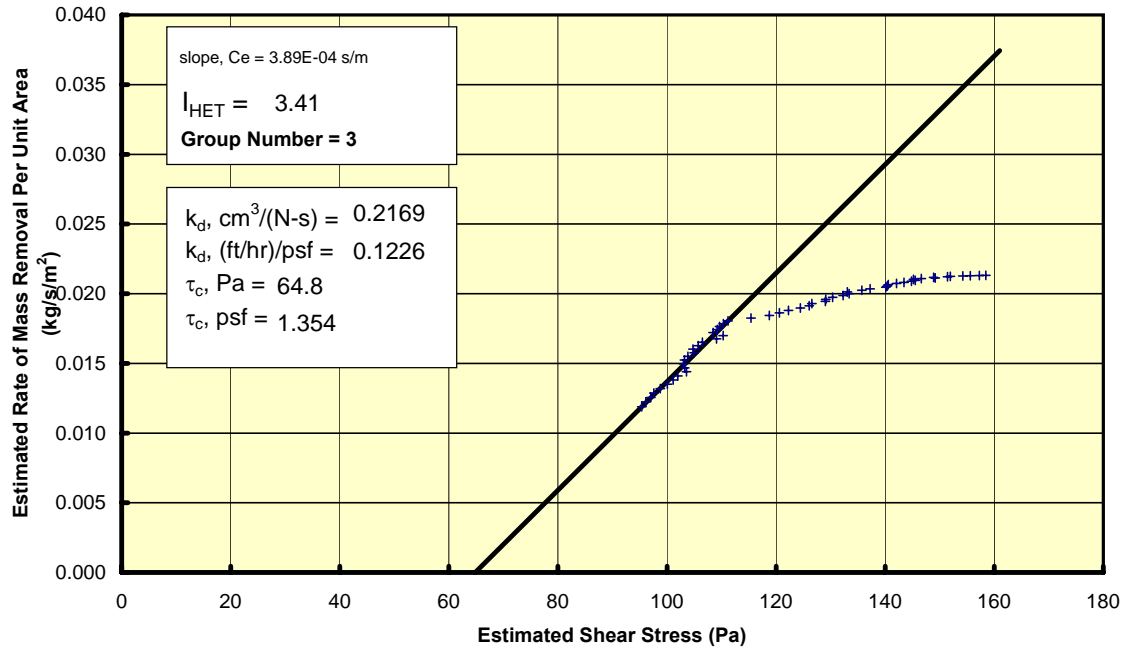
ARS-P2-HET, -4% Test ARS-P2-HET, -4% 09-15-2008



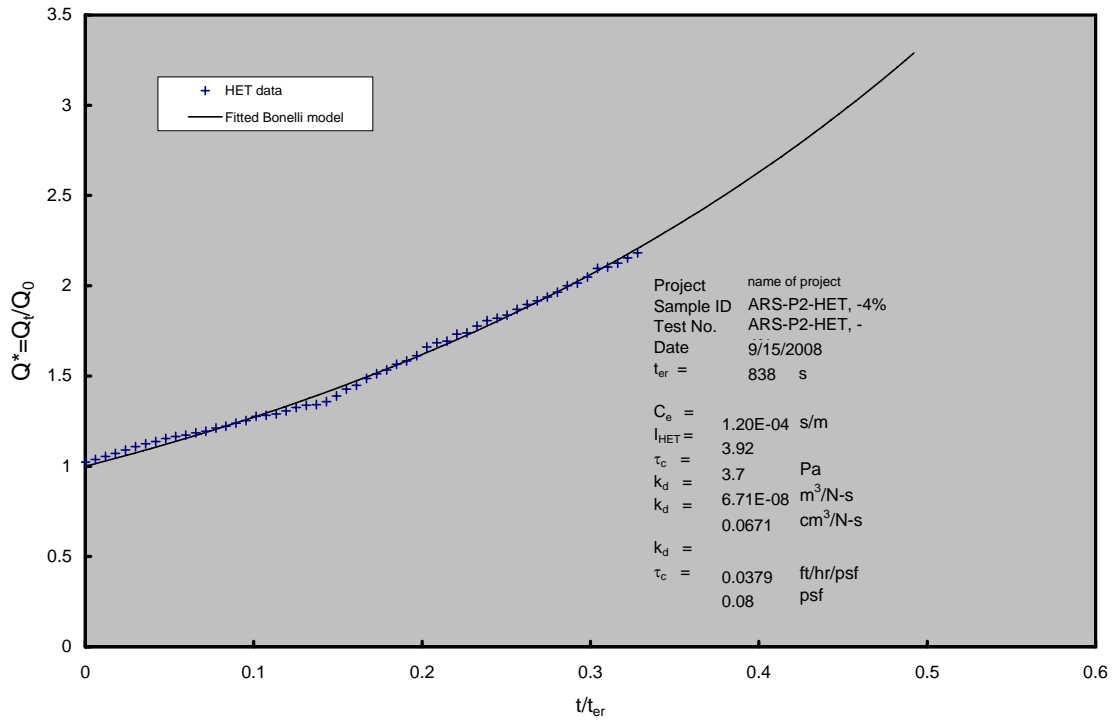
EROSION RATE VS. SHEAR STRESS

ERODS Phase 2

ARS-P2-HET, -4% Test ARS-P2-HET, -4% 09-15-2008



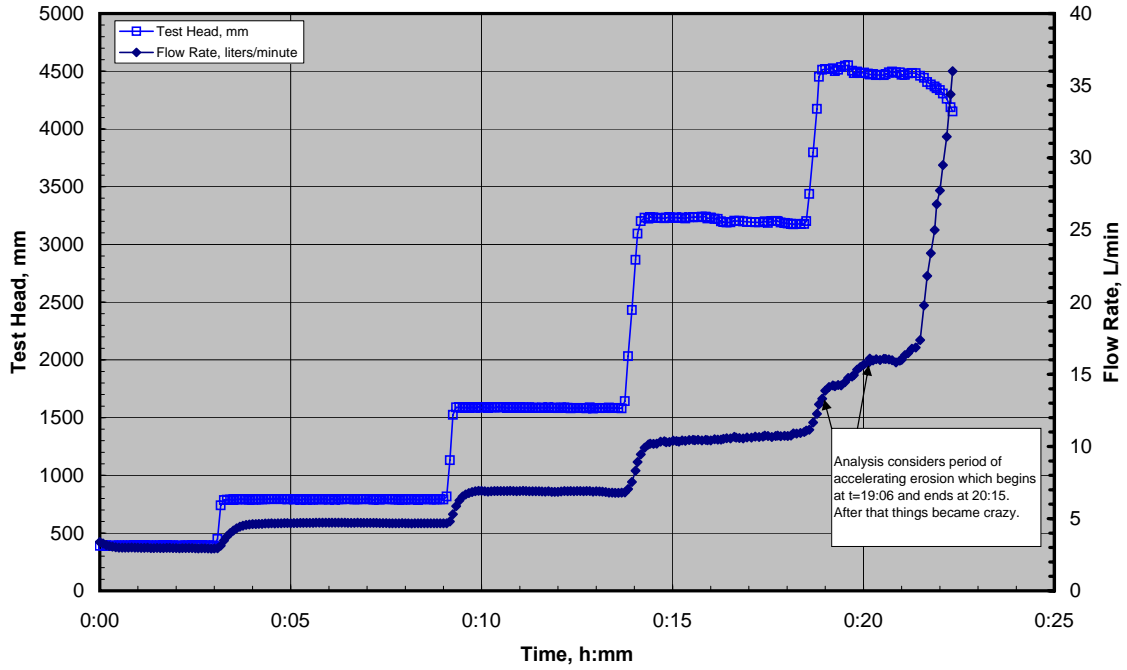
Bonelli Model - Dimensionless Flow vs. Dimensionless Time



ERODS - ARS Phase 2

HET Test Record

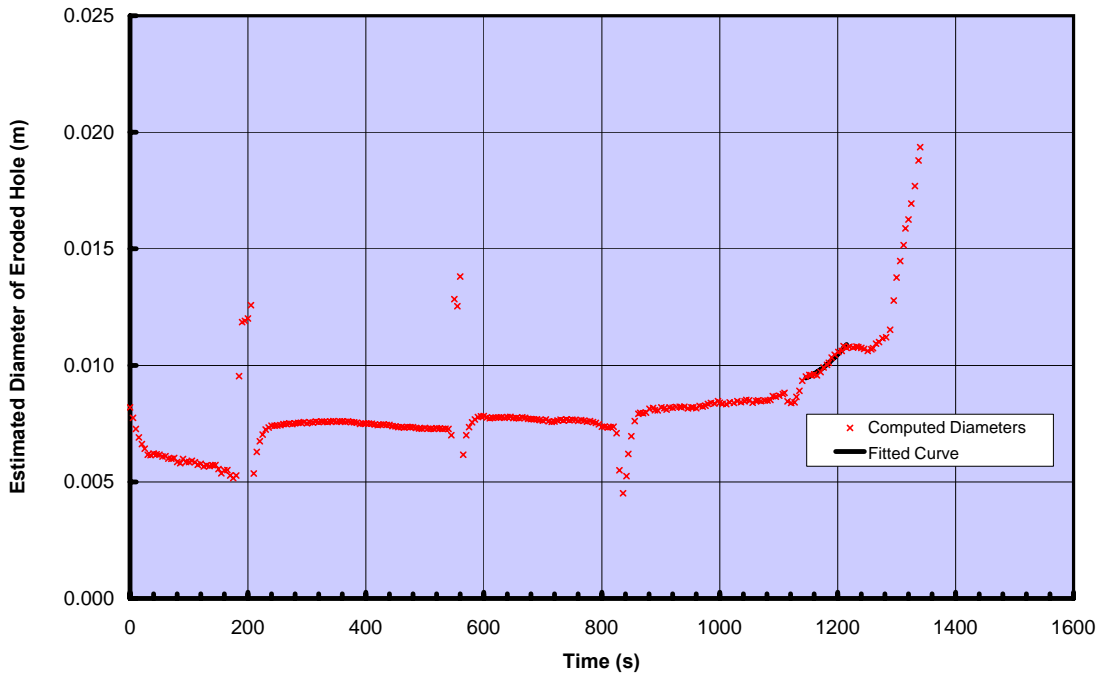
ARS-P2-HET-25, -2% Test ARS-P2-HET-25, -2% 08-27-2008



ERODS - ARS Phase 2

ESTIMATED DIAMETER OF ERODED HOLE

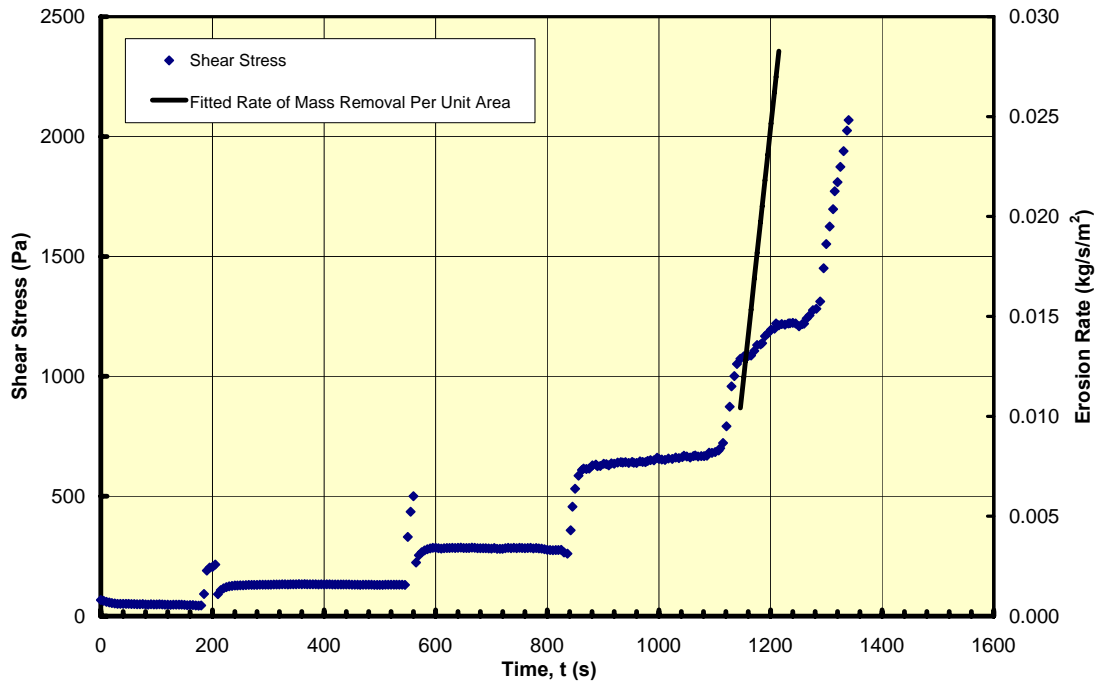
ARS-P2-HET-25, -2% Test ARS-P2-HET-25, -2% 08-27-2008



ERODS - ARS Phase 2

EROSION RATE AND SHEAR STRESS VS. TIME

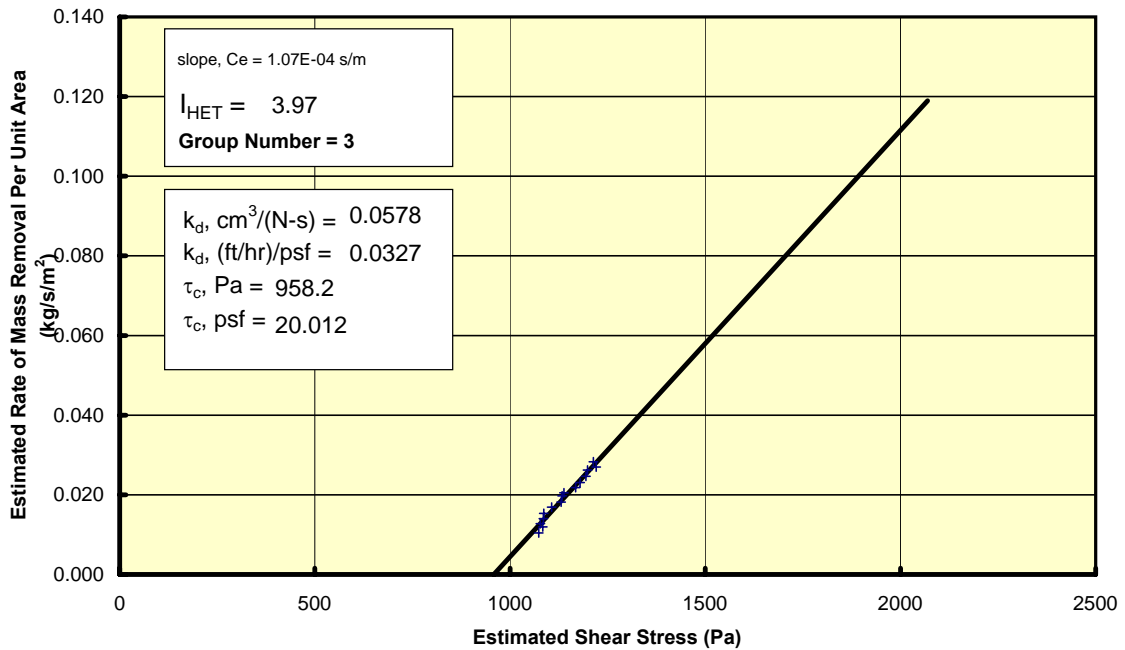
ARS-P2-HET-25, -2% Test ARS-P2-HET-25, -2% 08-27-2008



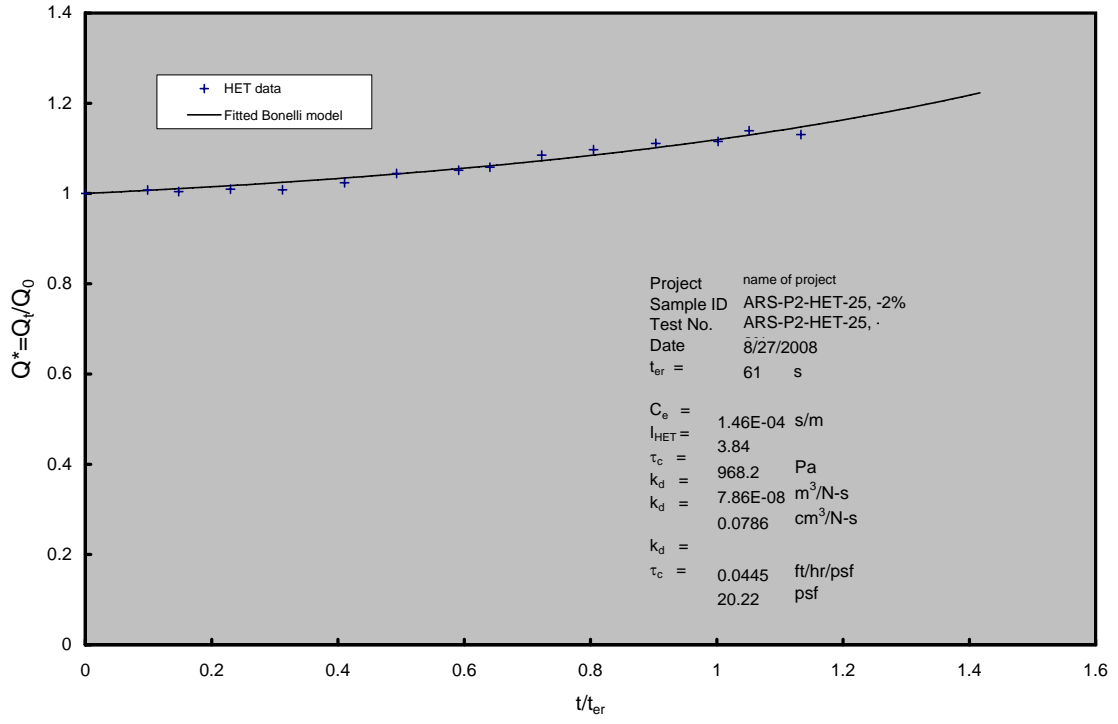
EROSION RATE VS. SHEAR STRESS

ERODS - ARS Phase 2

ARS-P2-HET-25, -2% Test ARS-P2-HET-25, -2% 08-27-2008



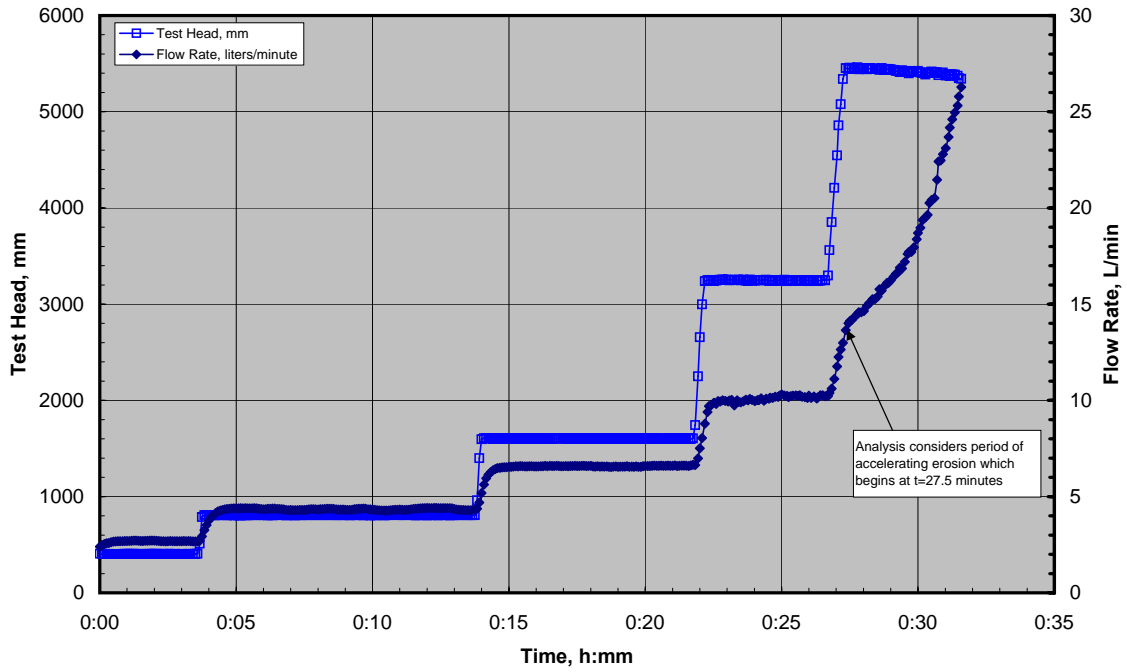
Bonelli Model - Dimensionless Flow vs. Dimensionless Time



ERODS phase 2

HET Test Record

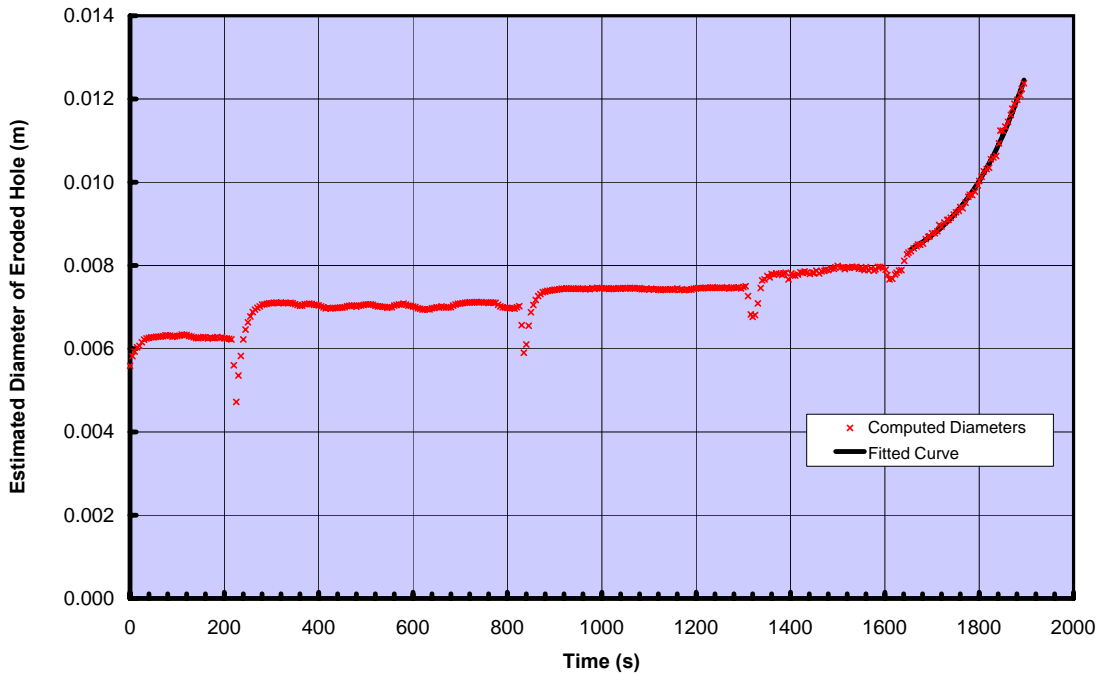
P2 @ OMC Test ARS-P2-HET-25-OMC 08-27-2008



ERODS phase 2

ESTIMATED DIAMETER OF ERODED HOLE

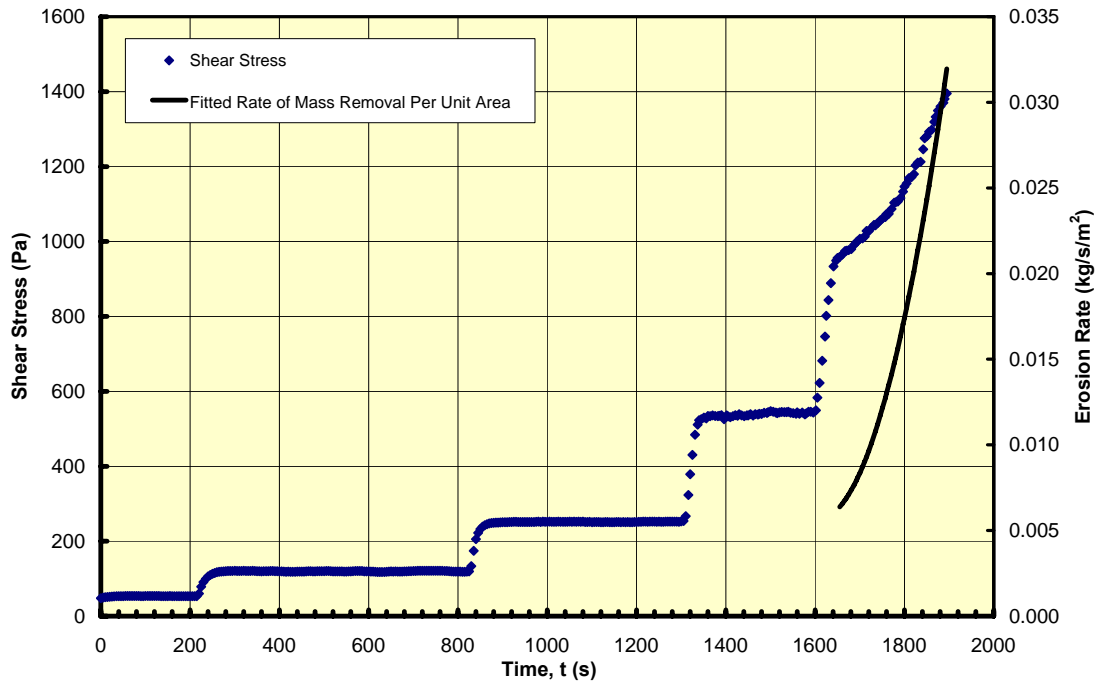
P2 @ OMC Test ARS-P2-HET-25-OMC 08-27-2008



ERODS phase 2

EROSION RATE AND SHEAR STRESS VS. TIME

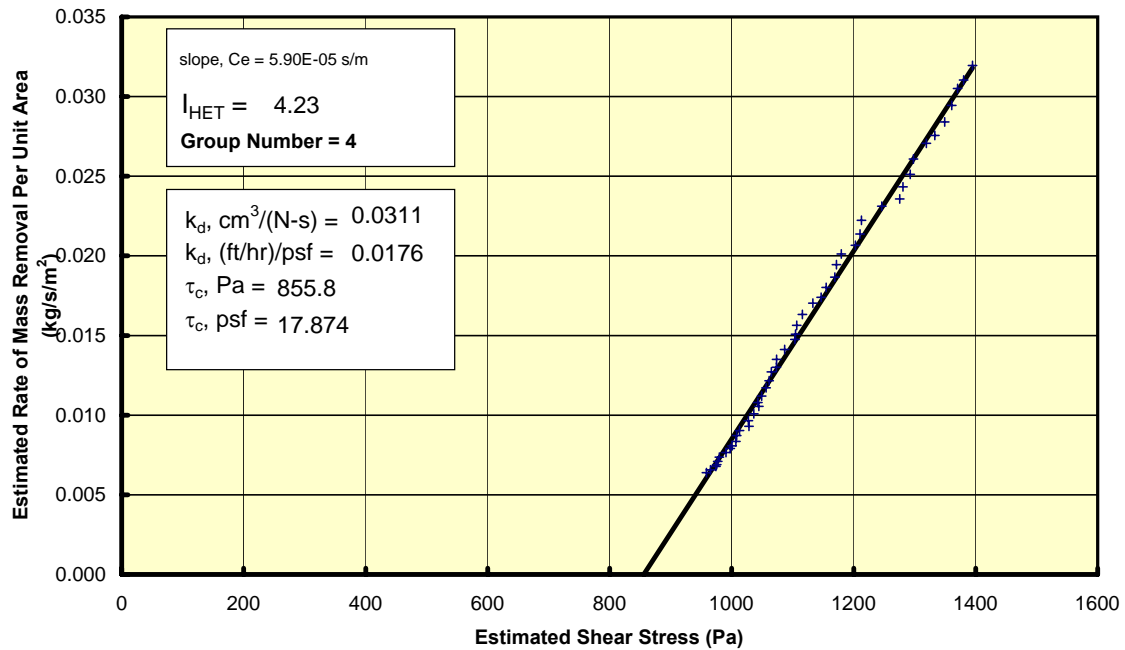
P2 @ OMC Test ARS-P2-HET-25-OMC 08-27-2008



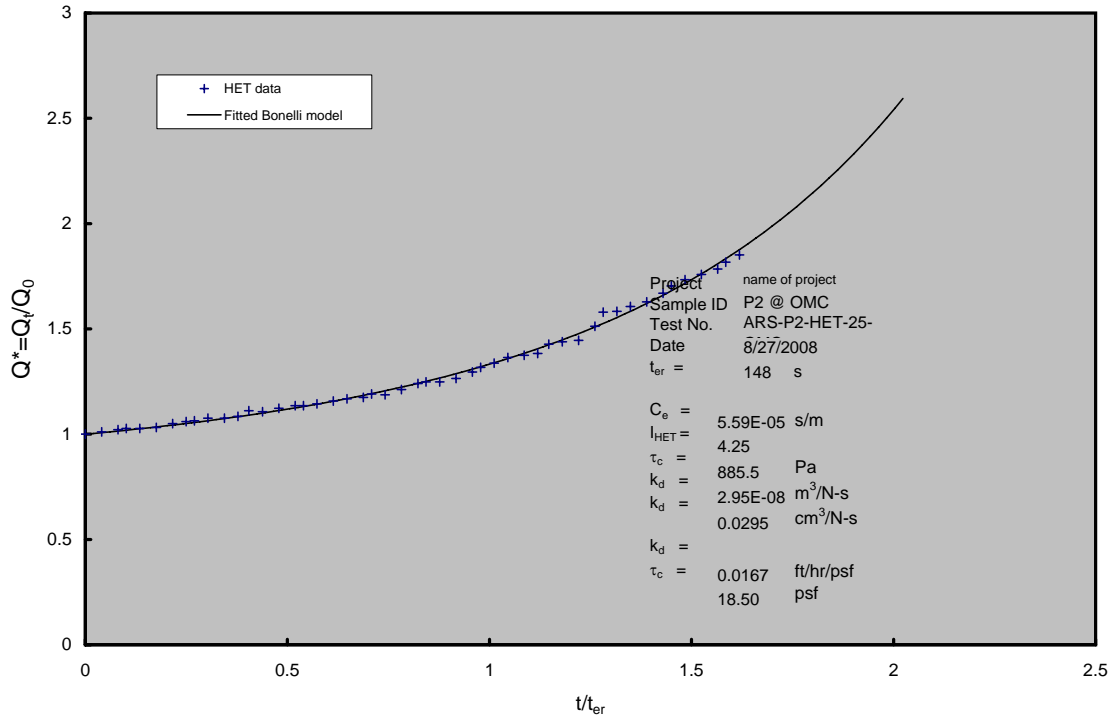
EROSION RATE VS. SHEAR STRESS

ERODS phase 2

P2 @ OMC Test ARS-P2-HET-25-OMC 08-27-2008



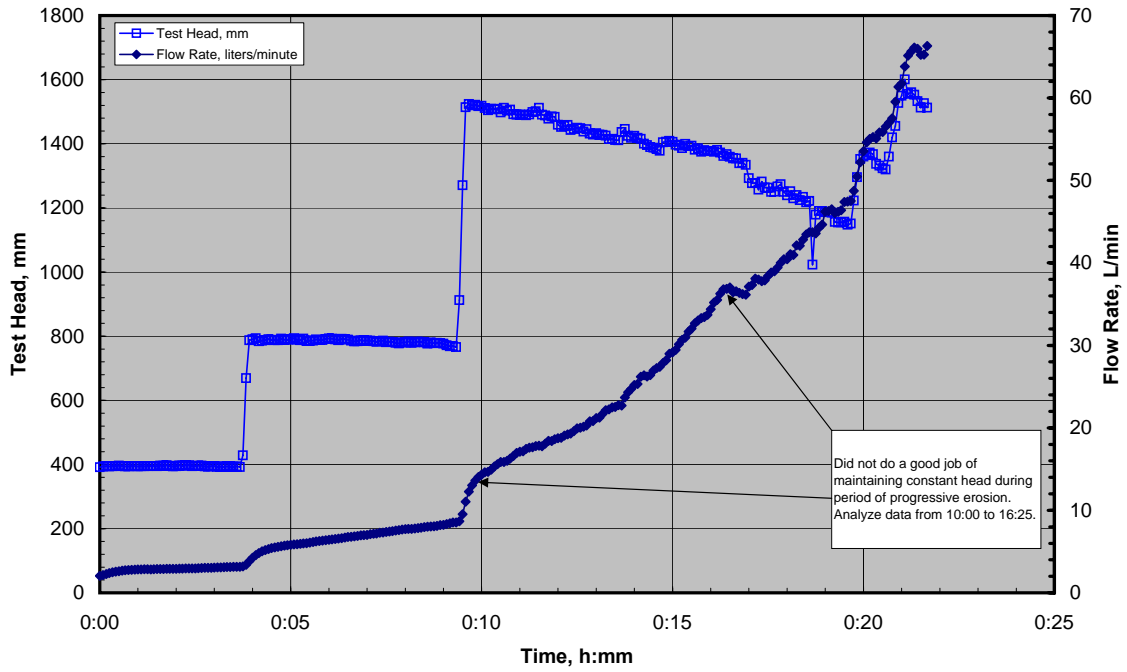
Bonelli Model - Dimensionless Flow vs. Dimensionless Time



ERODS Phase 2

HET Test Record

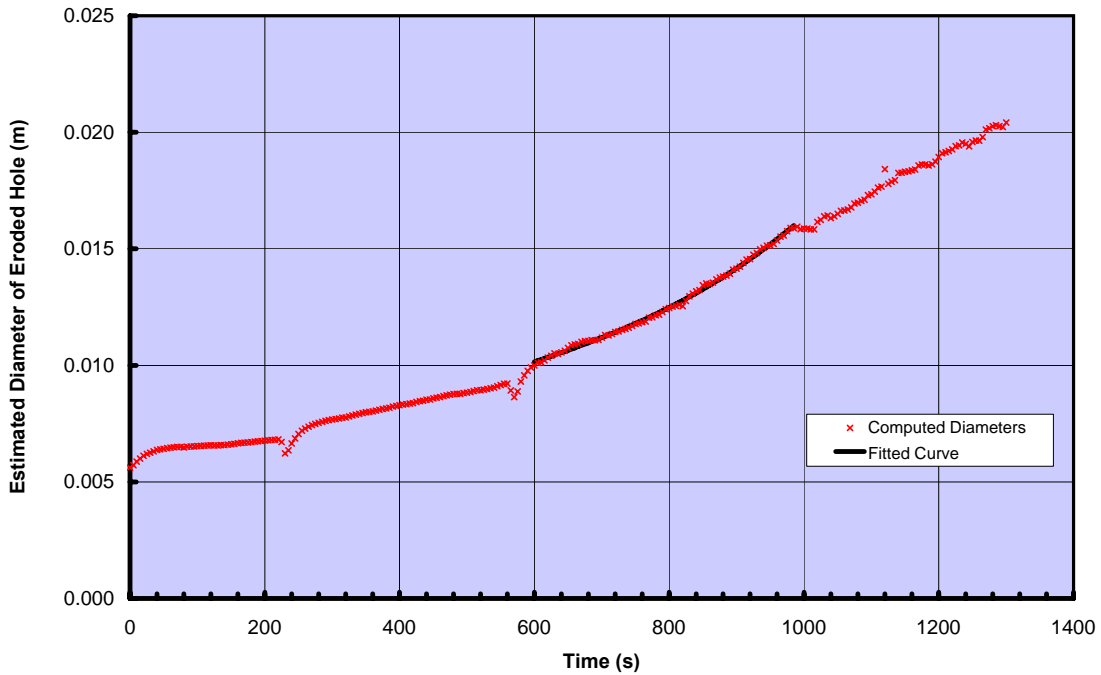
ARS-P2-HET-25, +2% Test ARS-P2-HET-25, +2% 08-27-2008



ERODS Phase 2

ESTIMATED DIAMETER OF ERODED HOLE

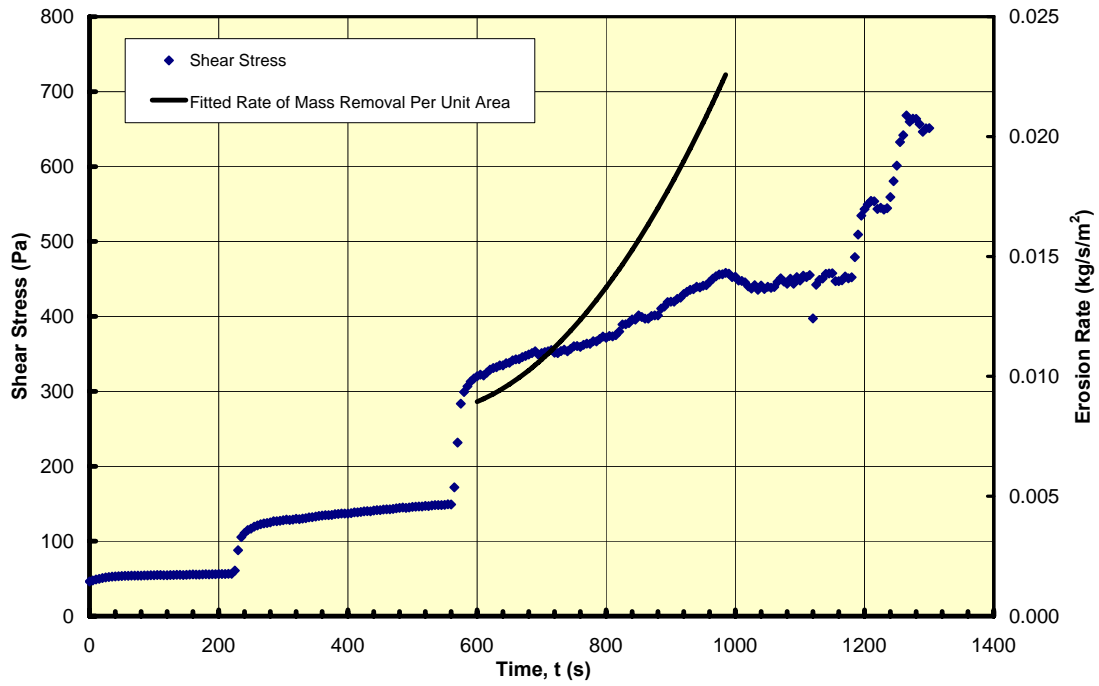
ARS-P2-HET-25, +2% Test ARS-P2-HET-25, +2% 08-27-2008



ERODS Phase 2

EROSION RATE AND SHEAR STRESS VS. TIME

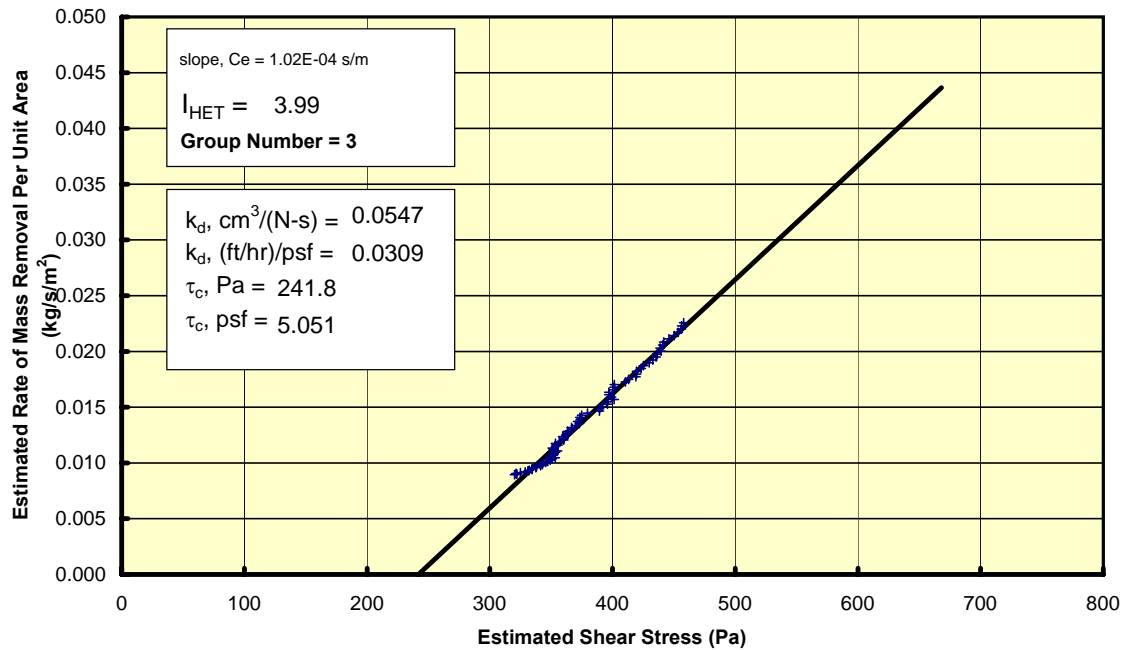
ARS-P2-HET-25, +2% Test ARS-P2-HET-25, +2% 08-27-2008



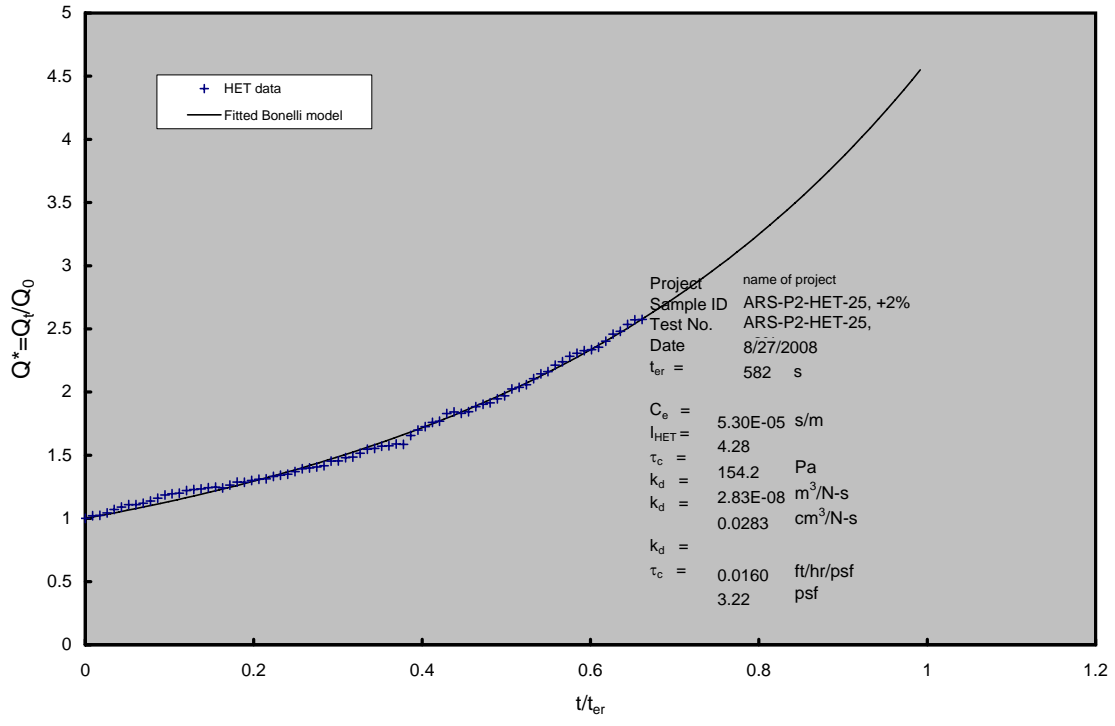
EROSION RATE VS. SHEAR STRESS

ERODS Phase 2

ARS-P2-HET-25, +2% Test ARS-P2-HET-25, +2% 08-27-2008



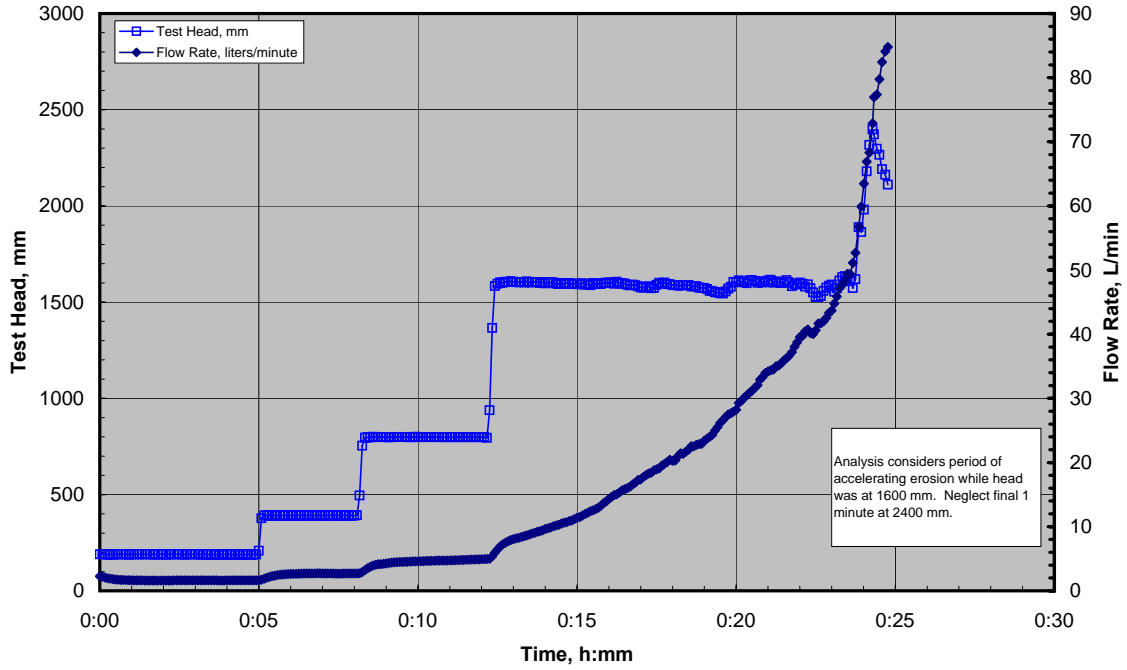
Bonelli Model - Dimensionless Flow vs. Dimensionless Time



ERODS Phase 2

HET Test Record

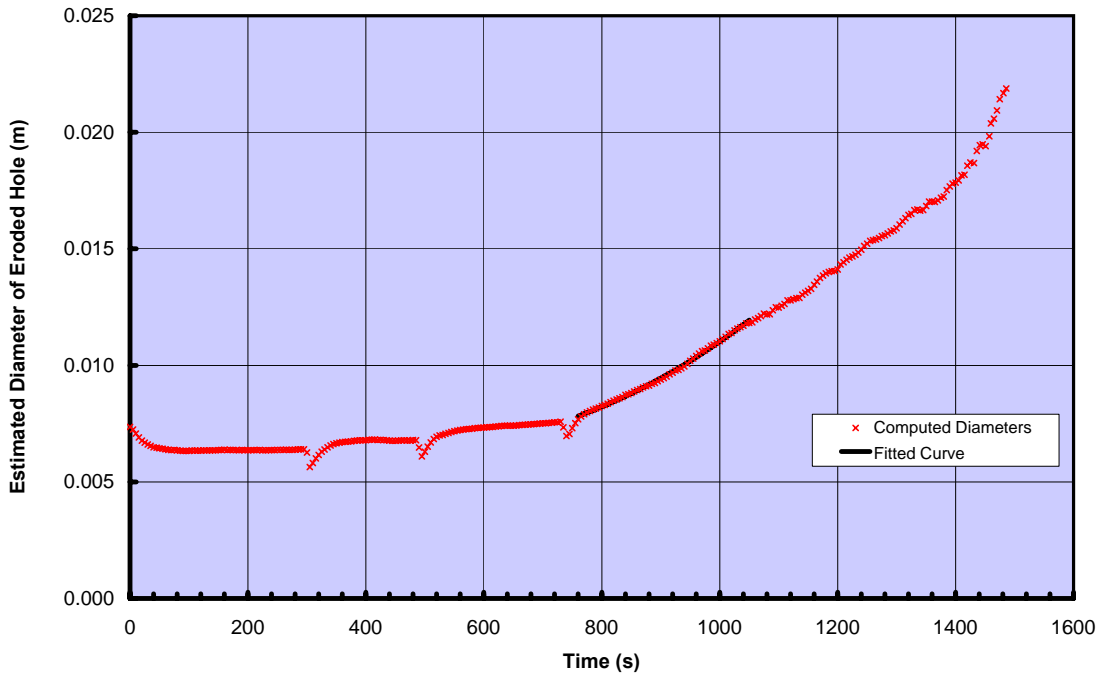
ARS-P2-HET-25, +4 Test ARS-P2-HET-25, +4 09-16-2008



ERODS Phase 2

ESTIMATED DIAMETER OF ERODED HOLE

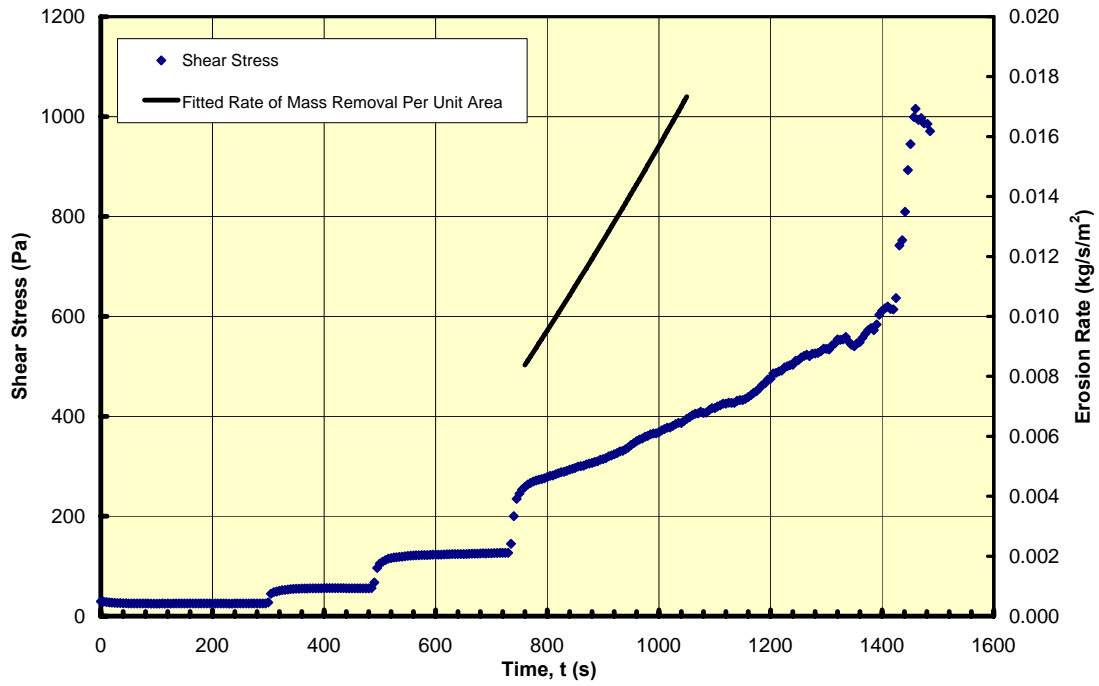
ARS-P2-HET-25, +4 Test ARS-P2-HET-25, +4 09-16-2008



ERODS Phase 2

EROSION RATE AND SHEAR STRESS VS. TIME

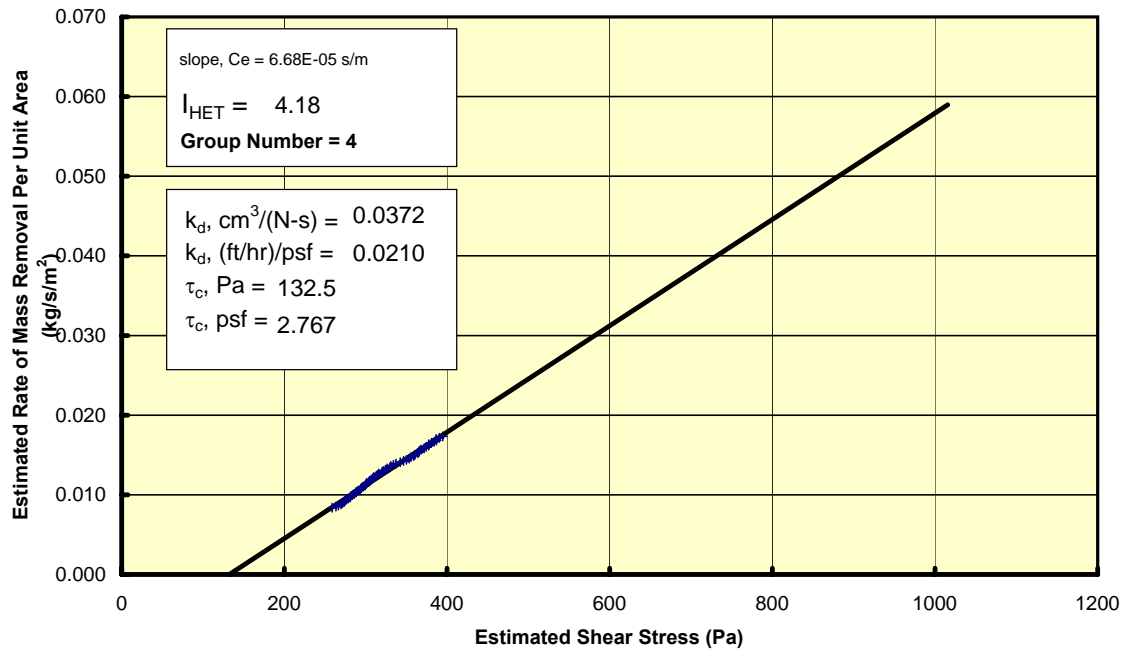
ARS-P2-HET-25, +4 Test ARS-P2-HET-25, +4 09-16-2008



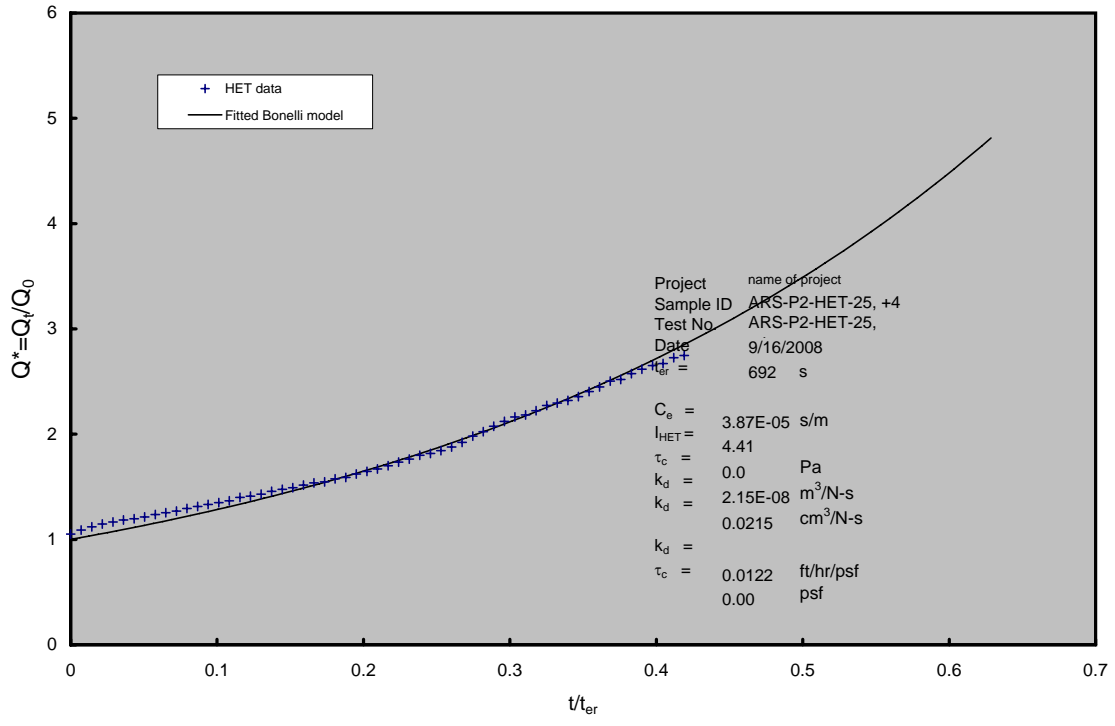
EROSION RATE VS. SHEAR STRESS

ERODS Phase 2

ARS-P2-HET-25, +4 Test ARS-P2-HET-25, +4 09-16-2008



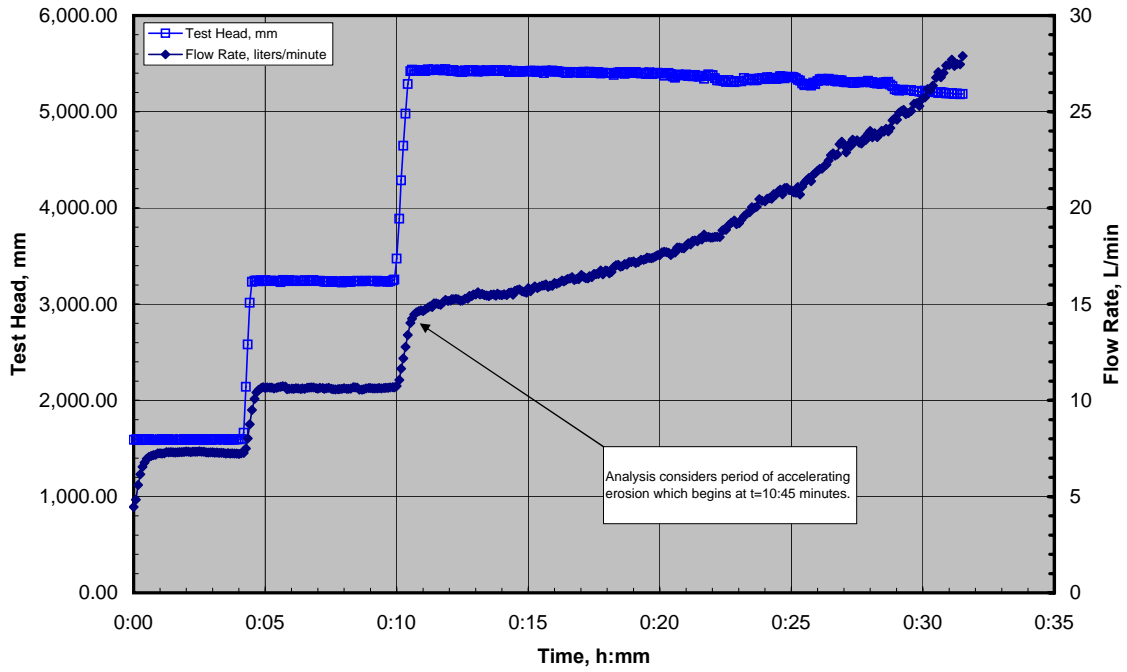
Bonelli Model - Dimensionless Flow vs. Dimensionless Time



ERODS Phase 2

HET Test Record

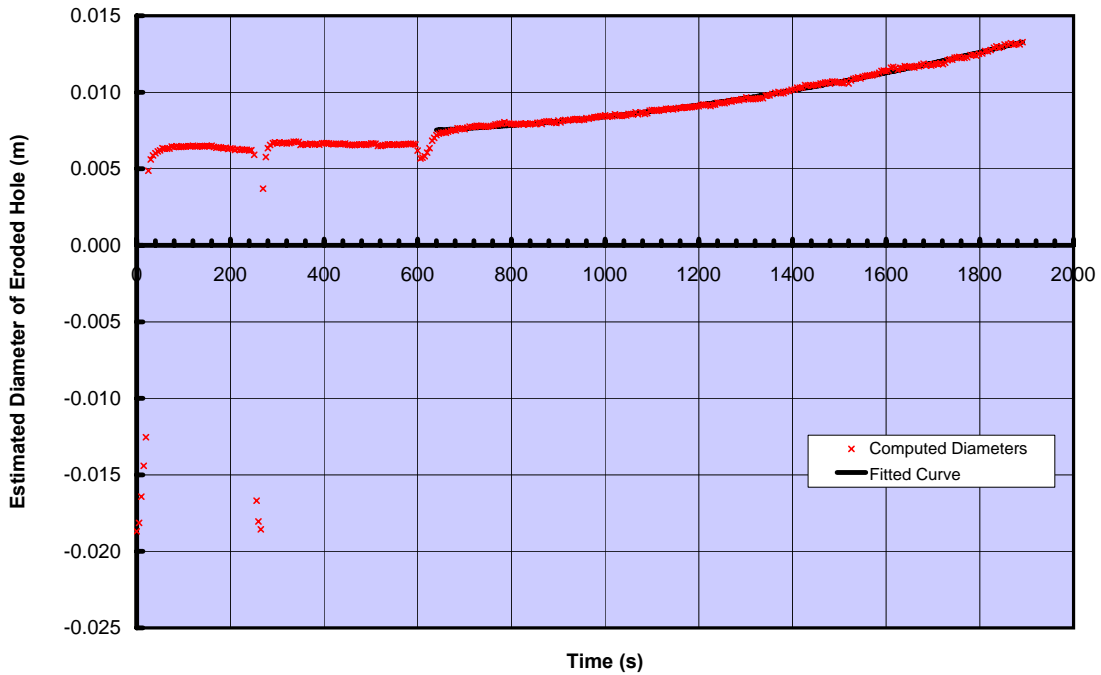
ARS-P3-HET-25, -2-b Test ARS-P3-HET-25, -2-b 09-17-2008



ERODS Phase 2

ESTIMATED DIAMETER OF ERODED HOLE

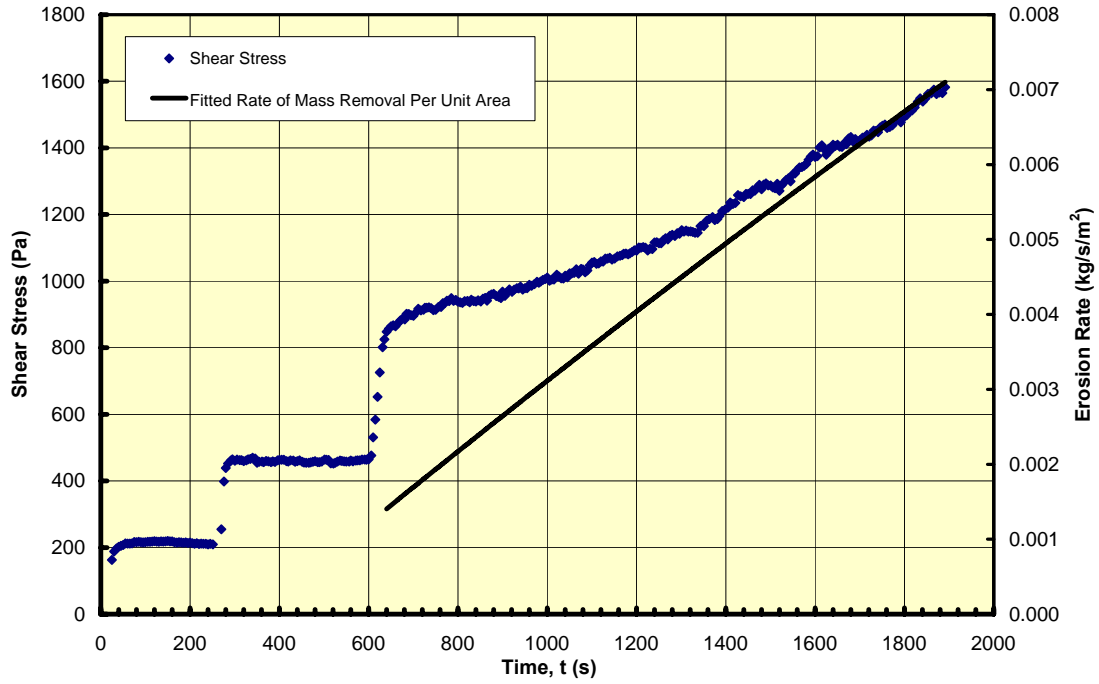
ARS-P3-HET-25, -2-b Test ARS-P3-HET-25, -2-b 09-17-2008



ERODS Phase 2

EROSION RATE AND SHEAR STRESS VS. TIME

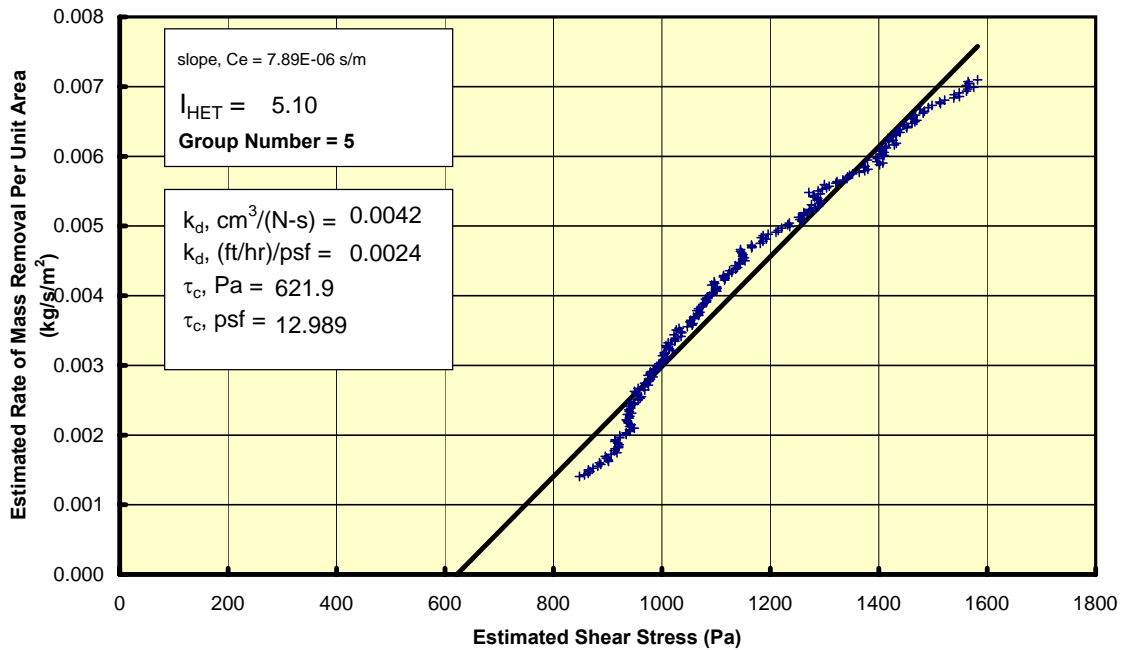
ARS-P3-HET-25, -2-b Test ARS-P3-HET-25, -2-b 09-17-2008



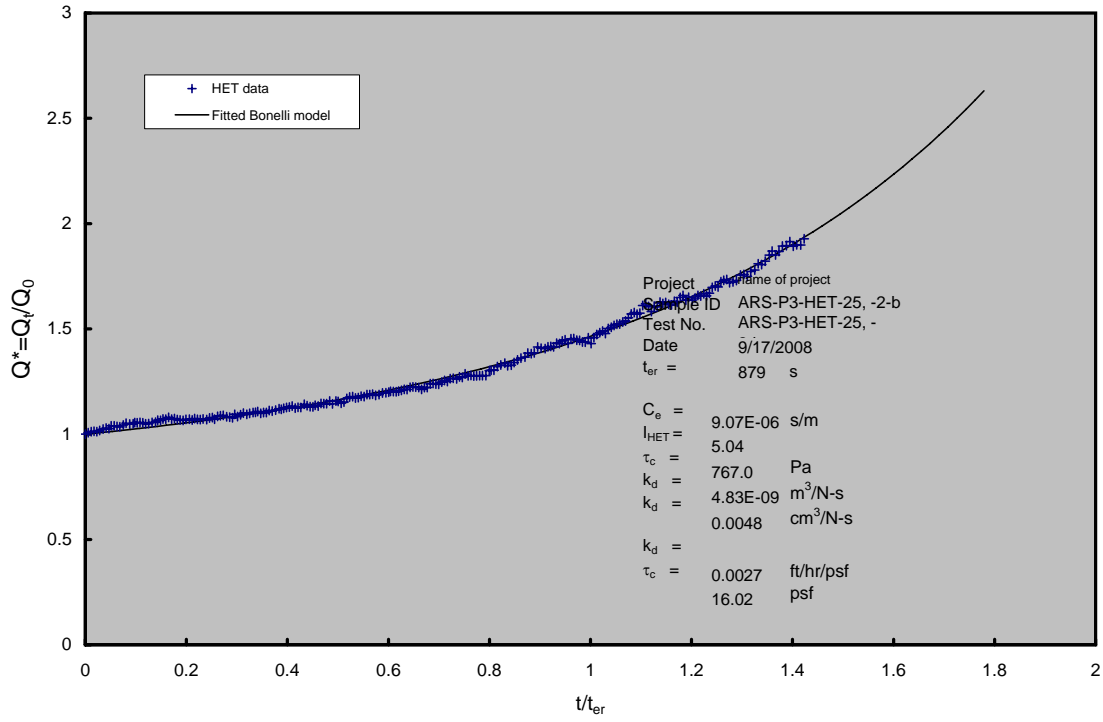
EROSION RATE VS. SHEAR STRESS

ERODS Phase 2

ARS-P3-HET-25, -2-b Test ARS-P3-HET-25, -2-b 09-17-2008



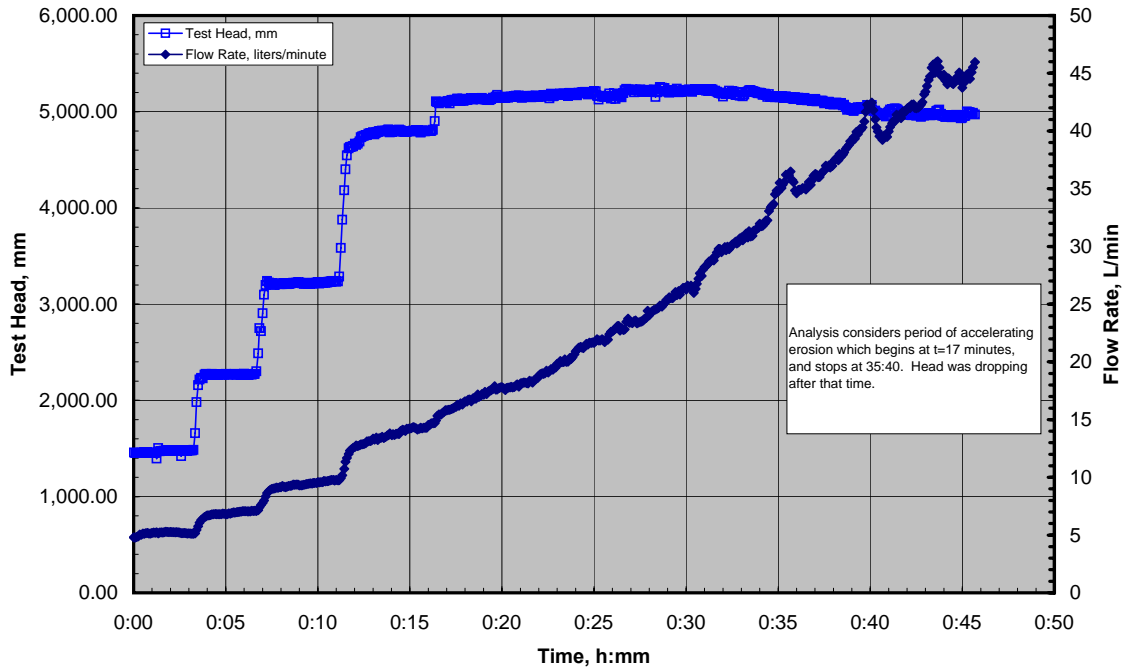
Bonelli Model - Dimensionless Flow vs. Dimensionless Time



ARS Phase 2

HET Test Record

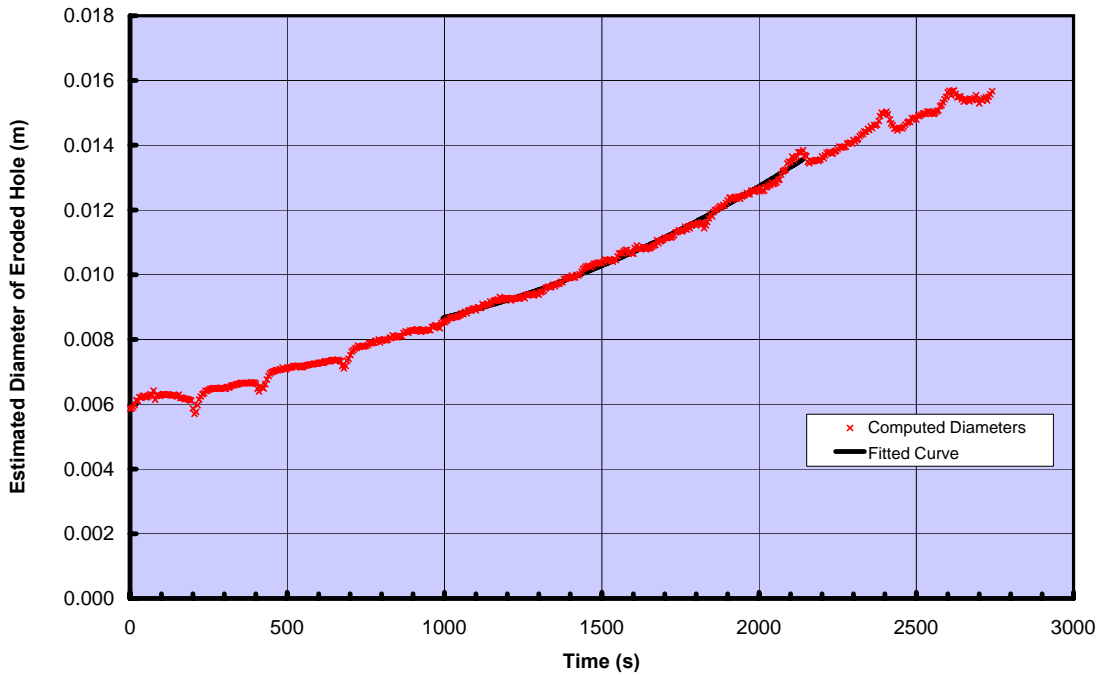
P3 at 2% dry, 25 blows Test ARS-P3-HET-25,-2 08-06-2008



ARS Phase 2

ESTIMATED DIAMETER OF ERODED HOLE

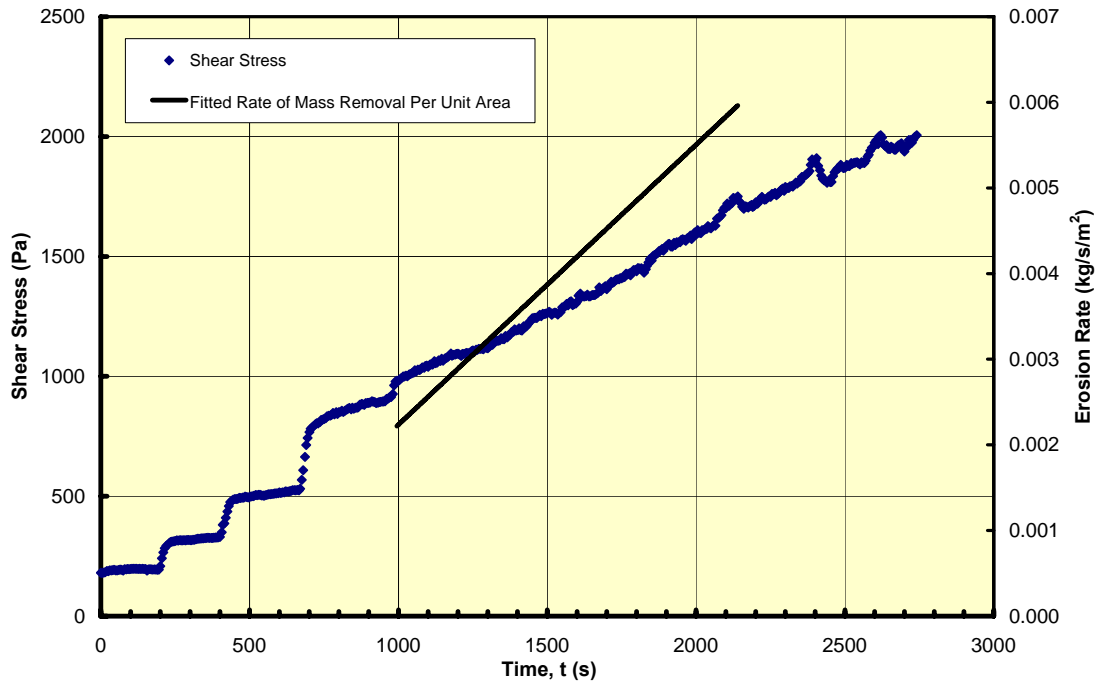
P3 at 2% dry, 25 blows Test ARS-P3-HET-25,-2 08-06-2008



ARS Phase 2

EROSION RATE AND SHEAR STRESS VS. TIME

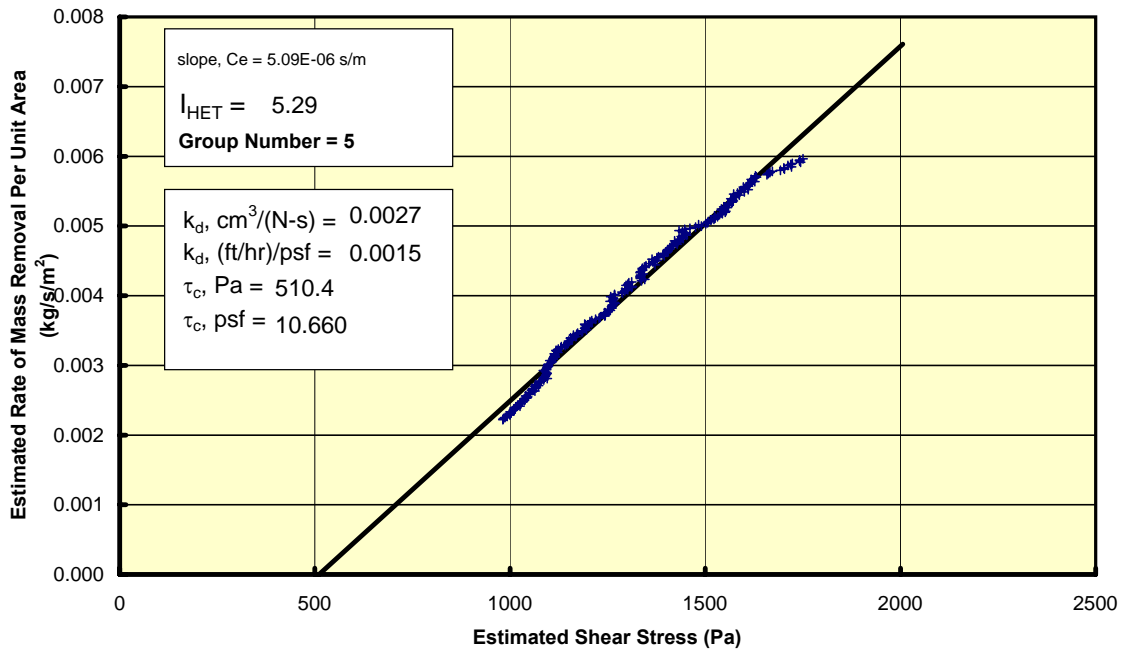
P3 at 2% dry, 25 blows Test ARS-P3-HET-25,-2 08-06-2008



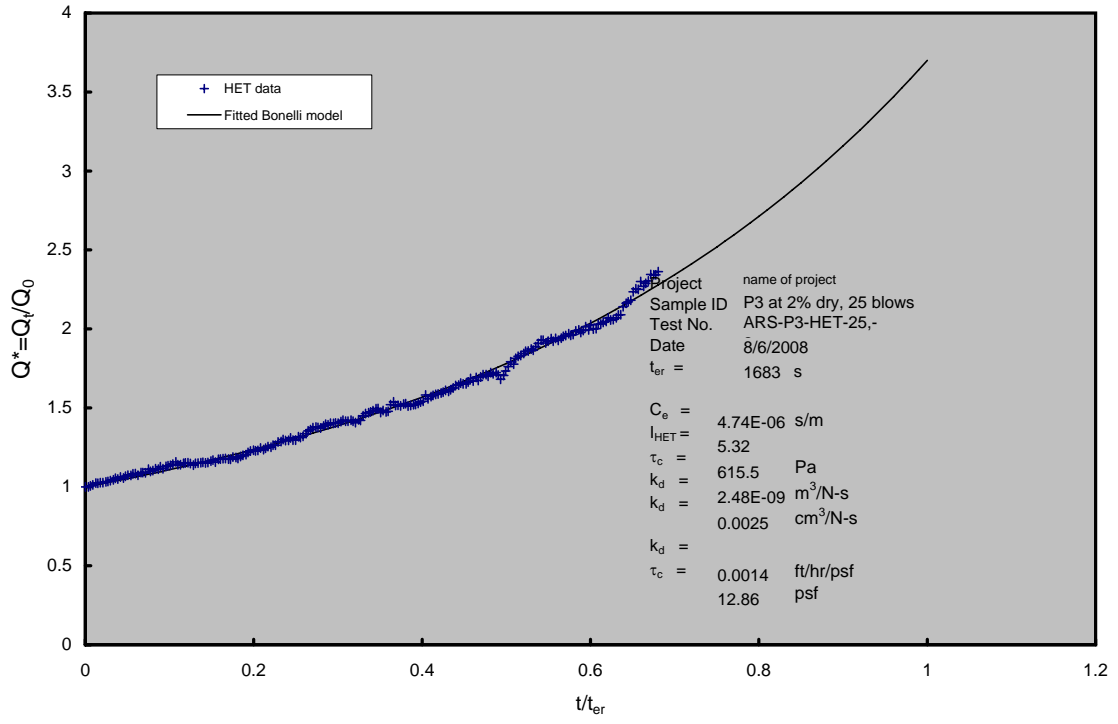
EROSION RATE VS. SHEAR STRESS

ARS Phase 2

P3 at 2% dry, 25 blows Test ARS-P3-HET-25,-2 08-06-2008



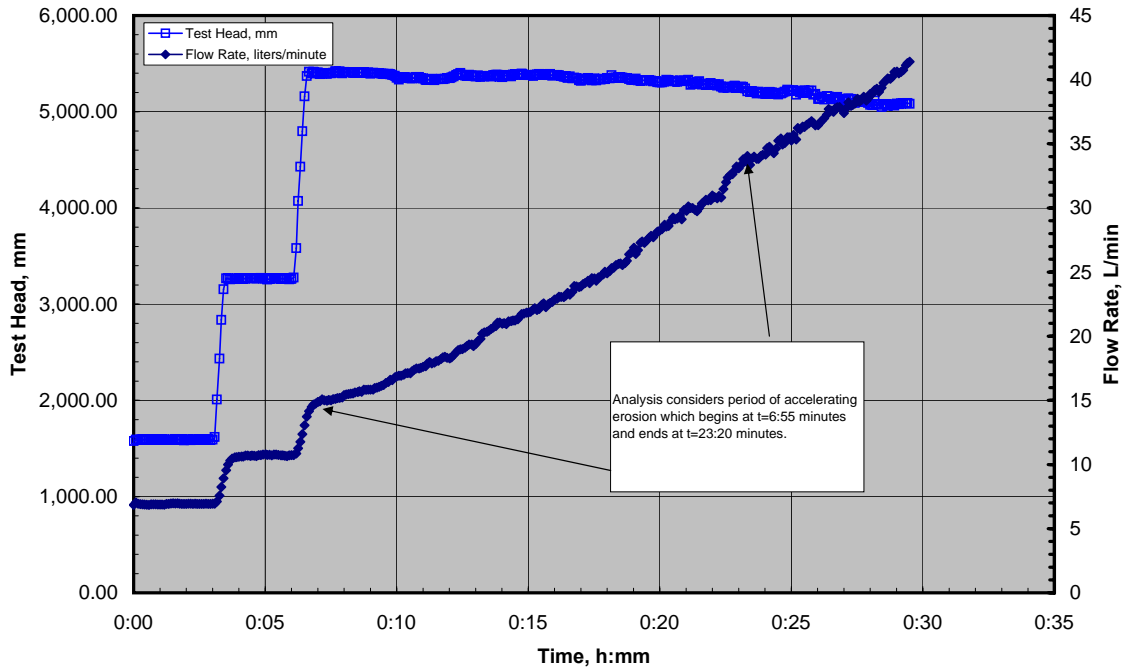
Bonelli Model - Dimensionless Flow vs. Dimensionless Time



ERODS Phase 2

HET Test Record

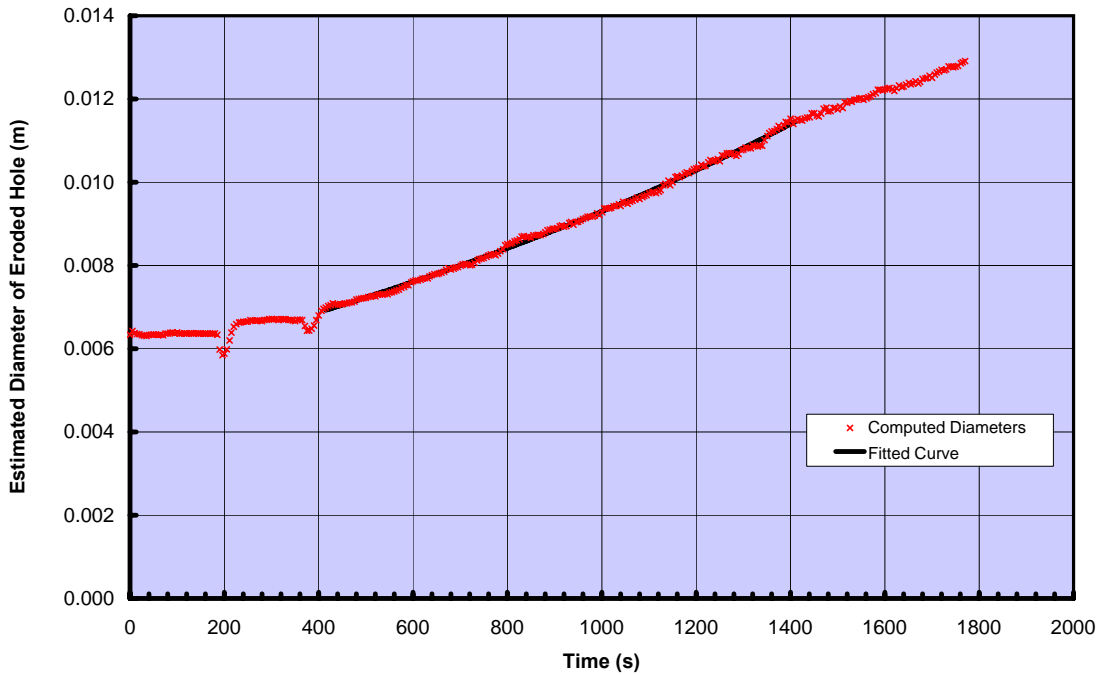
ARS-P3-HET-25-OMC-b Test ARS-P3-HET-25-OMC-b 09-17-2008



ERODS Phase 2

ESTIMATED DIAMETER OF ERODED HOLE

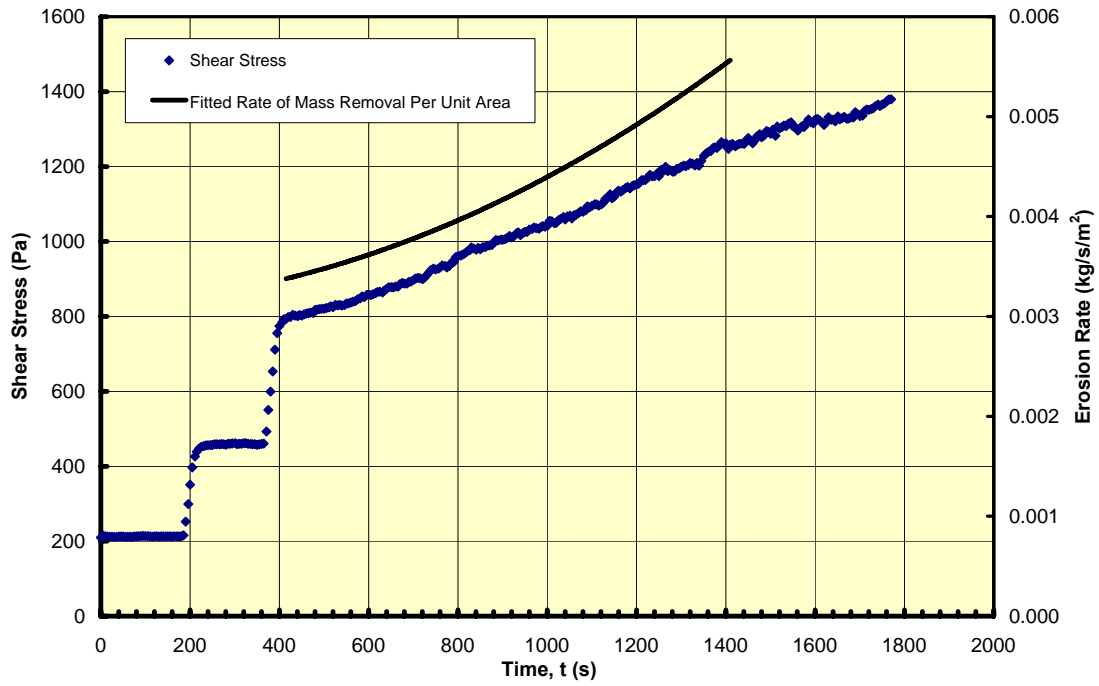
ARS-P3-HET-25-OMC-b Test ARS-P3-HET-25-OMC-b 09-17-2008



ERODS Phase 2

EROSION RATE AND SHEAR STRESS VS. TIME

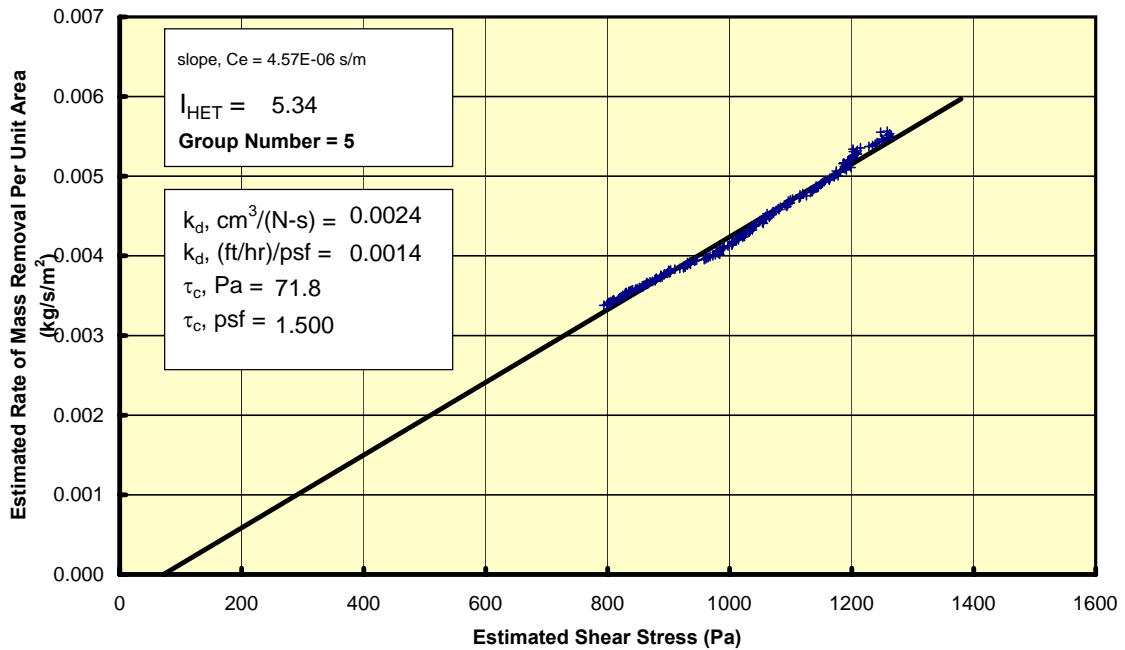
ARS-P3-HET-25-OMC-b Test ARS-P3-HET-25-OMC-b 09-17-2008



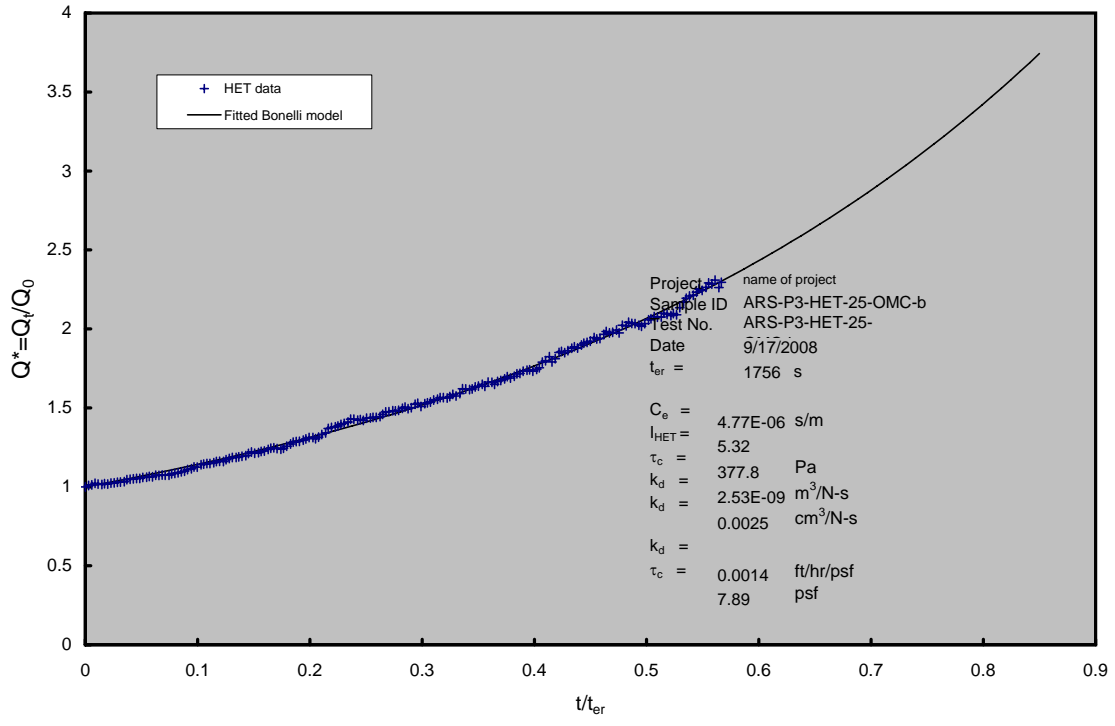
EROSION RATE VS. SHEAR STRESS

ERODS Phase 2

ARS-P3-HET-25-OMC-b Test ARS-P3-HET-25-OMC-b 09-17-2008



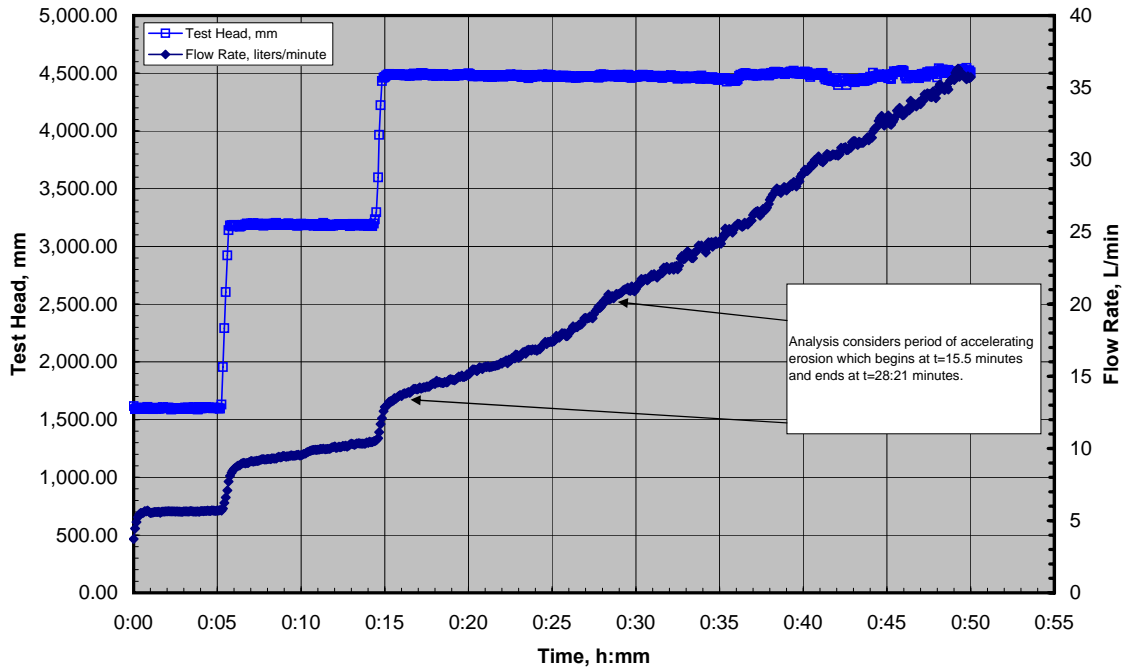
Bonelli Model - Dimensionless Flow vs. Dimensionless Time



ARS Phase 2

HET Test Record

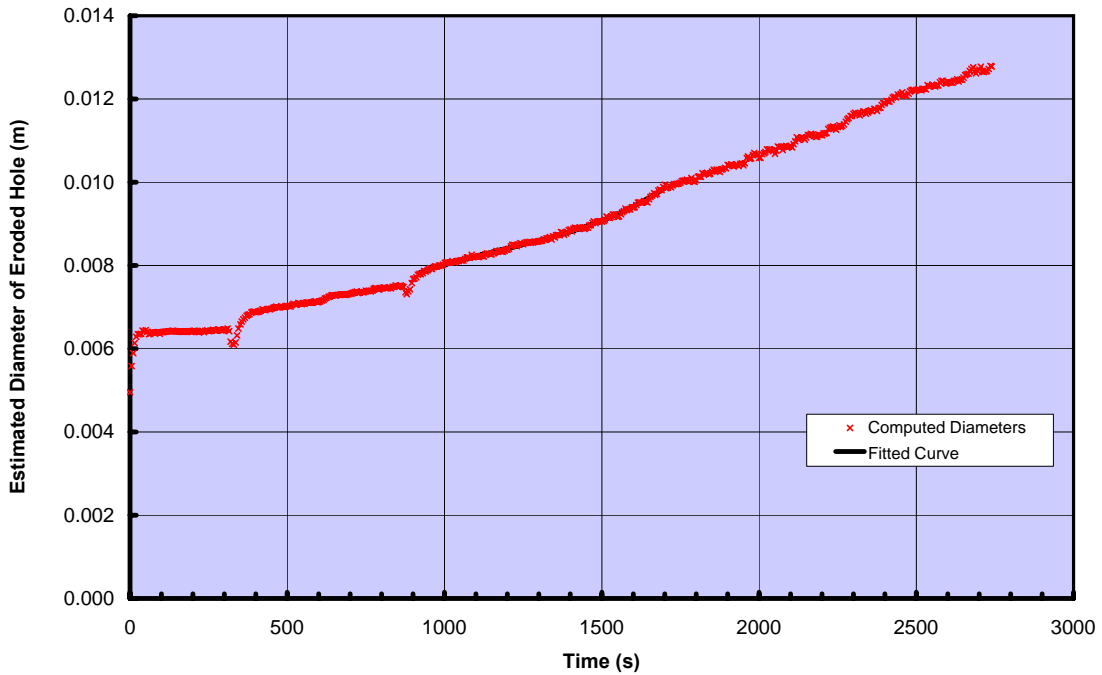
P3 at 2% dry, 25 blows Test ARS-P3-HET-25,-2 08-06-2008



ARS Phase 2

ESTIMATED DIAMETER OF ERODED HOLE

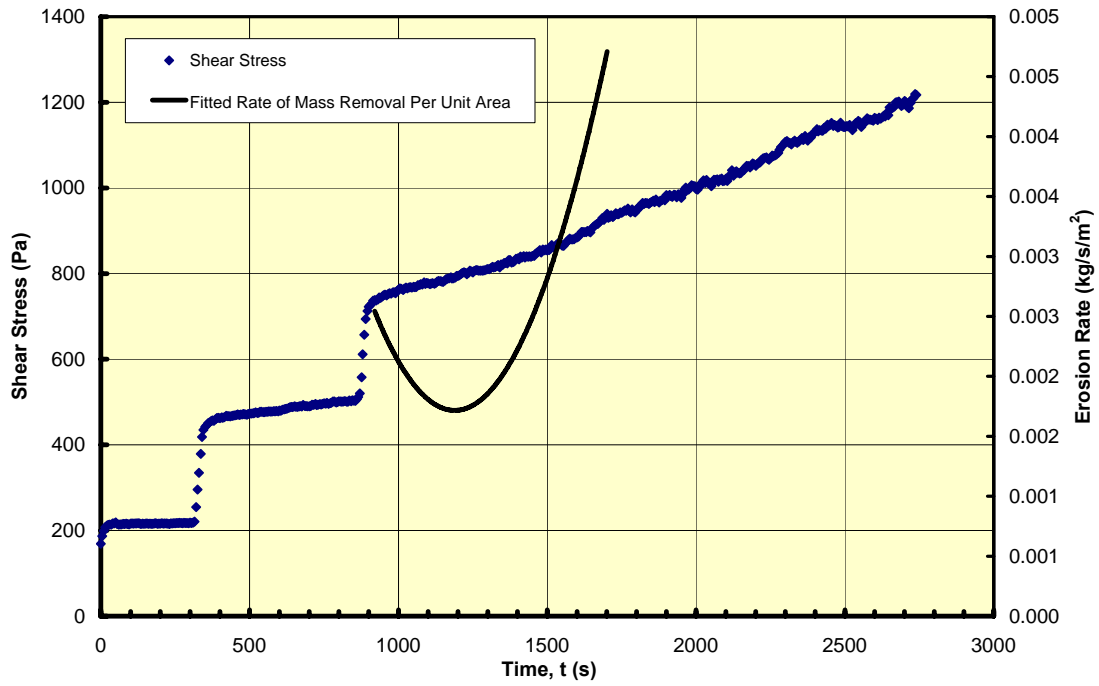
P3 at 2% dry, 25 blows Test ARS-P3-HET-25,-2 08-06-2008



ARS Phase 2

EROSION RATE AND SHEAR STRESS VS. TIME

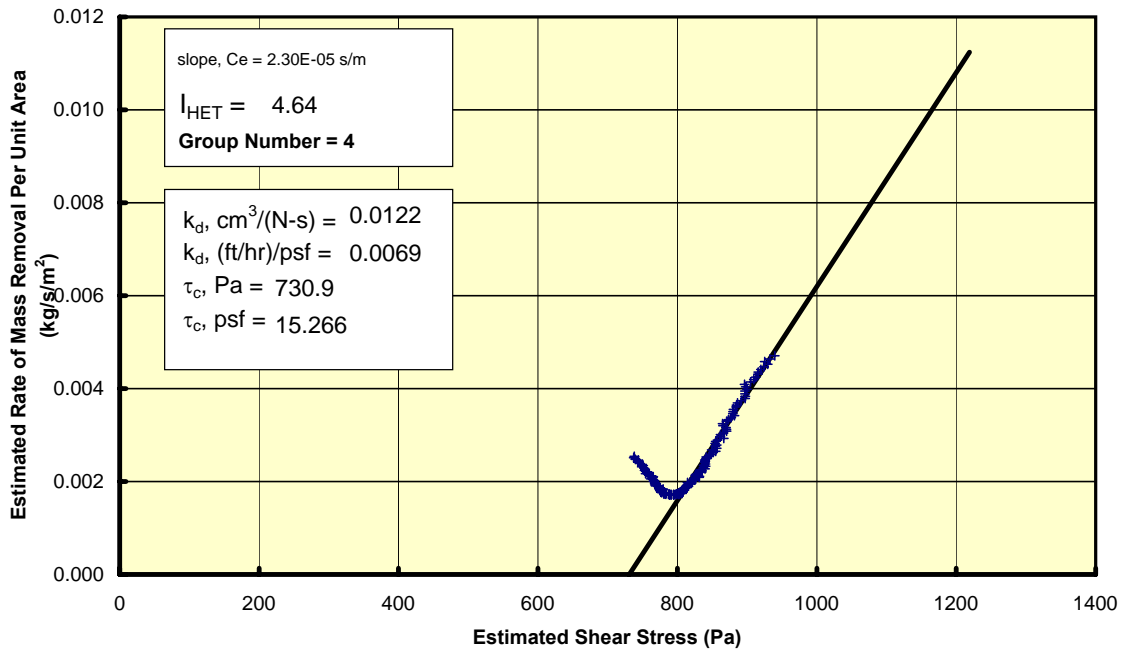
P3 at 2% dry, 25 blows Test ARS-P3-HET-25,-2 08-06-2008



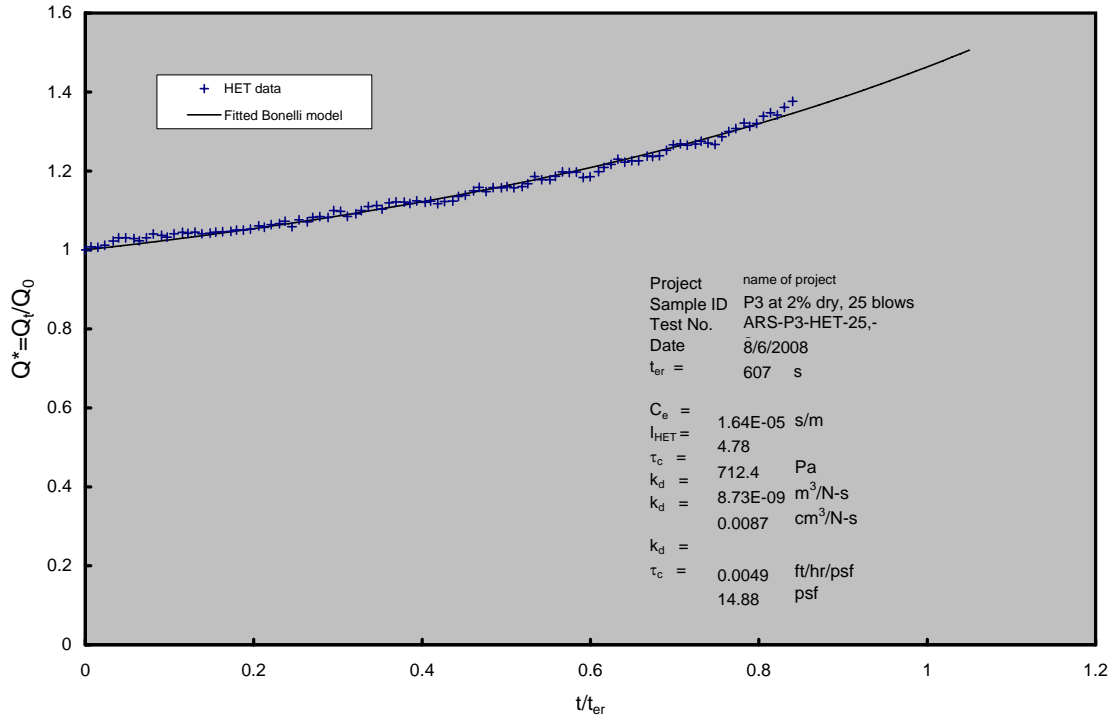
EROSION RATE VS. SHEAR STRESS

ARS Phase 2

P3 at 2% dry, 25 blows Test ARS-P3-HET-25,-2 08-06-2008



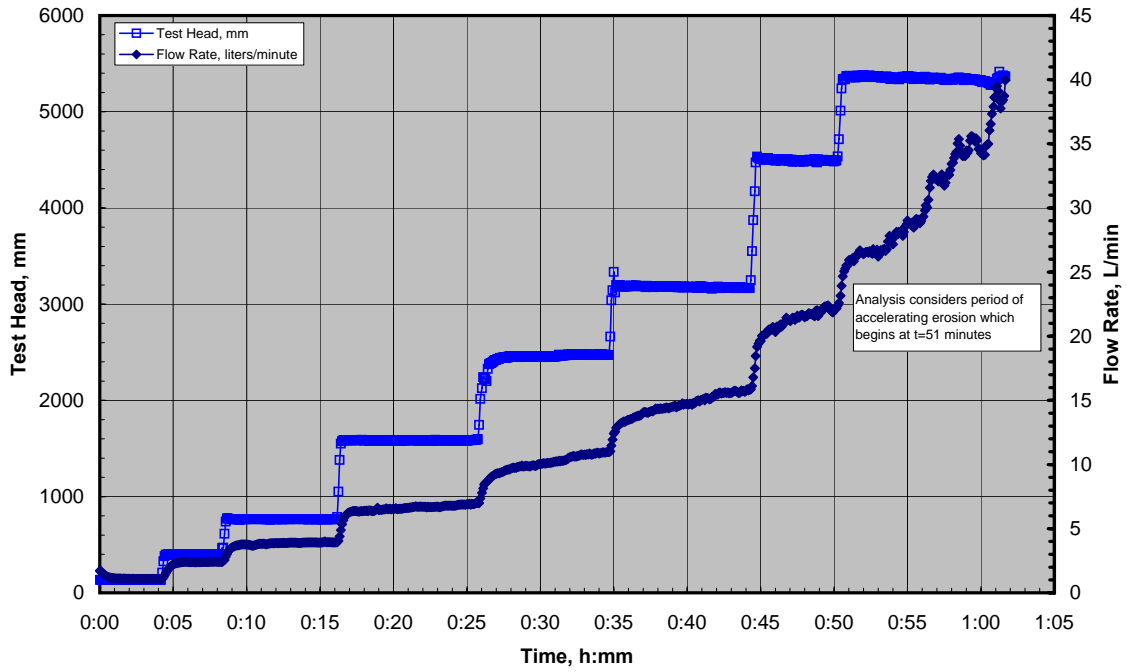
Bonelli Model - Dimensionless Flow vs. Dimensionless Time



ERODS (ARS Phase 2)

HET Test Record

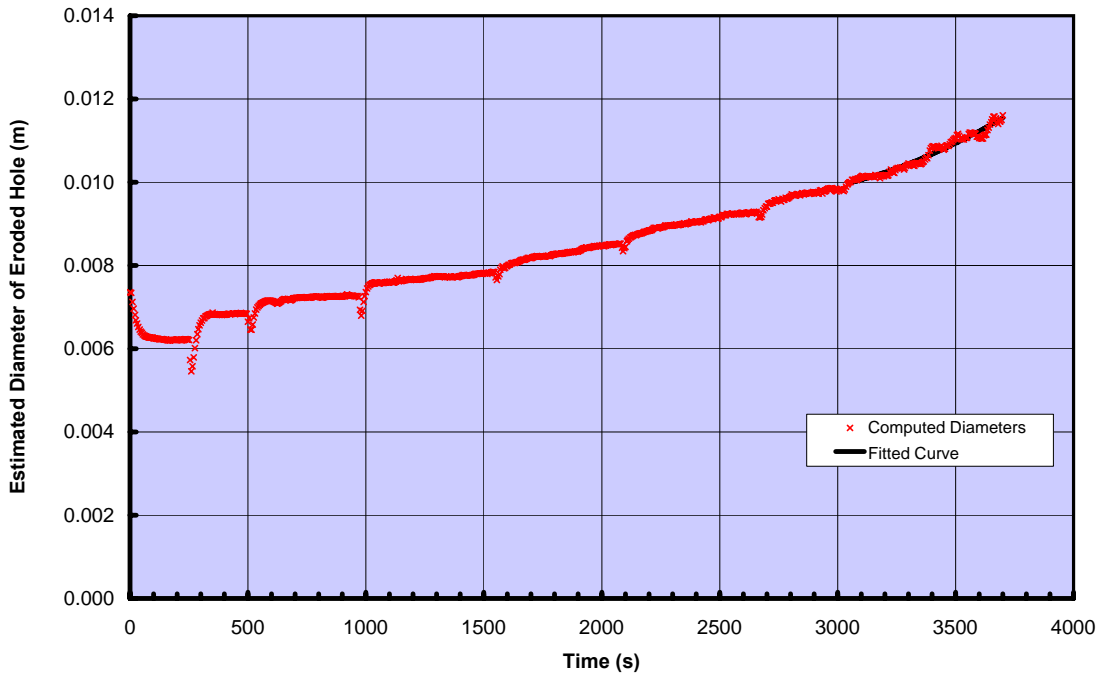
P3 @ Optimum moisture, 25 blows Test ARS-P3-25-OMC 07-28-2008



ERODS (ARS Phase 2)

ESTIMATED DIAMETER OF ERODED HOLE

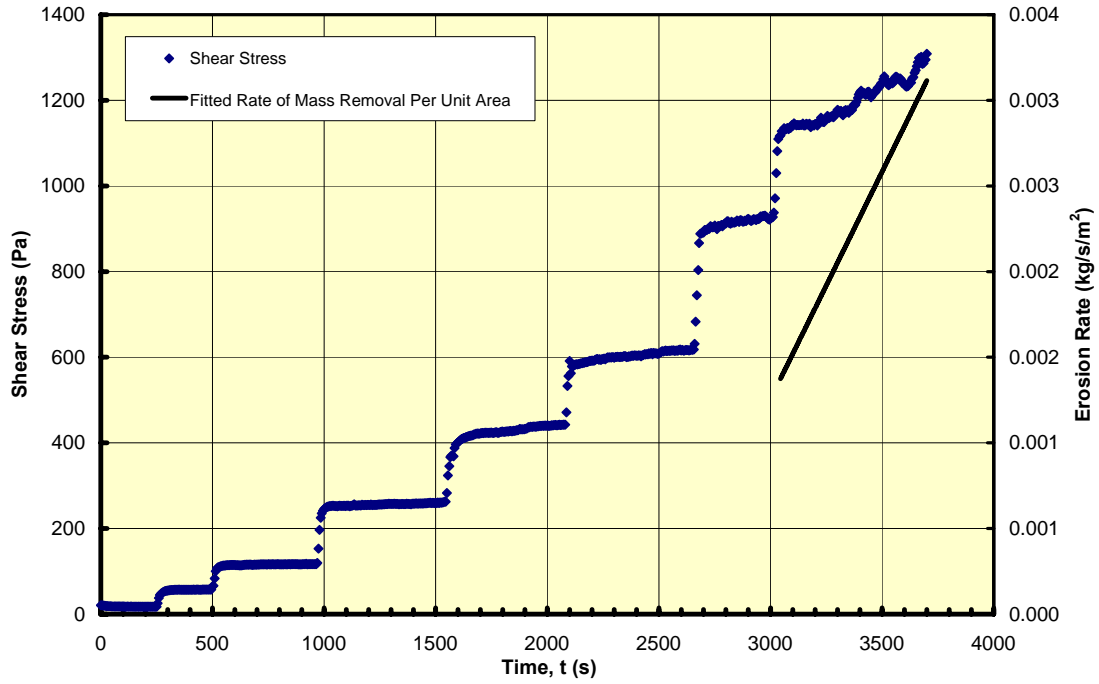
P3 @ Optimum moisture, 25 blows Test ARS-P3-25-OMC 07-28-2008



ERODS (ARS Phase 2)

EROSION RATE AND SHEAR STRESS VS. TIME

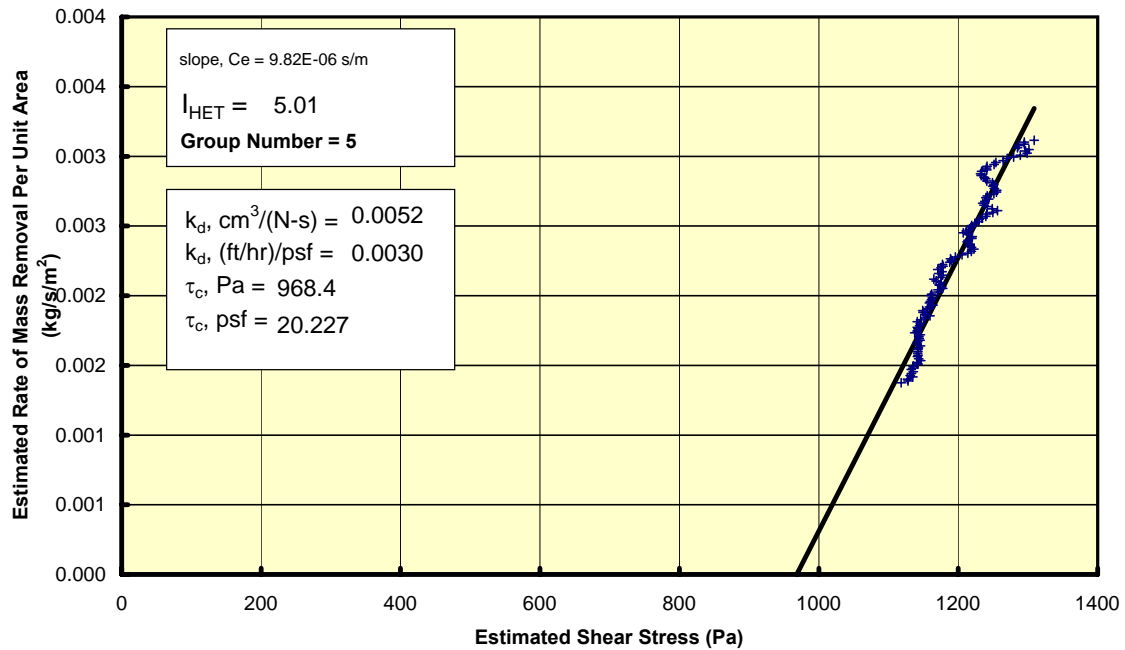
P3 @ Optimum moisture, 25 blows Test ARS-P3-25-OMC 07-28-2008



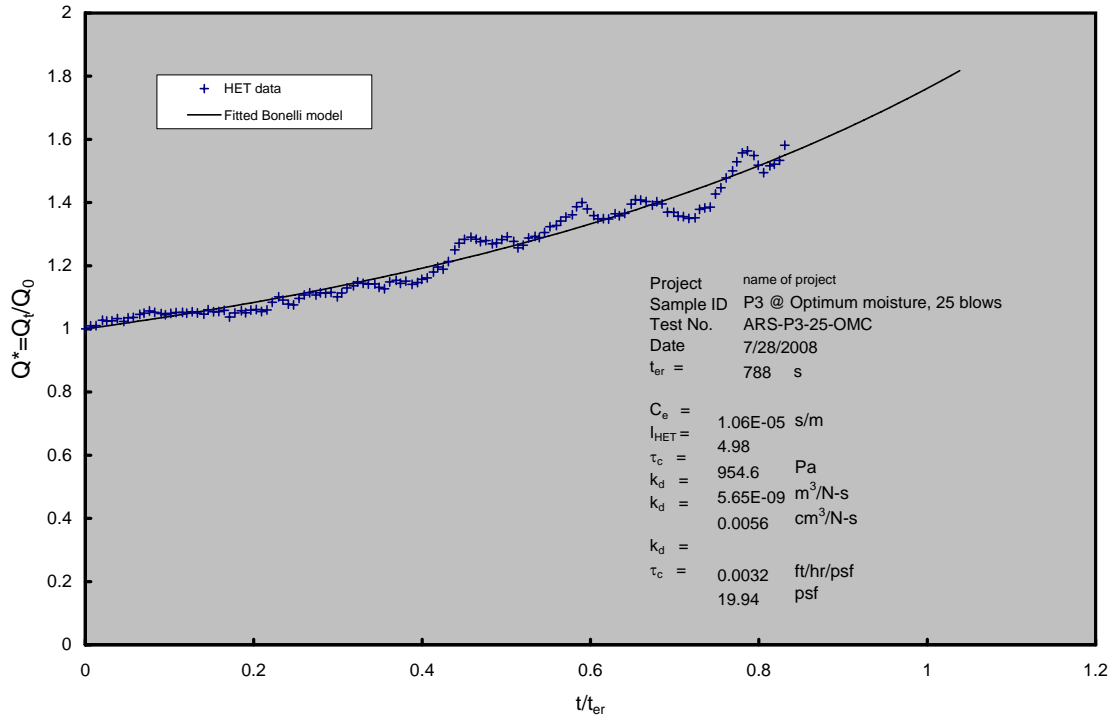
EROSION RATE VS. SHEAR STRESS

ERODS (ARS Phase 2)

P3 @ Optimum moisture, 25 blows Test ARS-P3-25-OMC 07-28-2008



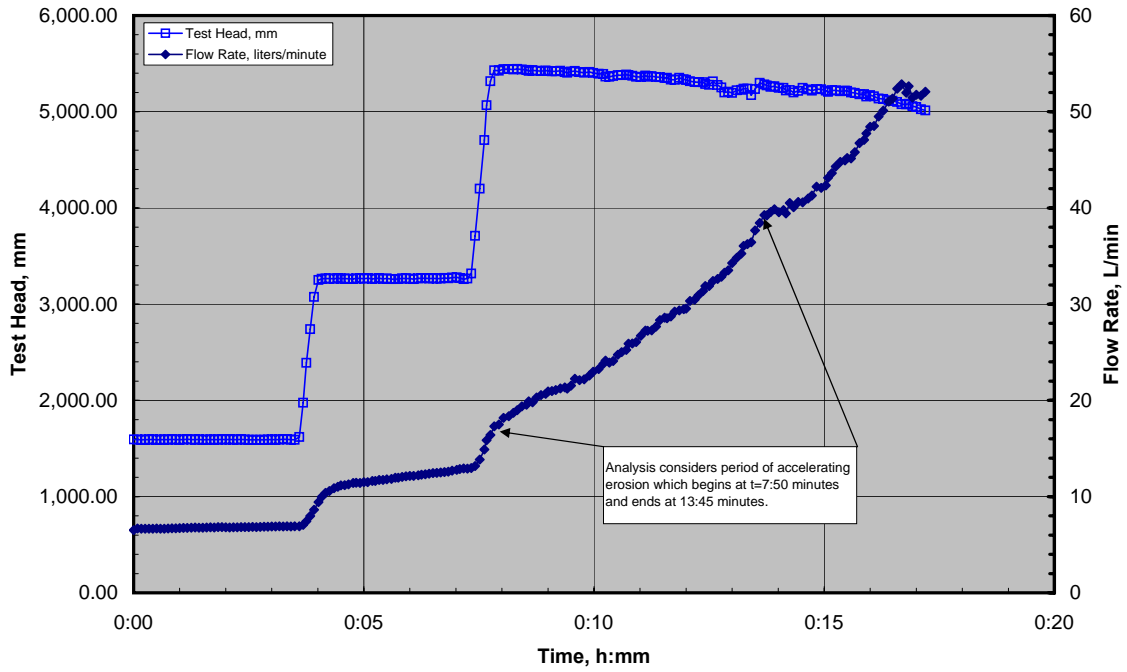
Bonelli Model - Dimensionless Flow vs. Dimensionless Time



ERODS Phase 2

HET Test Record

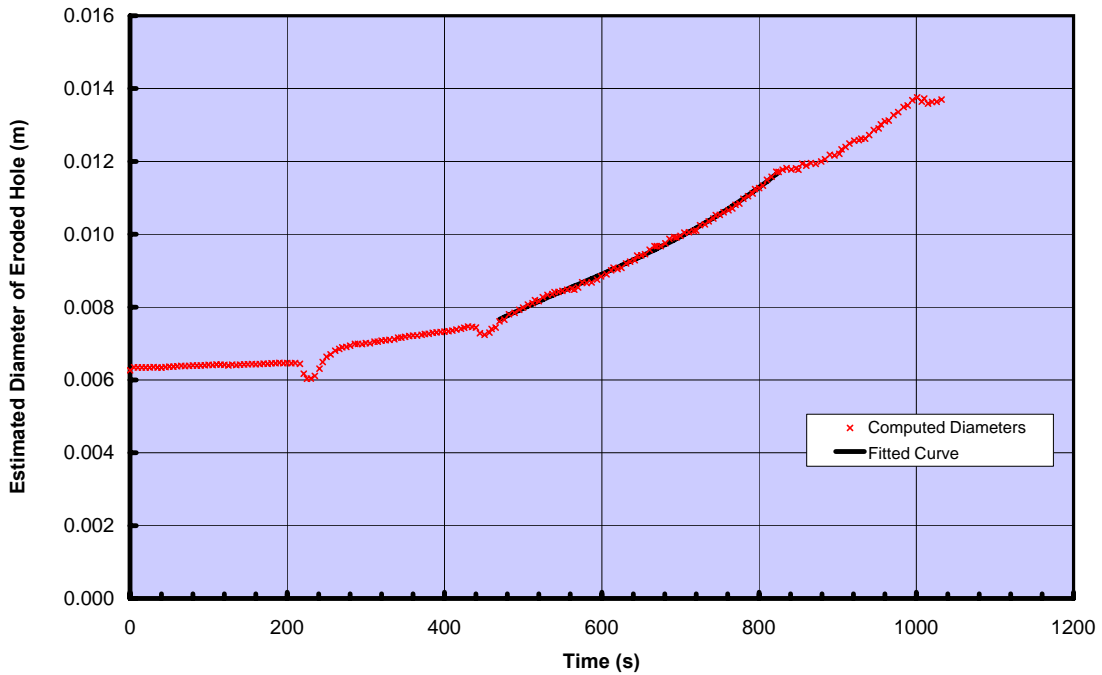
ARS-P3-HET-25, +2-b Test ARS-P3-HET-25, +2-b 09-17-2008



ERODS Phase 2

ESTIMATED DIAMETER OF ERODED HOLE

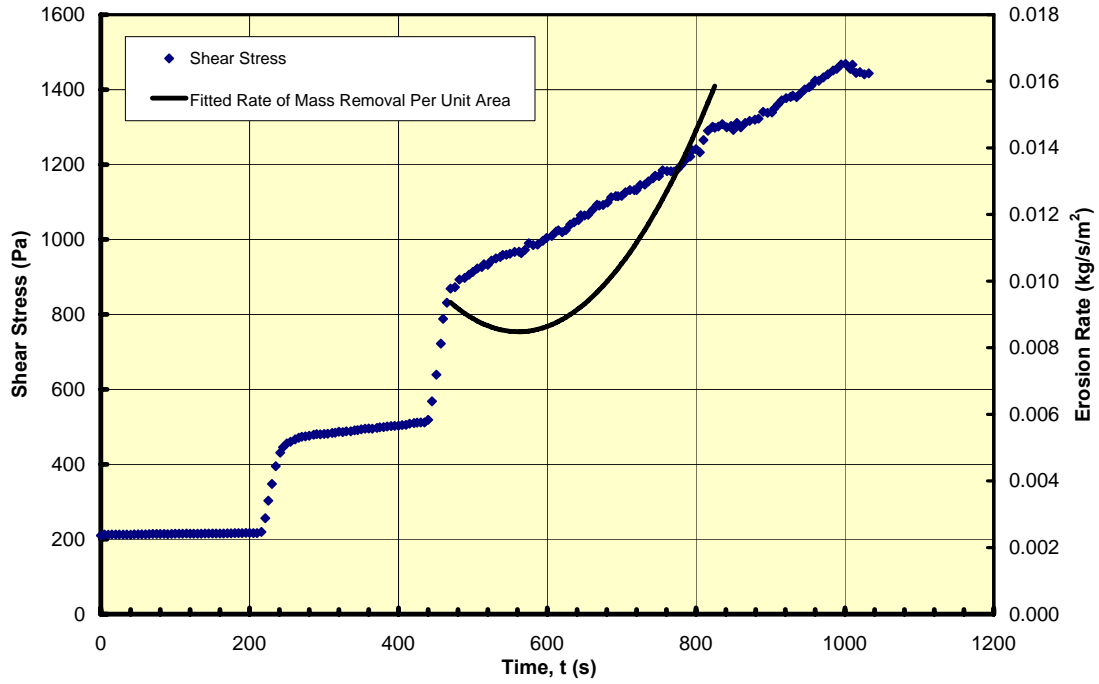
ARS-P3-HET-25, +2-b Test ARS-P3-HET-25, +2-b 09-17-2008



ERODS Phase 2

EROSION RATE AND SHEAR STRESS VS. TIME

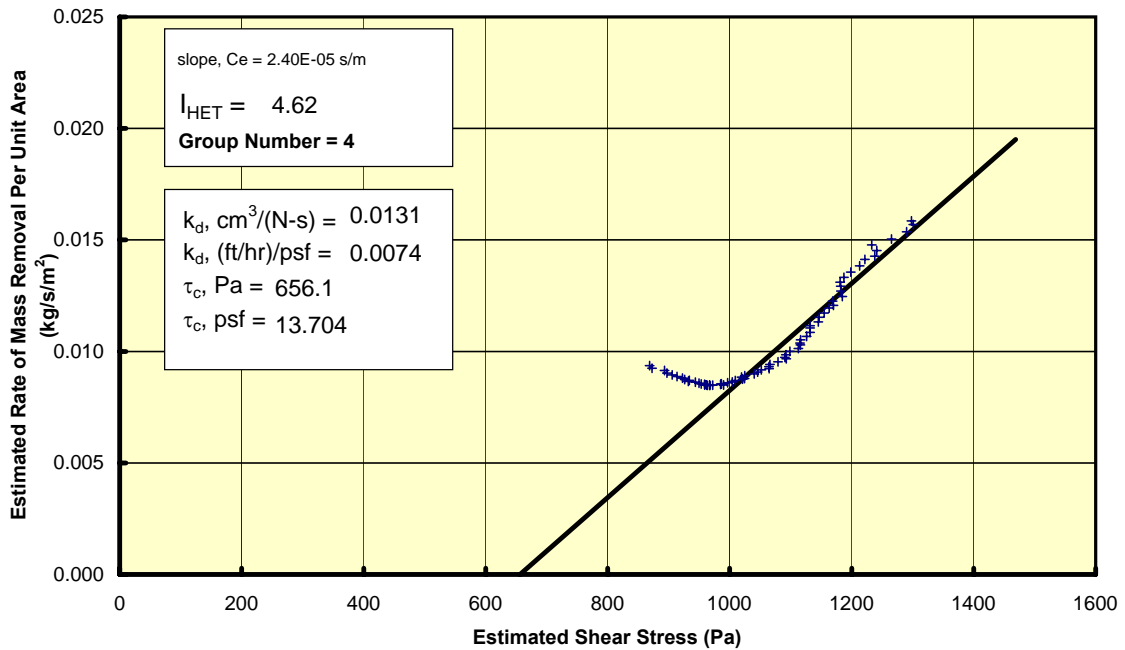
ARS-P3-HET-25, +2-b Test ARS-P3-HET-25, +2-b 09-17-2008



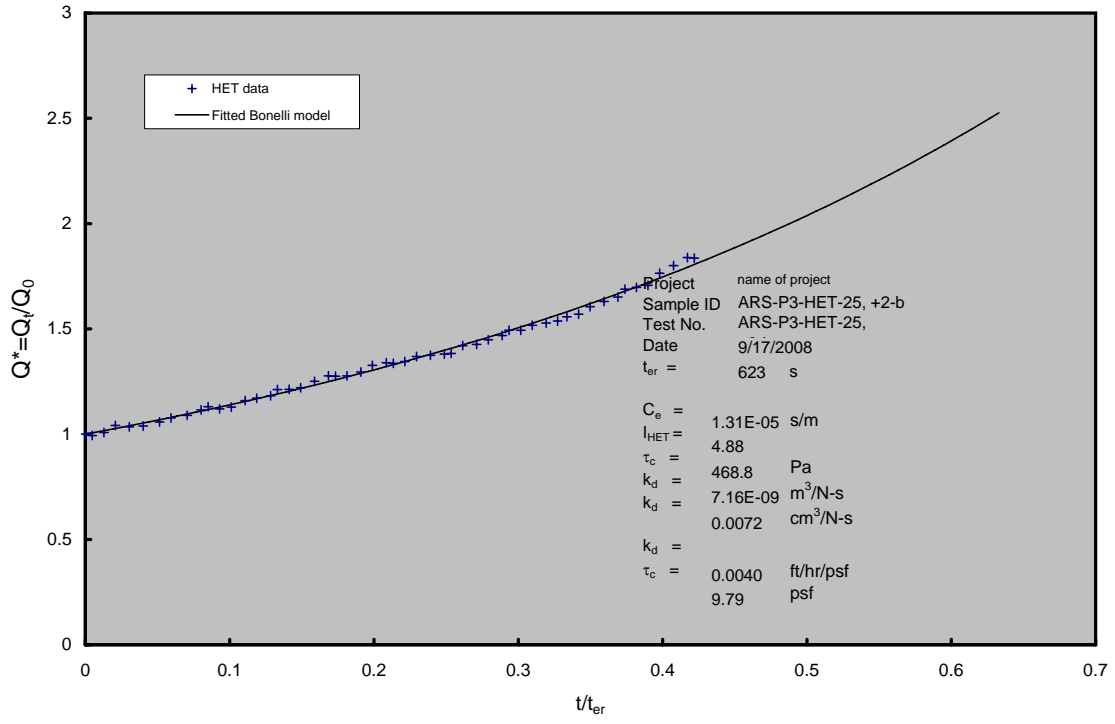
EROSION RATE VS. SHEAR STRESS

ERODS Phase 2

ARS-P3-HET-25, +2-b Test ARS-P3-HET-25, +2-b 09-17-2008



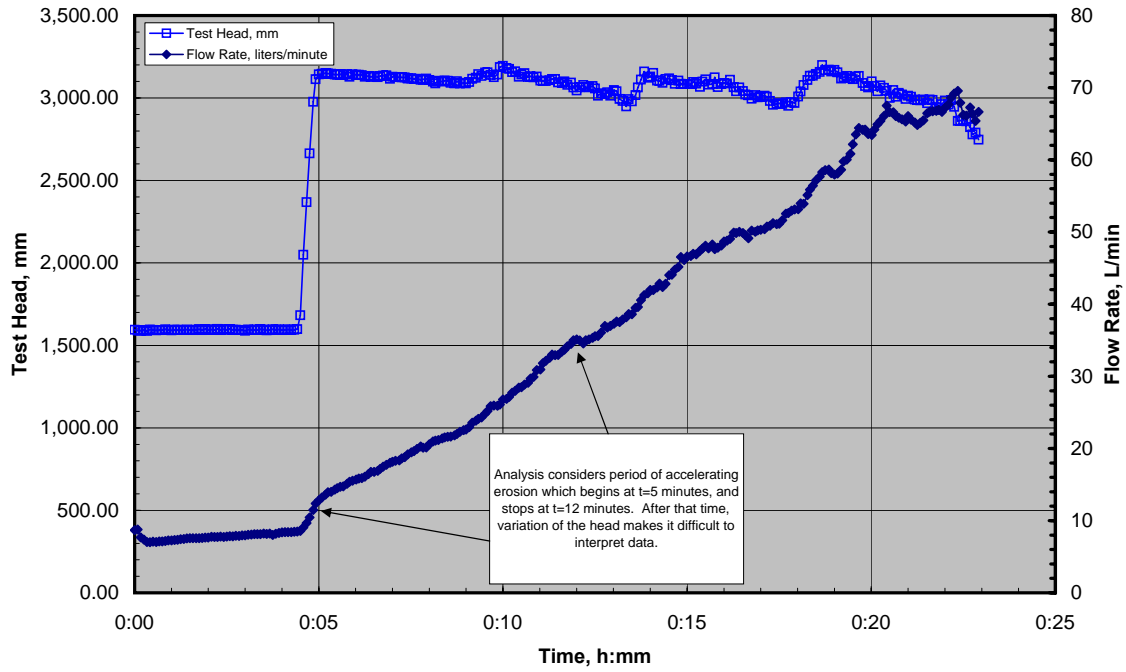
Bonelli Model - Dimensionless Flow vs. Dimensionless Time



ARS Phase 2

HET Test Record

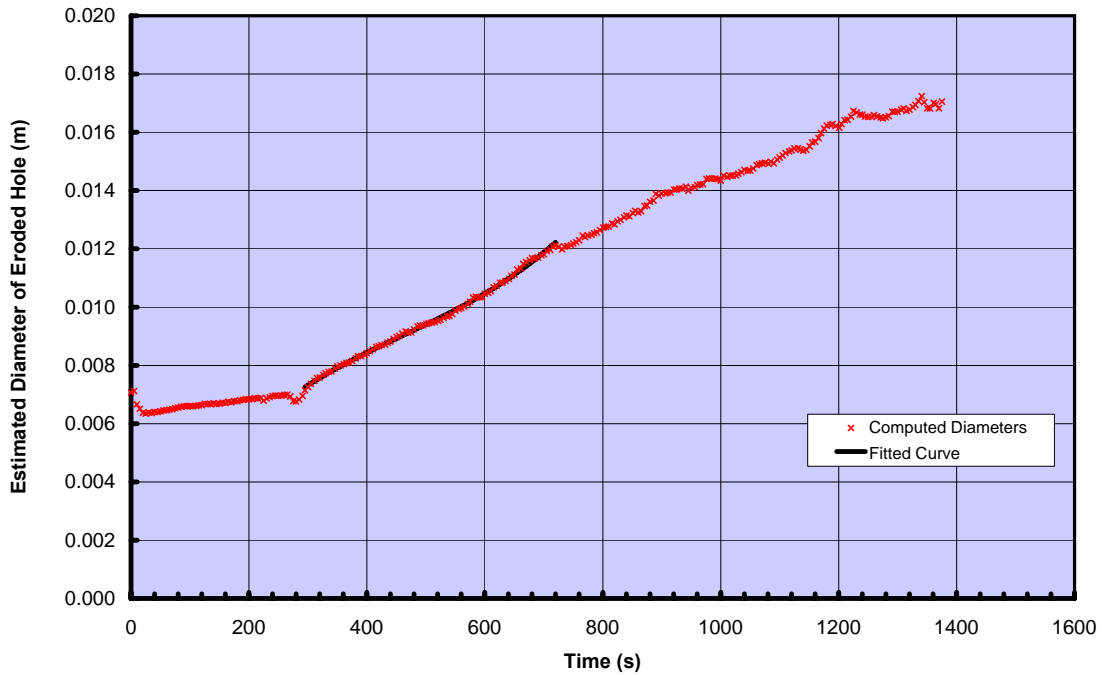
P3 4% wet, 25 blows Test ARS-P3-HET-25,+4 08-06-2008



ARS Phase 2

ESTIMATED DIAMETER OF ERODED HOLE

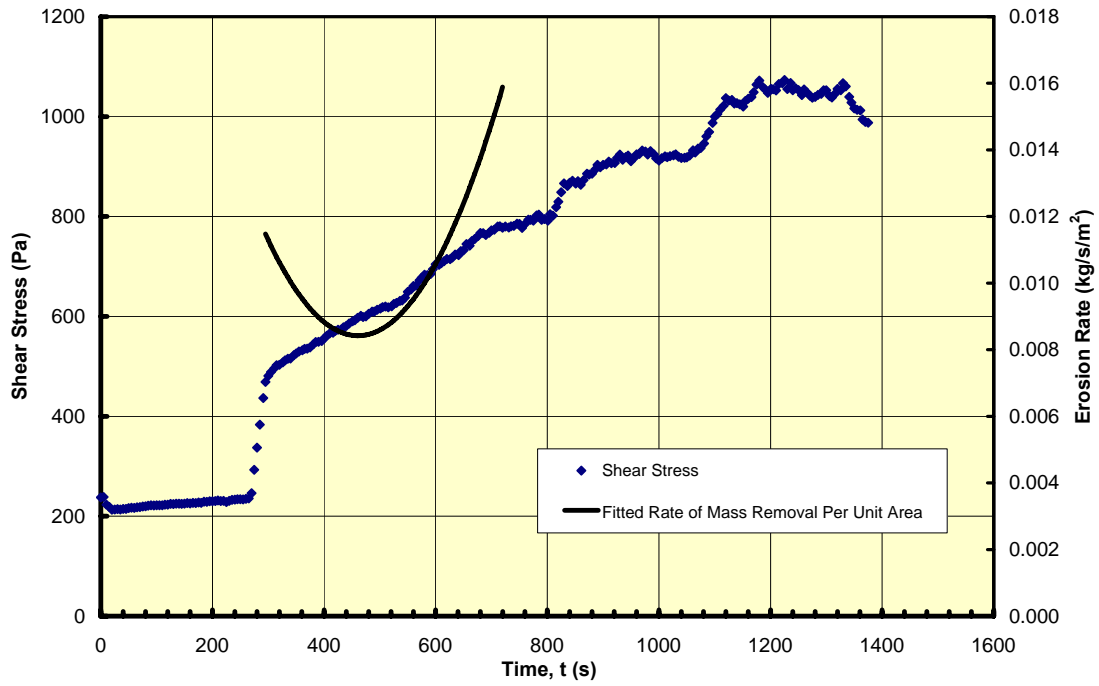
P3 4% wet, 25 blows Test ARS-P3-HET-25,+4 08-06-2008



ARS Phase 2

EROSION RATE AND SHEAR STRESS VS. TIME

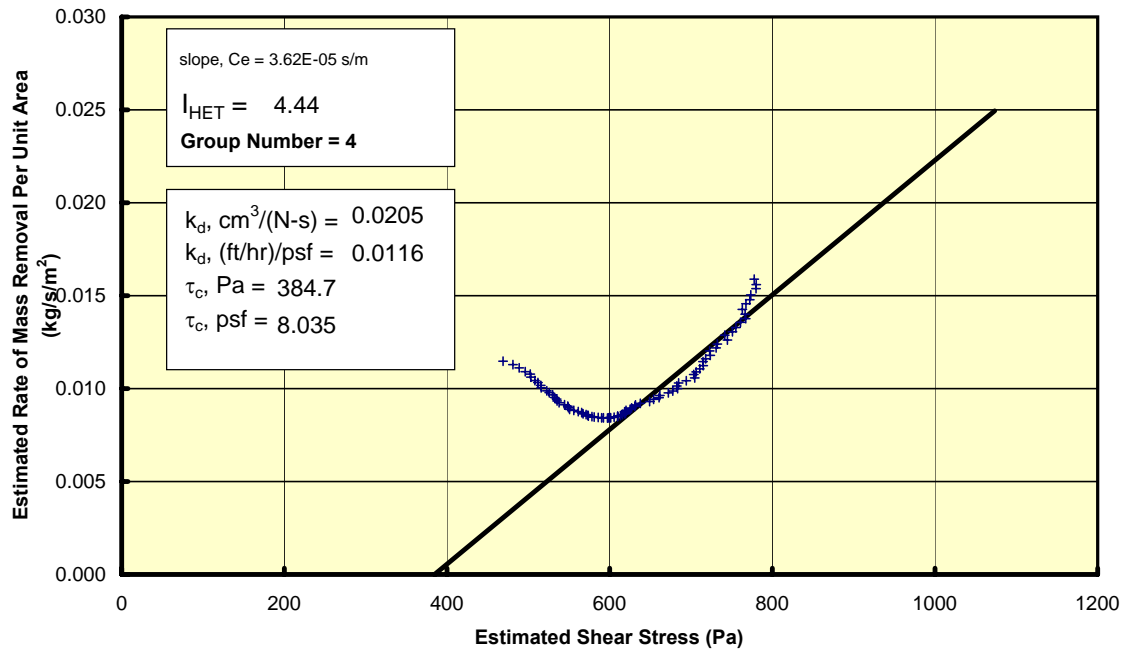
P3 4% wet, 25 blows Test ARS-P3-HET-25,+4 08-06-2008



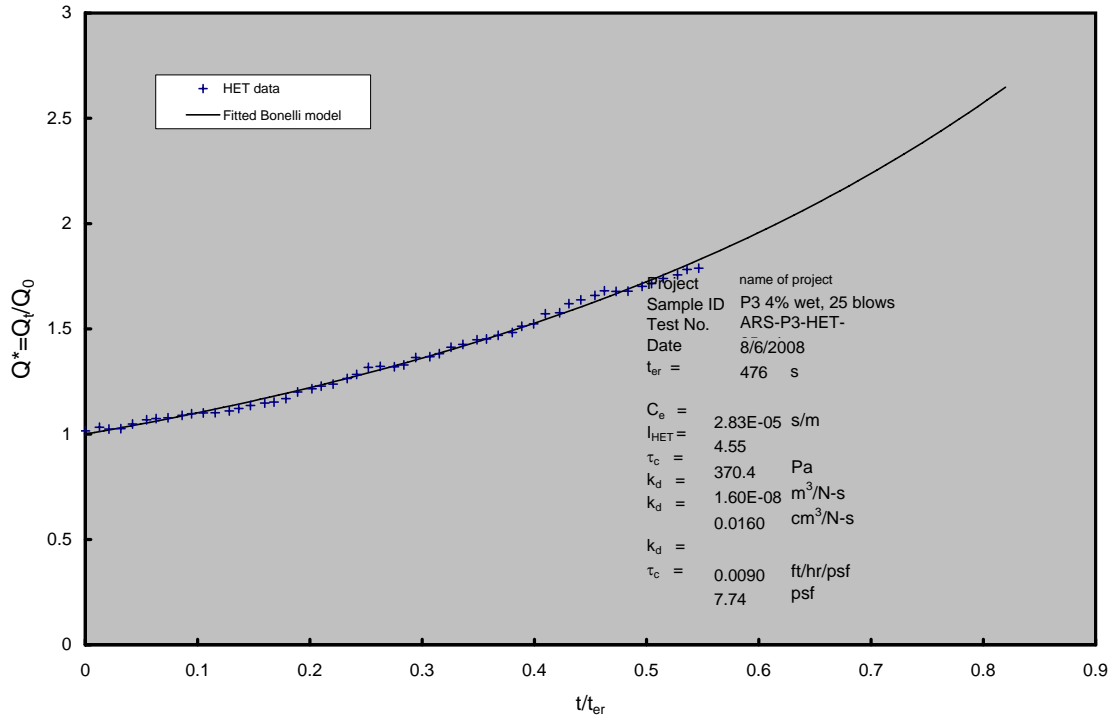
EROSION RATE VS. SHEAR STRESS

ARS Phase 2

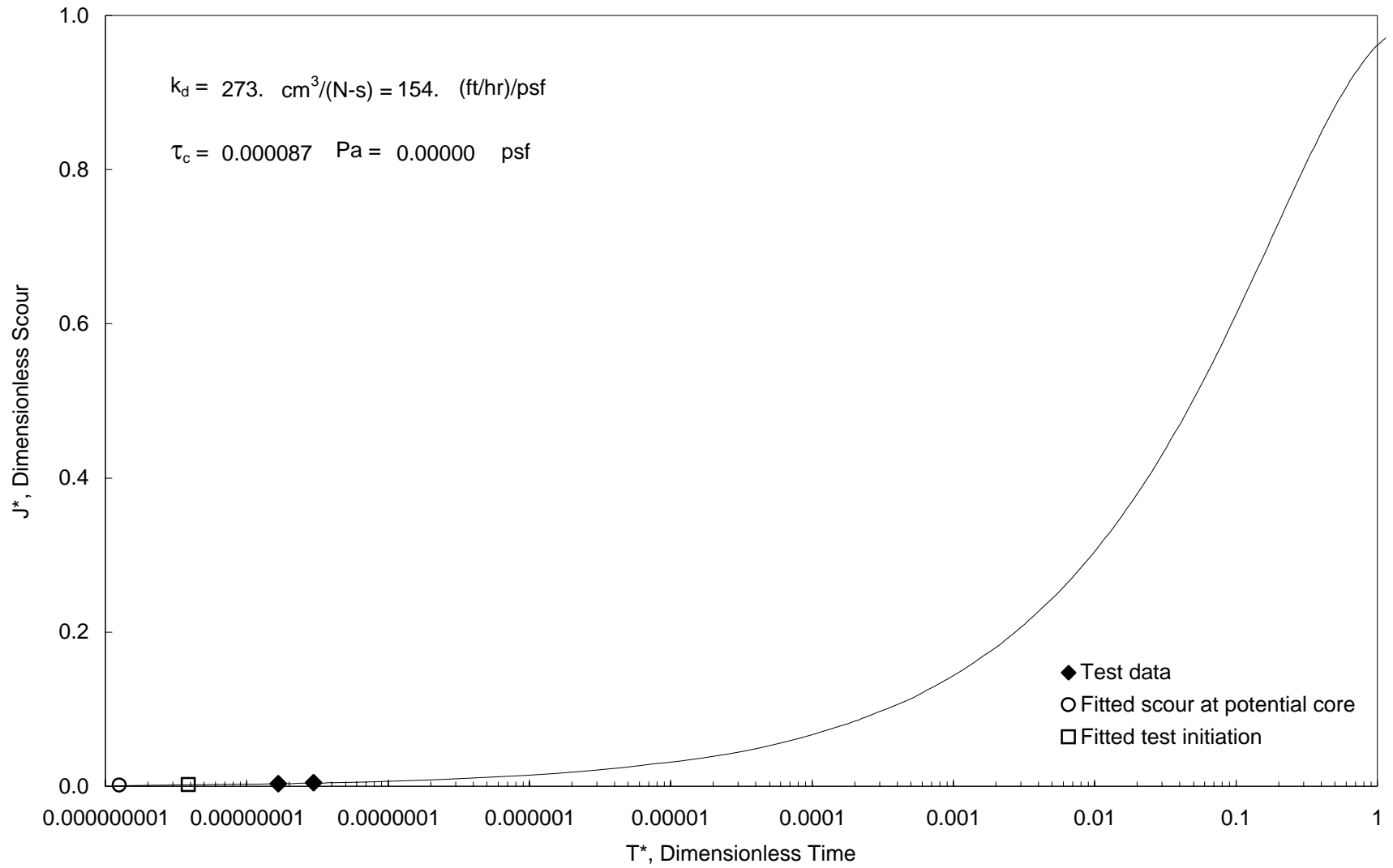
P3 4% wet, 25 blows Test ARS-P3-HET-25,+4 08-06-2008



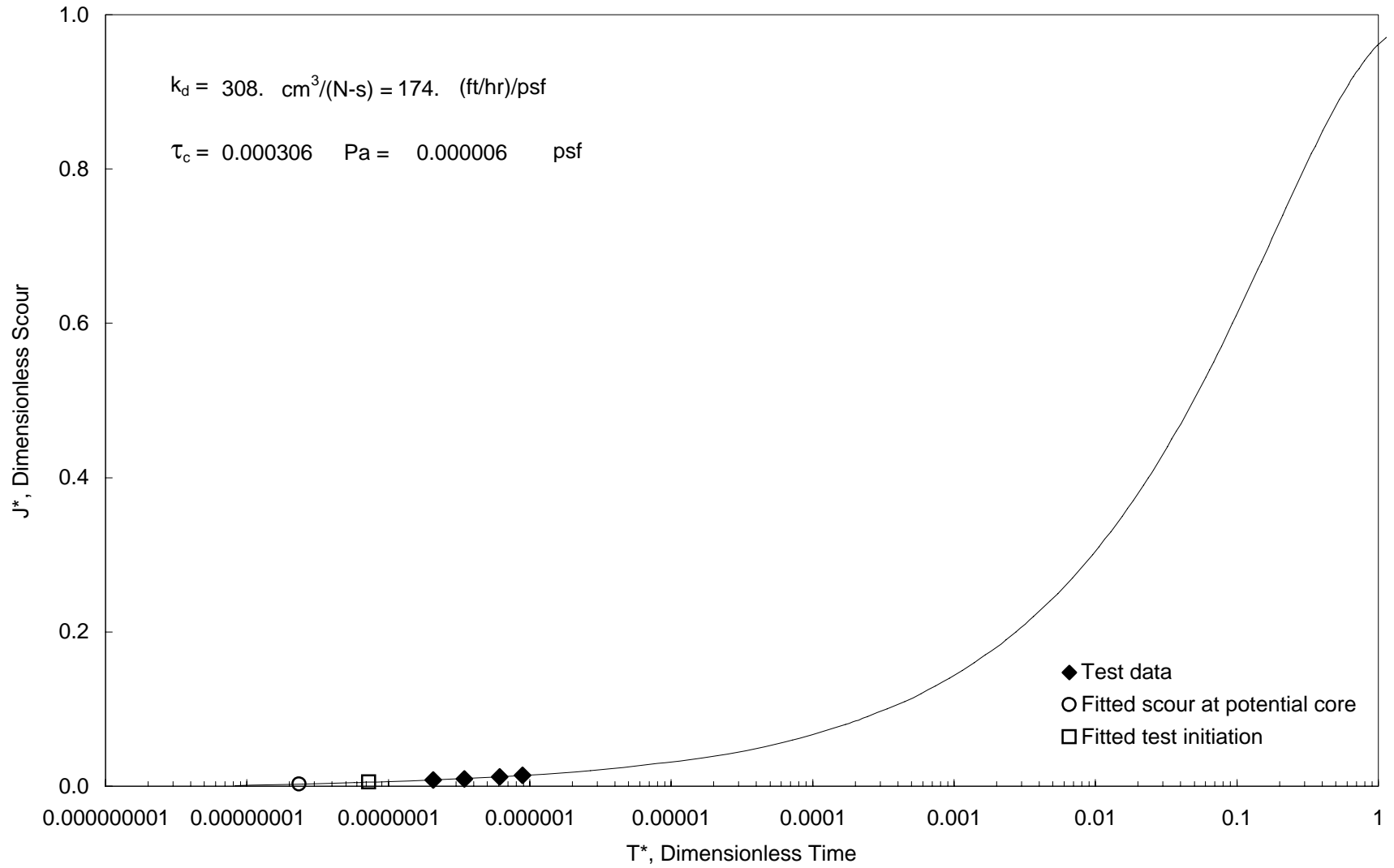
Bonelli Model - Dimensionless Flow vs. Dimensionless Time



Dimensionless Scour vs. Dimensionless Time (Blaisdell Method)



Dimensionless Scour vs. Dimensionless Time (Blaisdell Method)



SUBMERGED JET TEST DATA

P2-Jet 1.xls

DATE 3/20/2008

JET TEST

LOCATION ARS P2 soil (in P2A mold)

OPERATOR TLWahl

ZERO POINT GAGE

READING (on deflector plate) 1.226

TEST # 1

PRELIMINARY HEAD SETTING (IN.) 24

POINT GAGE RDG @ NOZZLE 1.262

NOZZLE DIAMETER (IN.) 0.25

INITIAL NOZZLE HEIGHT (FT) 0.144

SCOUR DEPTH READINGS			
TIME (MIN)	DIFF TIME (MIN)	PT GAGE READING (FT)	MAXIMUM DEPTH OF SCOUR (FT)
0		1.118	0.000
2	2	1.099	0.019
4	2	1.085	0.033
8	4	1.067	0.051
15	7	1.054	0.064
30	15	1.034	0.084
61	31	1.001	0.117
120	59	0.958	0.160

HEAD SETTING	
TIME (MIN)	HEAD (IN.)
0	24.00
2	24.00
4	24.00
8	24.00
15	24.00
30	24.00
61	24.00
120	24.00

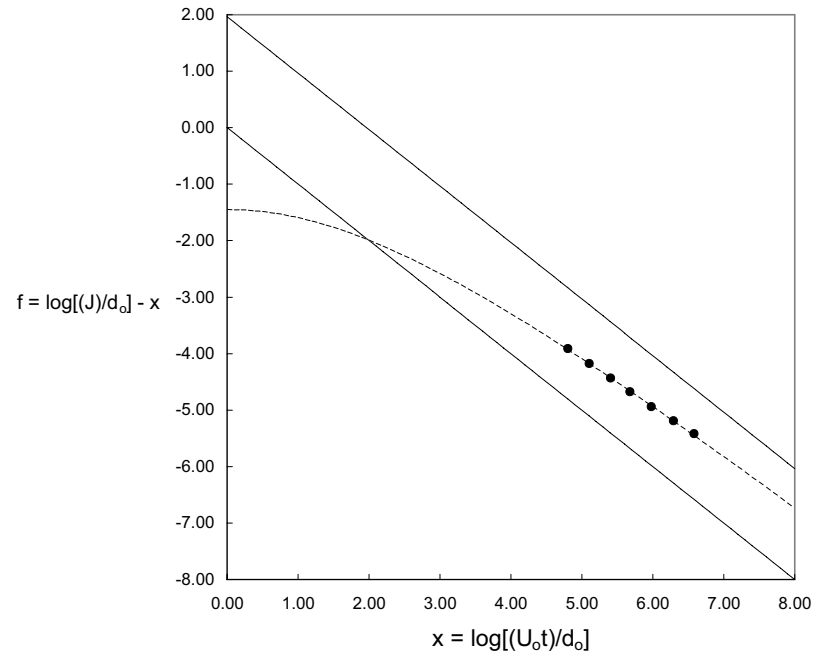
Solve Workbook

COMMENTS

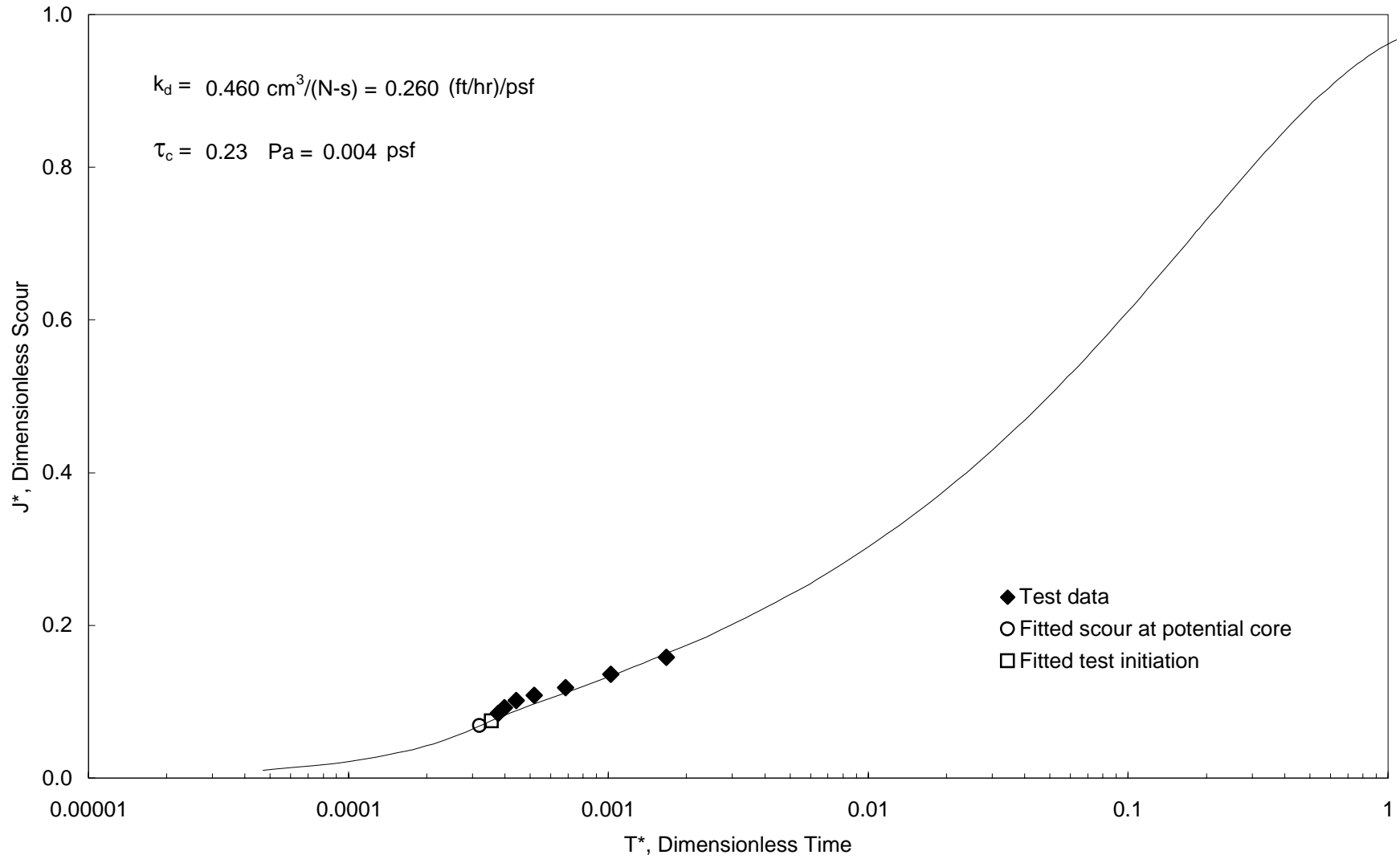
Moisture content % =	12.39%	optimum wc% =	12.2%
Mold volume (ft ³) =	0.03322	Mold weight =	4.234 Soil+mold weight = 8.35
γ_{wet} =	123.9012643		
γ_{dry} =	110.2436309		
$\gamma_{d,max}$ =	118.24		
	93.24%		

D:\BREACH\Erodibility\ARS Soils\Jet's\{P2-Jet 1.xls}\Data

Asymptote Plot to Predict Ultimate Scour



Dimensionless Scour vs. Dimensionless Time (Blaisdell Method)



SUBMERGED JET TEST DATA

PROJECT ARS Piping Soils for ERODS Research

DATE 3/21/2008

SAMPLE / LOCATION P2 @ 95% compaction and OMC

OPERATOR TLWahl

ZERO POINT GAGE
READING (on deflector plate) 1.226

TEST # 2

PRELIMINARY HEAD SETTING (IN.) 24

POINT GAGE RDG @ NOZZLE 1.262

NOZZLE DIAMETER (IN.) 0.25

INITIAL NOZZLE HEIGHT (FT) 0.144

Solve Workbook

SCOUR DEPTH READINGS			
TIME (MIN)	DIFF TIME (MIN)	PT GAGE READING (FT)	MAXIMUM DEPTH OF SCOUR (FT)
0		1.118	0.000
2	2	1.112	0.006
4	2	1.103	0.015
10	6	1.085	0.033
18	8	1.073	0.045
30	12	1.063	0.055
60	30	1.046	0.072
135	75	1.021	0.097

HEAD SETTING	
TIME (MIN)	HEAD (IN.)
0	24.00
2	24.00
4	24.00
10	24.00
18	24.00
30	24.00
60	24.00
135	24.00

REMOLDED SAMPLES

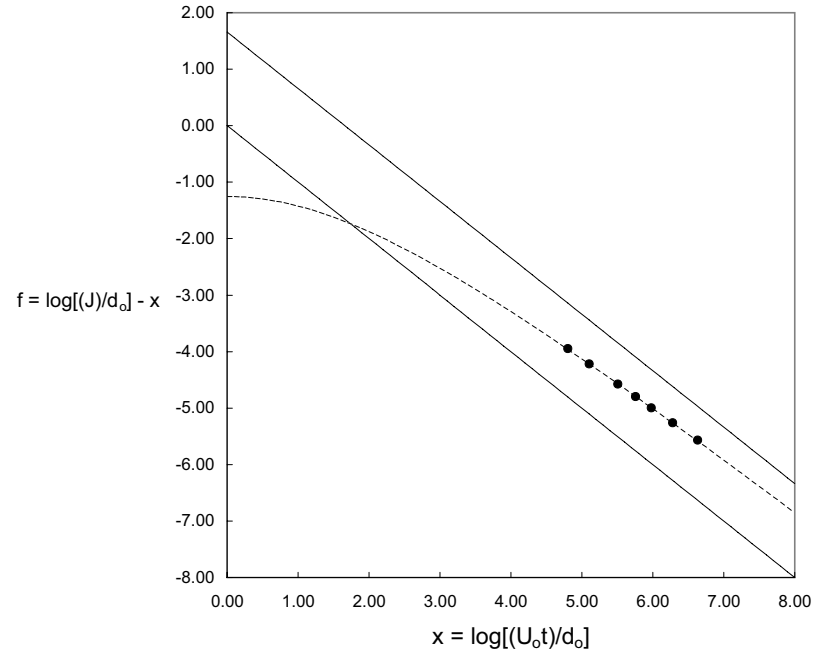
Compaction Properties
 Method 10 blows/layer, 3 layers
 Compaction Energy 4950 ft-lb/ft³
 Optimum Moisture Content 12.20 % $\gamma_{d,max}$ 118.24 lb/ft³

Moisture Content Determination
 Tare Container CL-125 Tare Mass 211.6 g
 Tare+Wet Mass 593.5 g
 Tare+Dry Mass 550.3 g

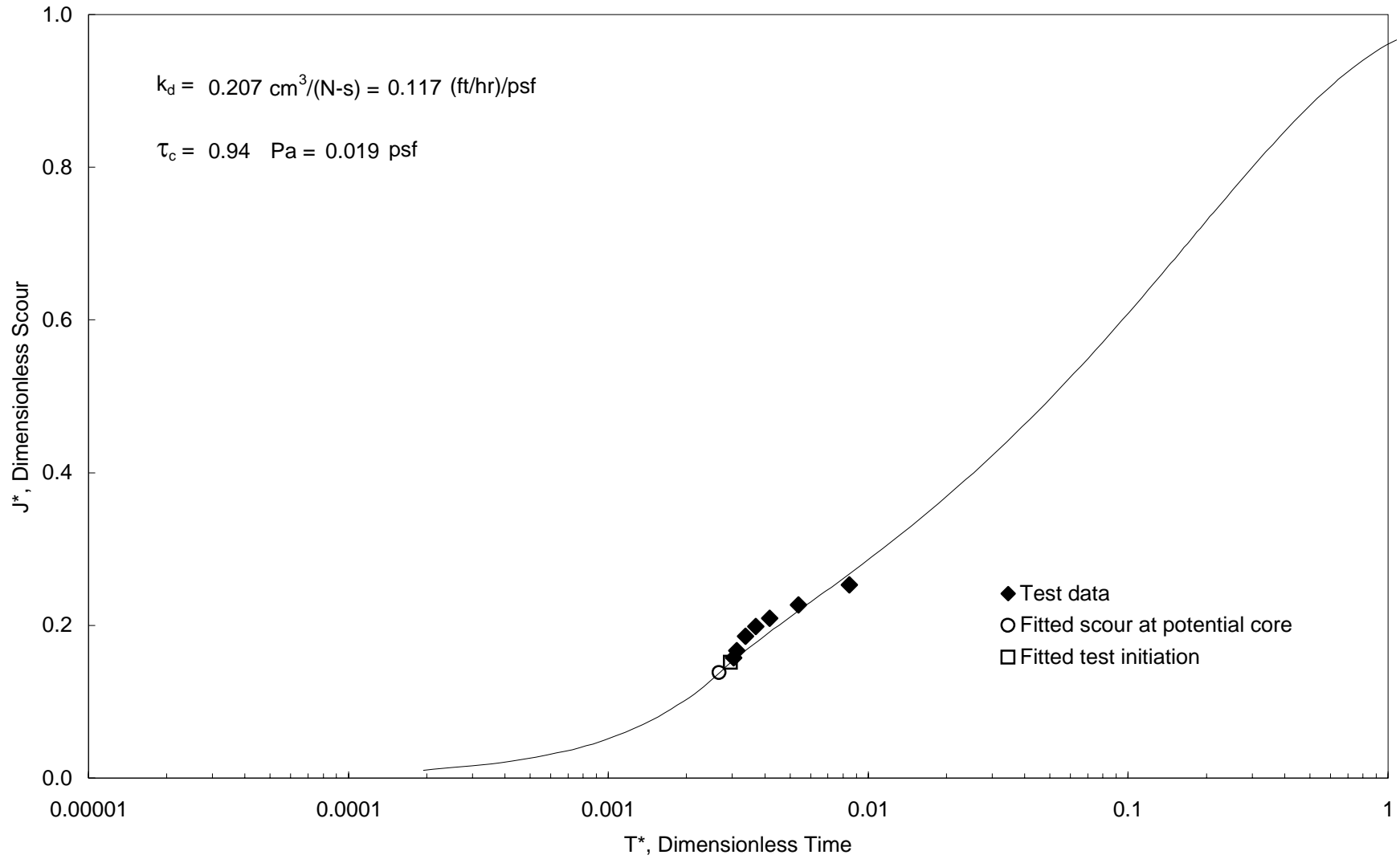
Dry Density Determination
 Mold ID P2C Mold Height 4.5858 in.
 Mold Volume 0.03313 ft³ Mold Diam. 3.987 in.
 Mold Weight 4.218 lb γ_{wet} 127.488257 lb/ft³
 Soil+mold weight 8.442 lb γ_{dry} 113.066962 lb/ft³
 Relative compaction 95.62 %

COMMENTS

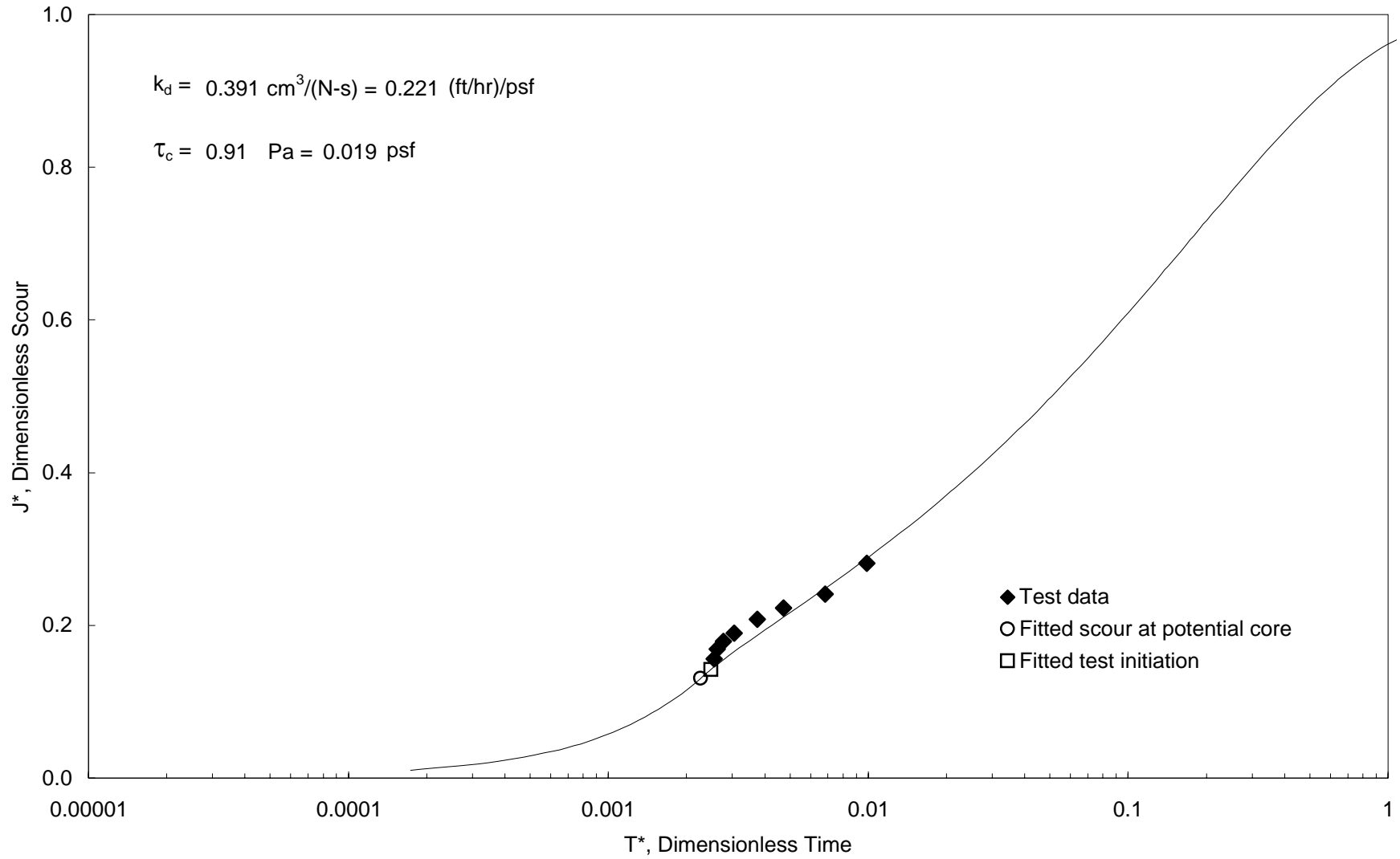
Asymptote Plot to Predict Ultimate Scour



Dimensionless Scour vs. Dimensionless Time (Blaisdell Method)



Dimensionless Scour vs. Dimensionless Time (Blaisdell Method)



SUBMERGED JET TEST DATA

PROJECT ARS DATE 4/8/2008
 SAMPLE / LOCATION P2 at breach test conditions OPERATOR TLW
 ZERO POINT GAGE READING (on deflector plate) 1.184 TEST # P2 - Jet 4
 PRELIMINARY HEAD SETTING (IN.) 36 POINT GAGE RDG @ NOZZLE 1.262
 NOZZLE DIAMETER (IN.) 0.25 INITIAL NOZZLE HEIGHT (FT) 0.133

Solve Workbook

SCOUR DEPTH READINGS			
TIME (MIN)	DIFF TIME (MIN)	PT GAGE READING (FT)	MAXIMUM DEPTH OF SCOUR (FT)
0		1.129	0.000
1	1	1.121	0.008
2	1	1.112	0.017
4	2	1.103	0.026
8	4	1.092	0.037
18	10	1.078	0.051
30	12	1.065	0.064
54	24	1.045	0.084
93	39	1.014	0.115
188	95	0.957	0.172

HEAD SETTING	
TIME (MIN)	HEAD (IN.)
0	36.00
1	36.00
2	36.00
2	36.00
8	36.00
18	36.00
30	36.00
54	36.00
93	36.00
188	36.00

Compaction Properties

Method Standard Proctor, with 7 blows/layer $\gamma_{d,max}$ 118.24 lb/ft³
 Compaction Energy 3465 ft-lb/ft³ Optimum Moisture 12.20 %

Moisture Content Determination

Tare Container CL-207 Tare Mass 207 Moisture Content 12.50 %
 Tare+Wet Mass 653.4 % Dry(-) / Wet(+)
 Tare+Dry Mass 603.8 +0.30 %

Dry Density Determination

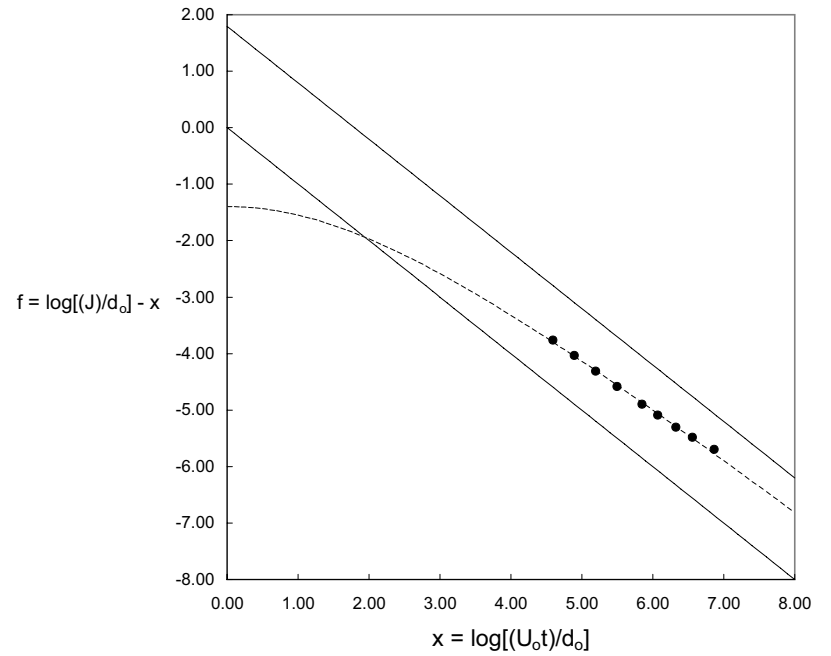
Mold ID 3 of 4 Mold Weight 4.238 lb
 Mold Height 4.6032 in. Soil+mold weight 8.336 lb
 Mold Diam. 3.9895 in. γ_{wet} 123.06 lb/ft³
 γ_{dry} 109.39 lb/ft³
 Mold Volume 0.0333 ft³ Relative compaction 92.5 %

COMMENTS

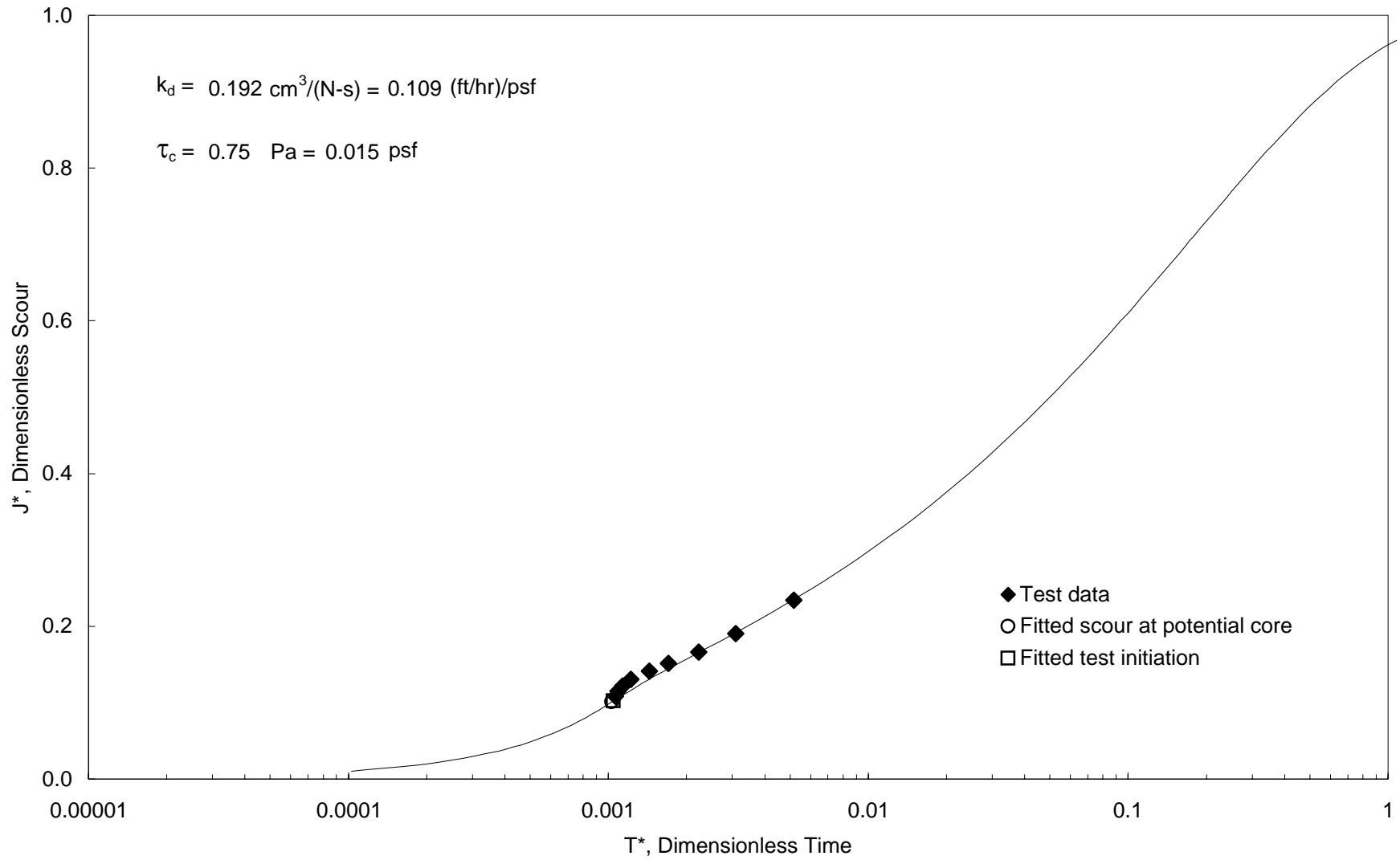
D:\BREACHErodibility\ARS Sols\Jets\P2-Jet 4.xls\Data

P2-Jet 4.xls

Asymptote Plot to Predict Ultimate Scour



Dimensionless Scour vs. Dimensionless Time (Blaisdell Method)



SUBMERGED JET TEST DATA

P3-Jet 1.xls

DATE 3/17/2008

JET TEST
LOCATION ARS P3 (P3A)

OPERATOR TLW

ZERO POINT GAGE
READING (on deflector plate) 0.980

TEST # 1

PRELIMINARY HEAD SETTING (IN.) 48

POINT GAGE RDG @ NOZZLE 1.017

NOZZLE DIAMETER (IN.) 0.25

INITIAL NOZZLE HEIGHT (FT) 0.145

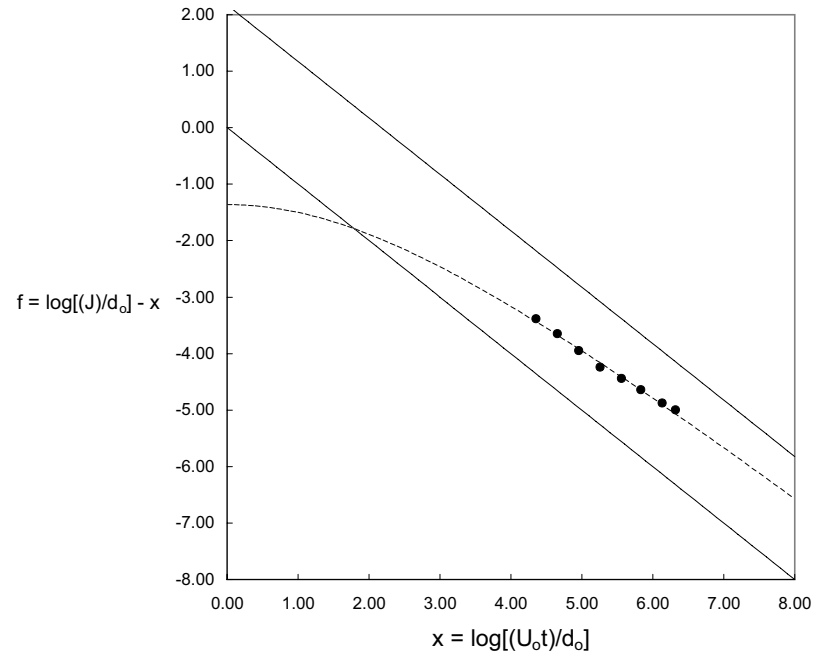
SCOUR DEPTH READINGS			
TIME (MIN)	DIFF TIME (MIN)	PT GAGE READING (FT)	MAXIMUM DEPTH OF SCOUR (FT)
0		0.872	0.000
0.5	0.5	0.825	0.047
1	0.5	0.807	0.065
2	1	0.806	0.066
4	2	0.803	0.069
8	4	0.747	0.125
15	7	0.696	0.176
30	15	0.642	0.230
46	16	0.580	0.292

HEAD SETTING	
TIME (MIN)	HEAD (IN.)
0	48.00
0.5	48.00
1	48.00
2	48.00
4	48.00
8	48.00
15	48.00
30	48.00
46	48.00

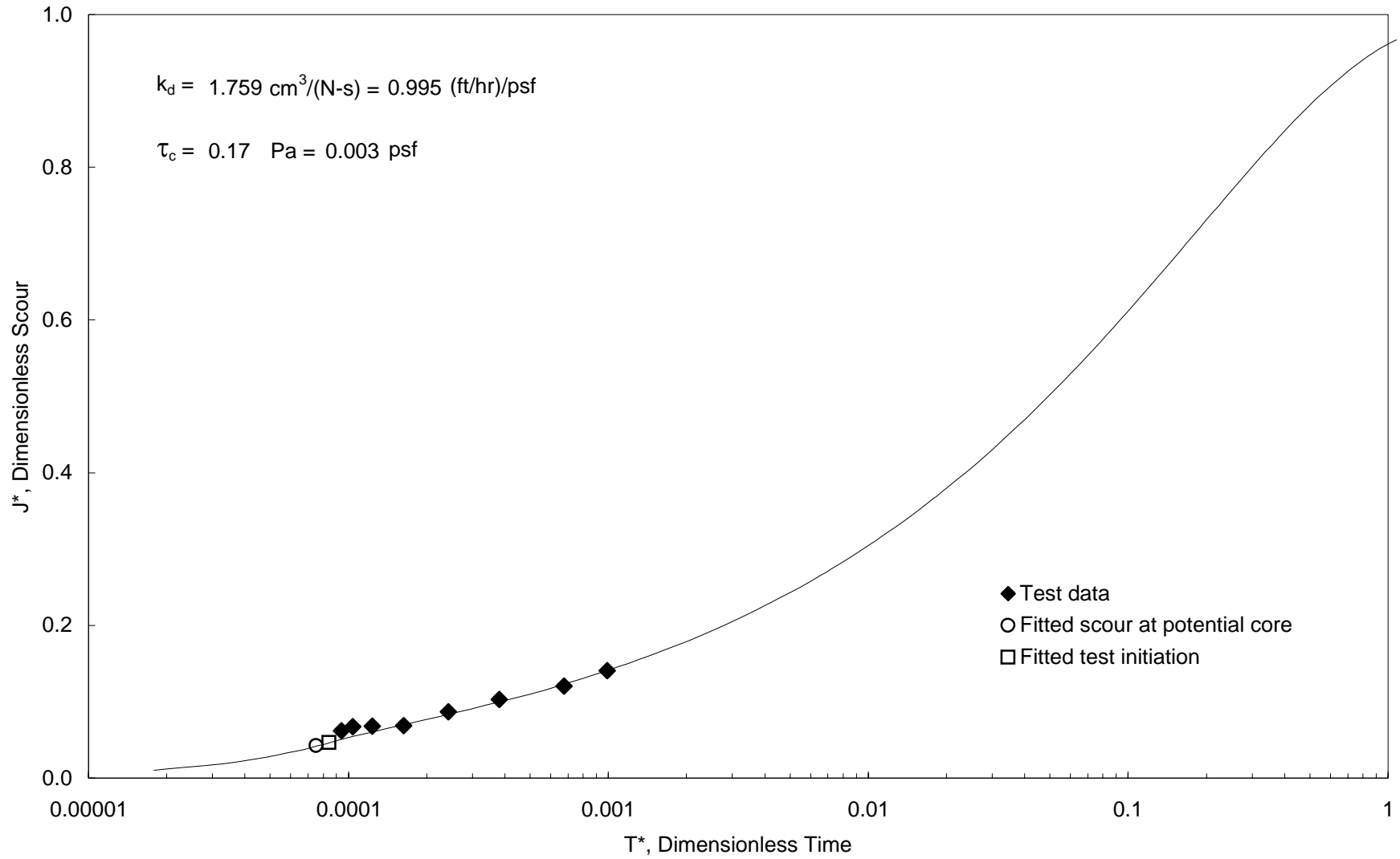
Solve Workbook

COMMENTS _____

Asymptote Plot to Predict Ultimate Scour



Dimensionless Scour vs. Dimensionless Time (Blaisdell Method)



SUBMERGED JET TEST DATA

P3-Jet 2.xls

DATE 3/18/2008

JET TEST
LOCATION ARS P3 (P3C)

OPERATOR TLW

ZERO POINT GAGE
READING (on deflector plate) 0.980

TEST # 1

PRELIMINARY HEAD SETTING (IN.) 30.3

POINT GAGE RDG @ NOZZLE 1.0165

NOZZLE DIAMETER (IN.) 0.25

INITIAL NOZZLE HEIGHT (FT) 0.144

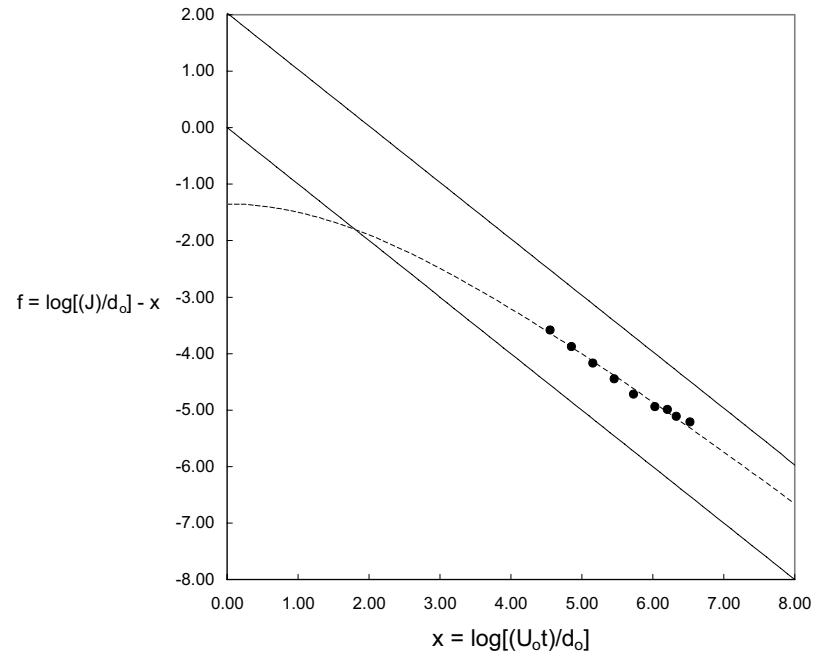
SCOUR DEPTH READINGS			
TIME (MIN)	DIFF TIME (MIN)	PT GAGE READING (FT)	MAXIMUM DEPTH OF SCOUR (FT)
0		0.873	0.000
1	1	0.822	0.051
2	1	0.818	0.055
4	2	0.814	0.059
8	4	0.806	0.068
15	7	0.802	0.071
30	15	0.760	0.113
45	15	0.676	0.197
60	15	0.669	0.204
93	33	0.588	0.285

HEAD SETTING	
TIME (MIN)	HEAD (IN.)
0	30.30
1	30.30
2	30.30
4	30.30
8	30.30
15	30.30
30	30.30
45	30.30
60	30.30
93	30.30

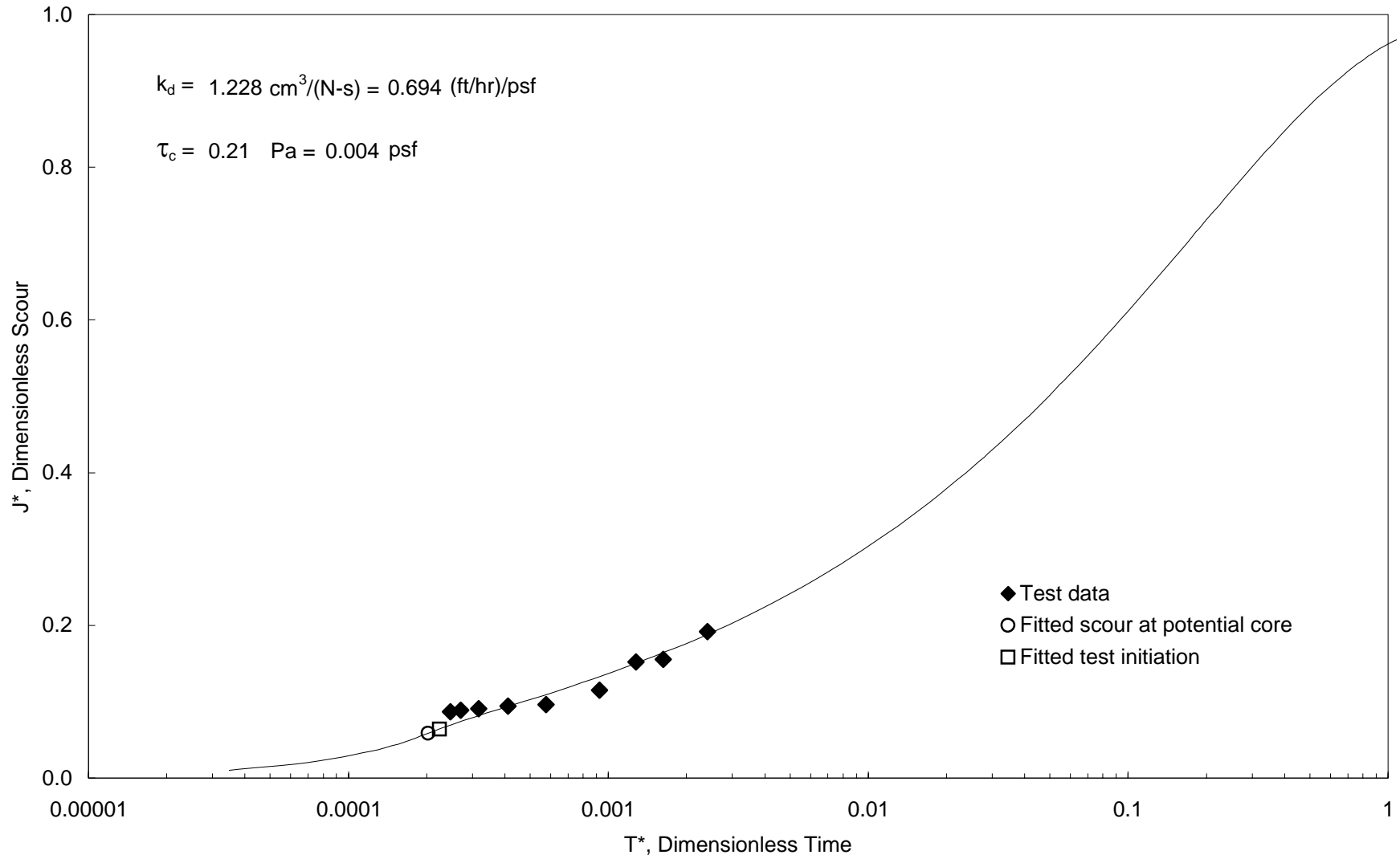
Solve Workbook

COMMENTS _____

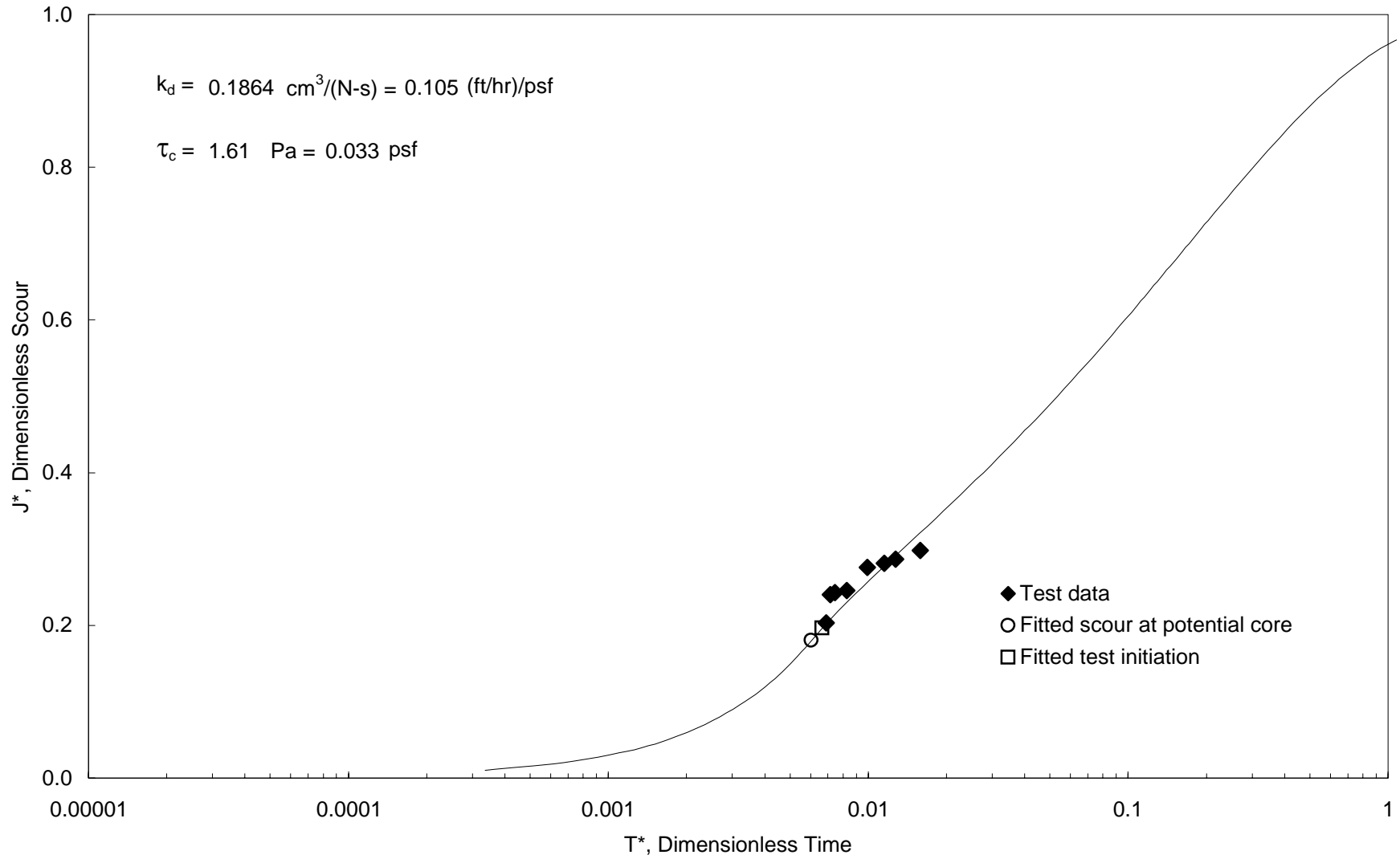
Asymptote Plot to Predict Ultimate Scour



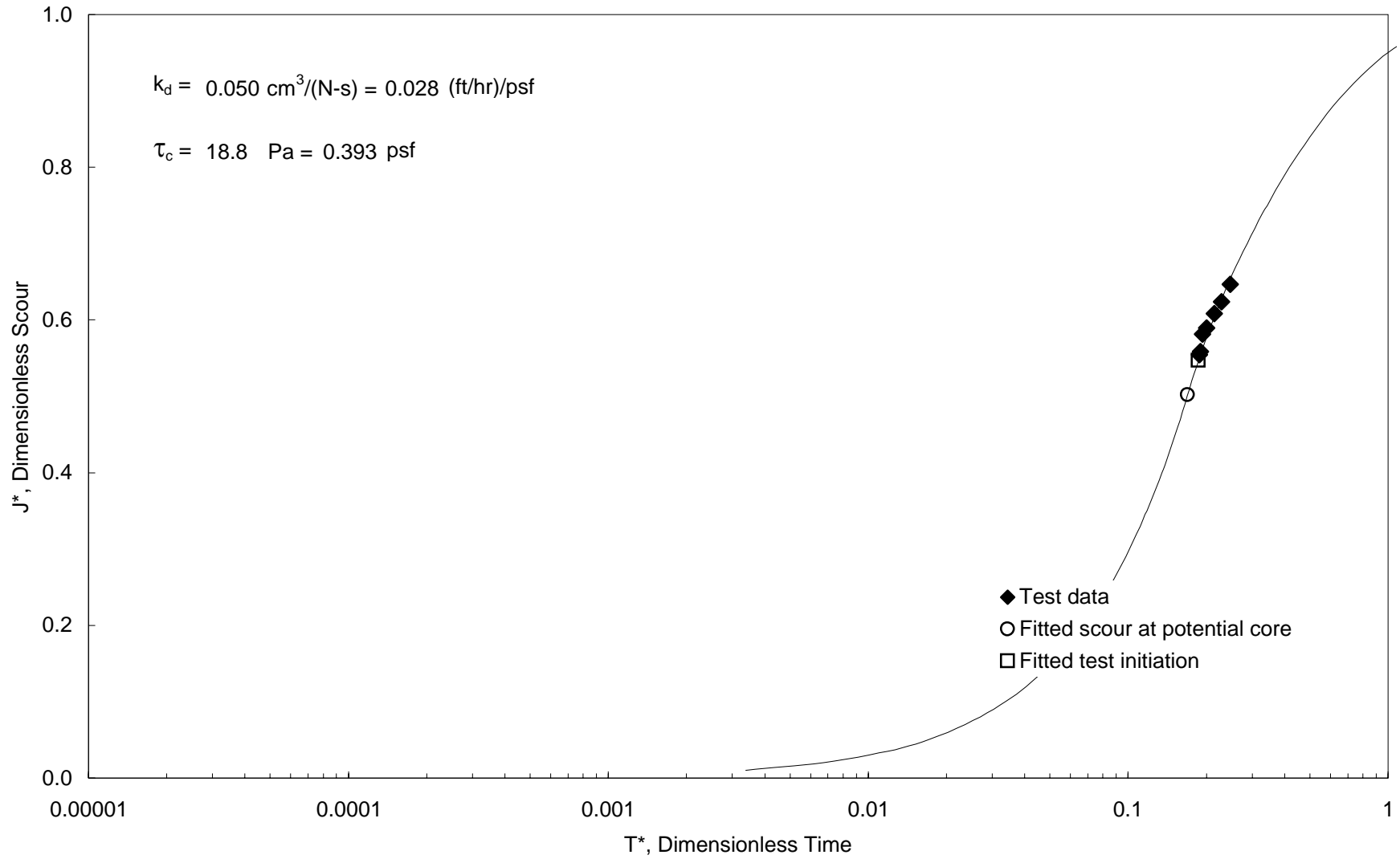
Dimensionless Scour vs. Dimensionless Time (Blaisdell Method)



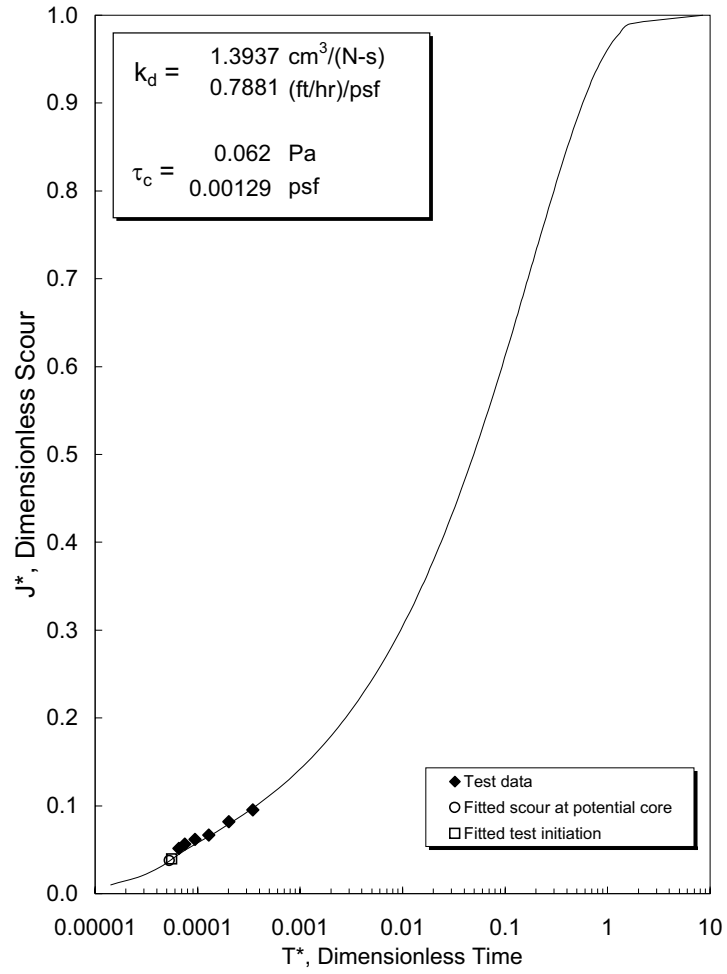
Dimensionless Scour vs. Dimensionless Time (Blaisdell Method)



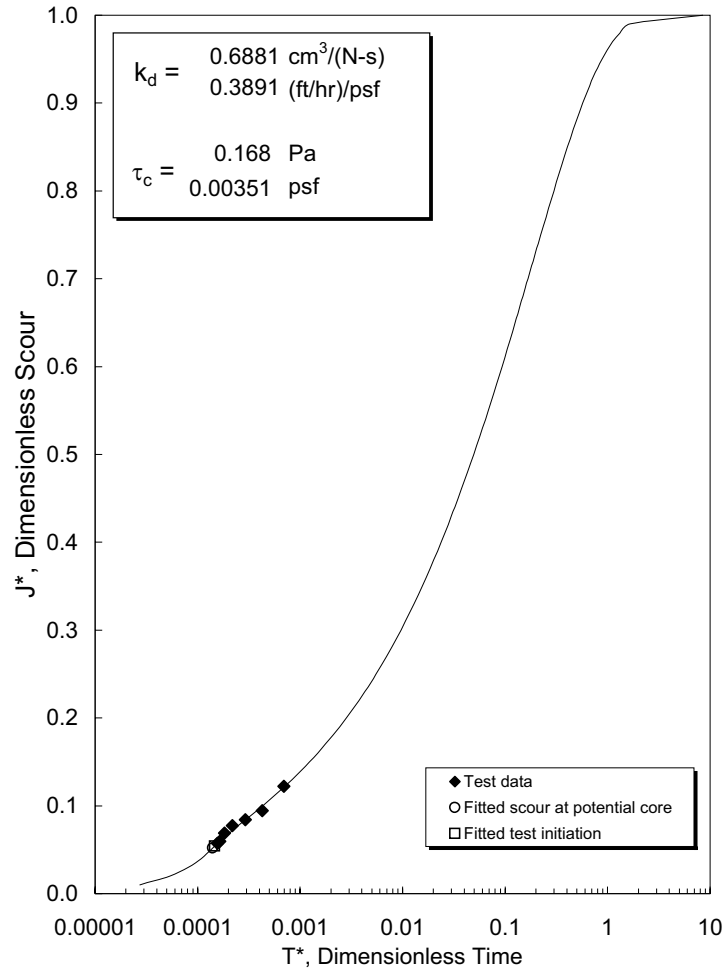
Dimensionless Scour vs. Dimensionless Time (Blaisdell Method)



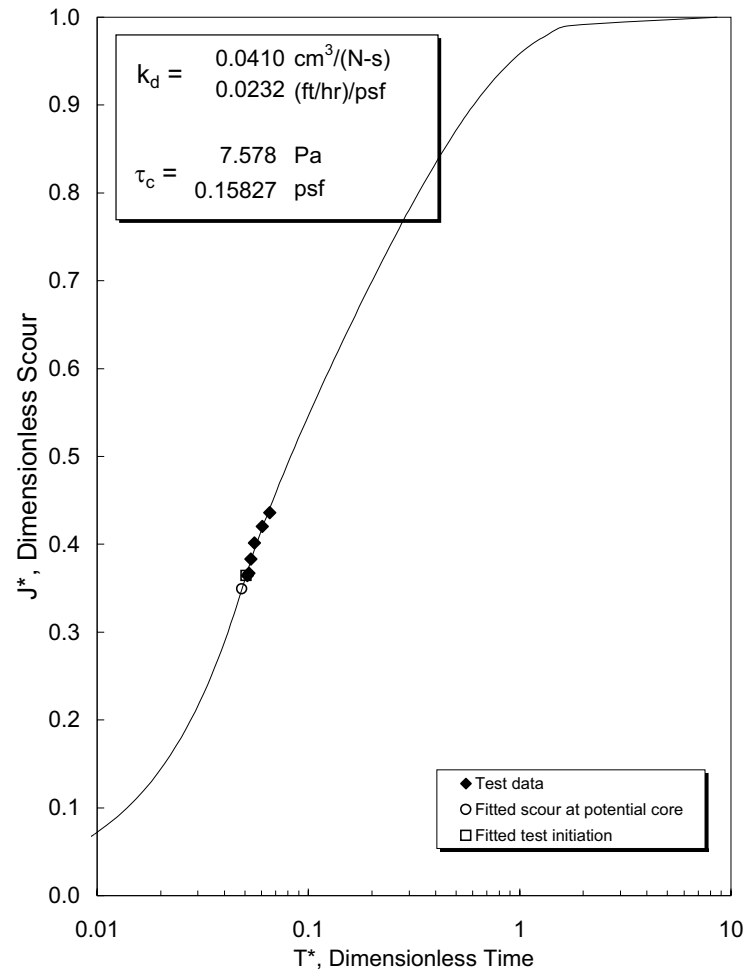
Dimensionless Scour-Time Plot (Blaisdell Method)



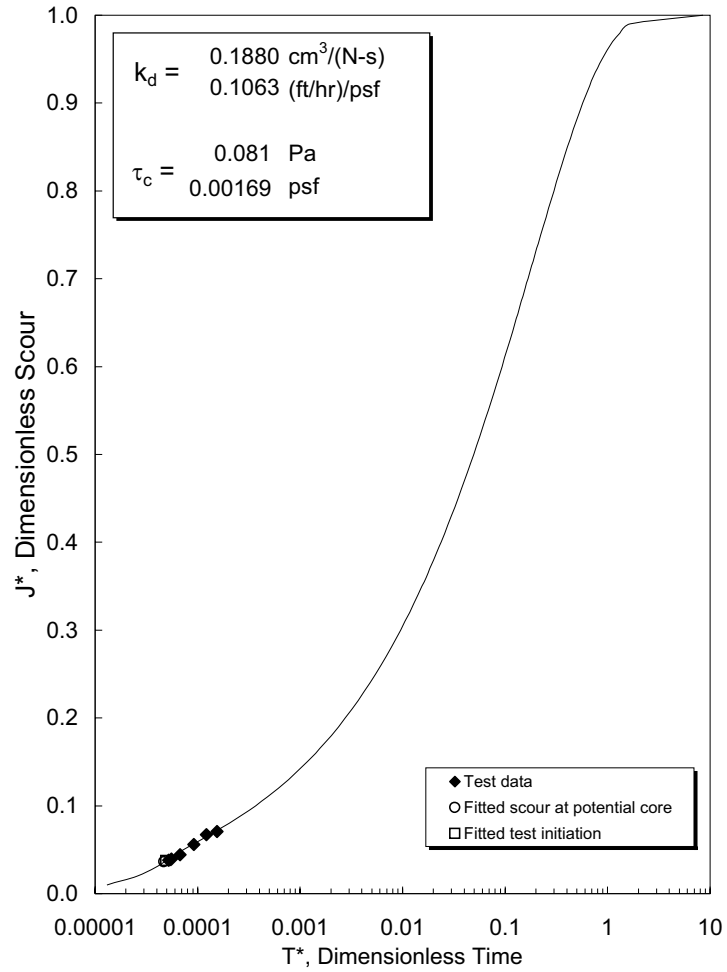
Dimensionless Scour-Time Plot (Blaisdell Method)



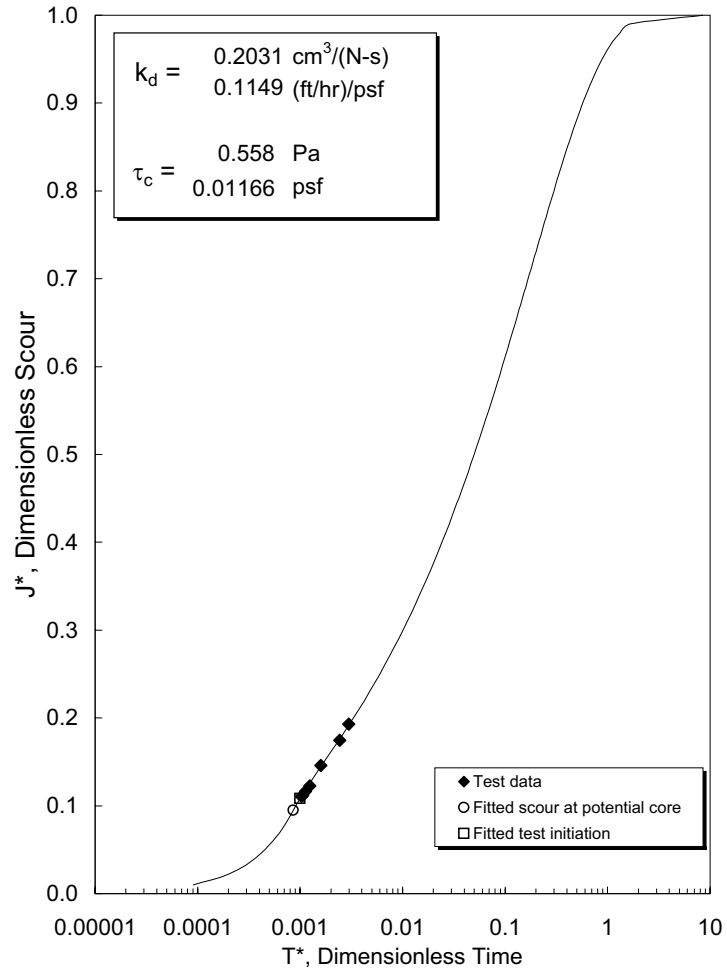
Dimensionless Scour-Time Plot (Blaisdell Method)

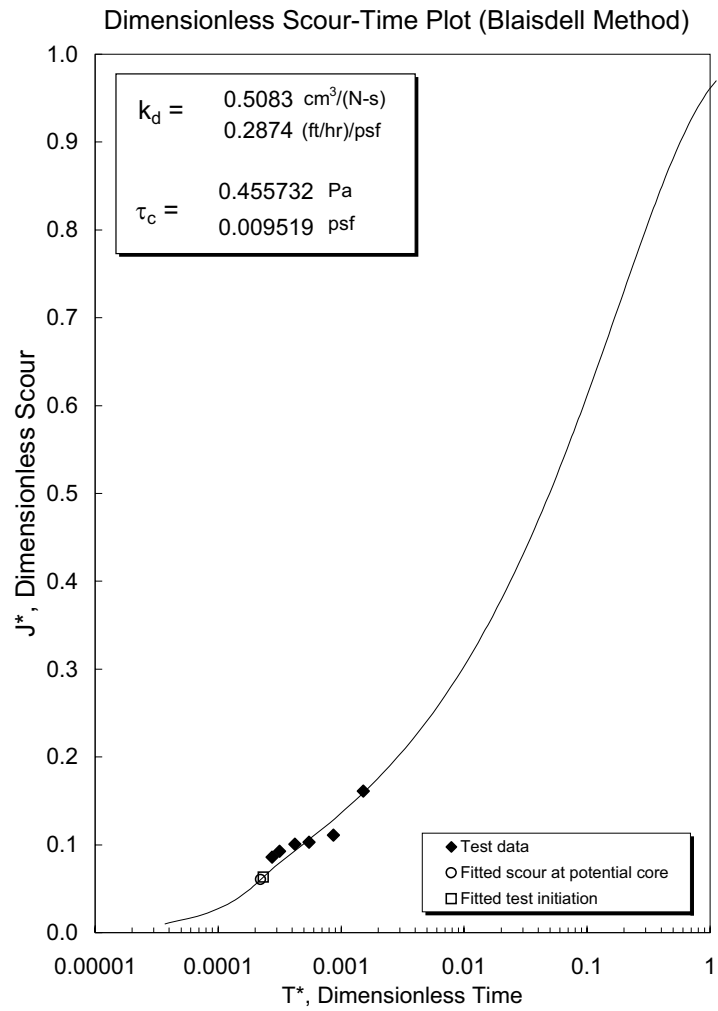


Dimensionless Scour-Time Plot (Blaisdell Method)



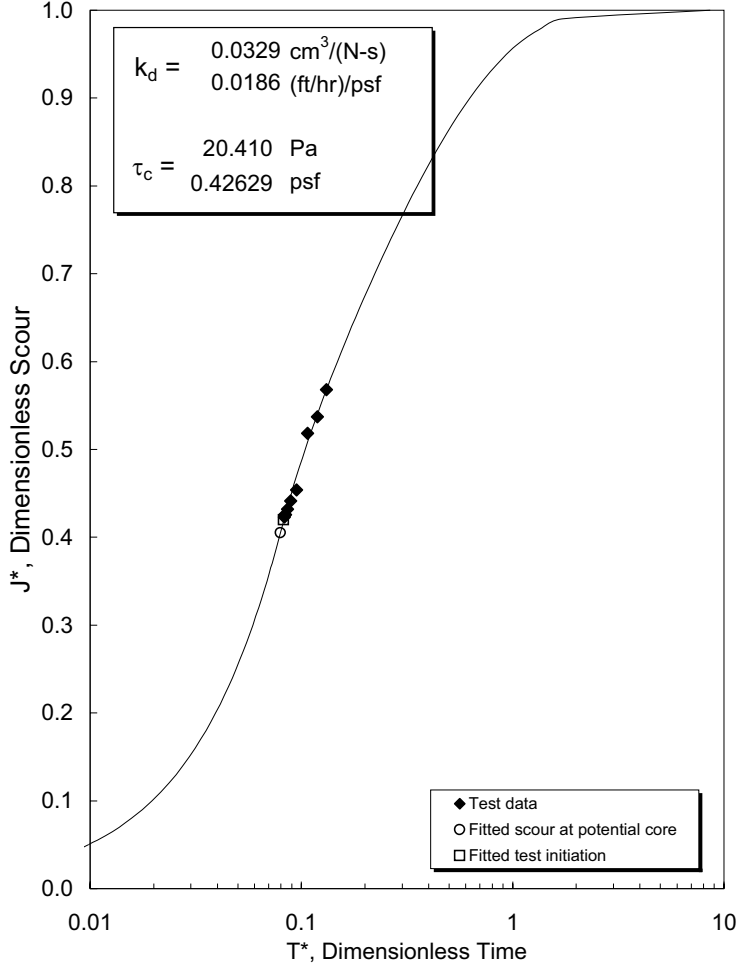
Dimensionless Scour-Time Plot (Blaisdell Method)



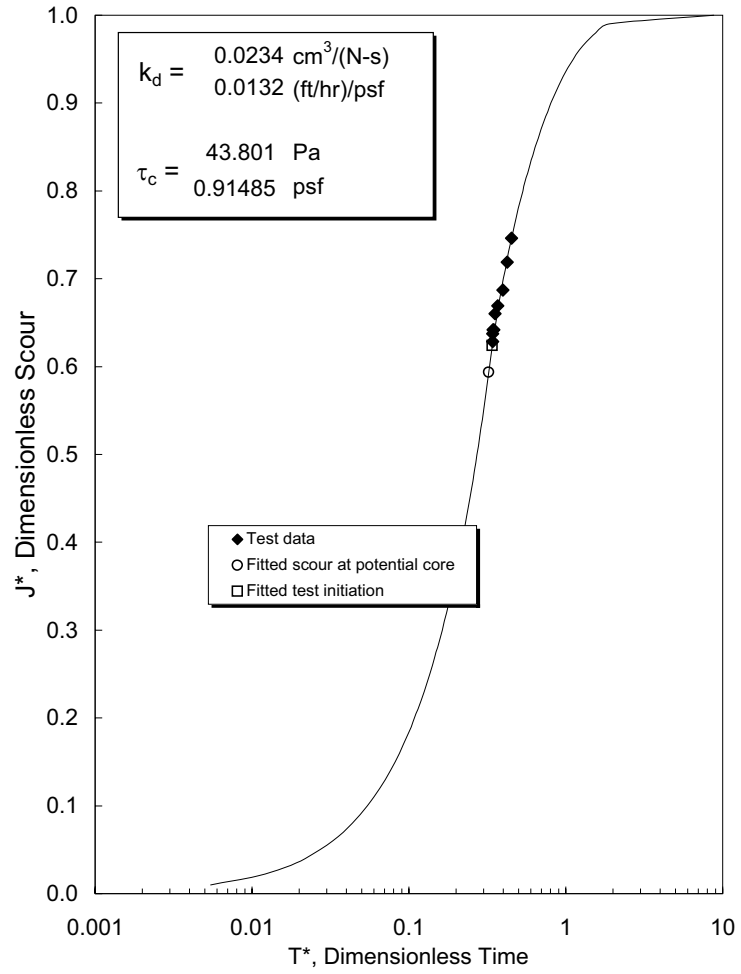


x

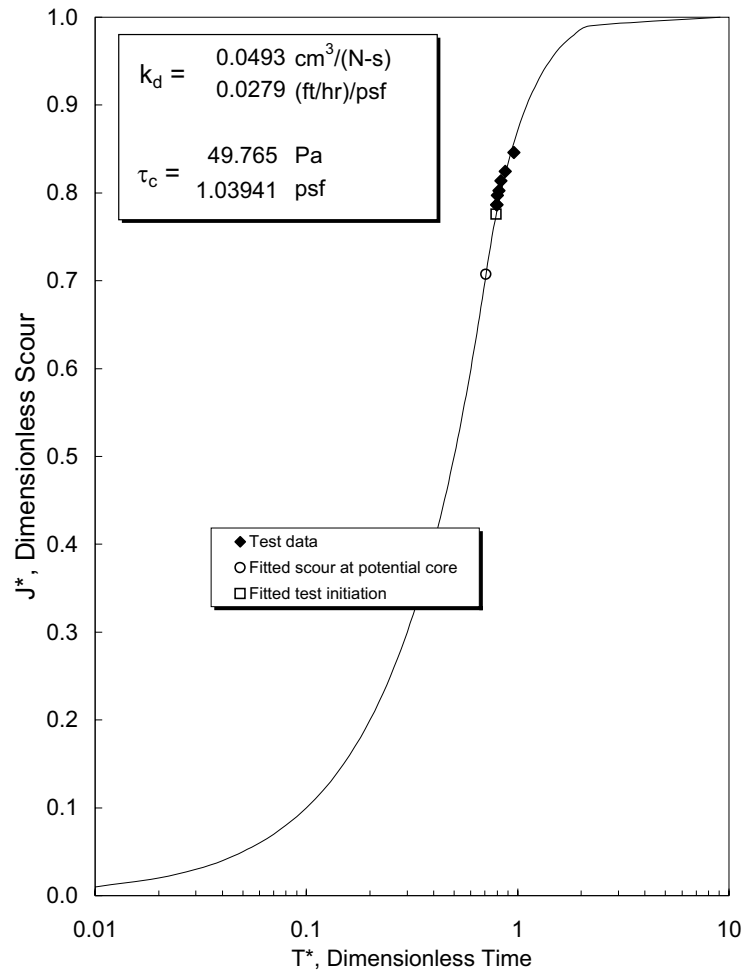
Dimensionless Scour-Time Plot (Blaisdell Method)



Dimensionless Scour-Time Plot (Blaisdell Method)



Dimensionless Scour-Time Plot (Blaisdell Method)



SUBMERGED JET TEST DATA

PROJECT ARS - ERODS - Phase 2 DATE 8/4/2008
 SAMPLE / LOCATION P3, 25 blows, OMC OPERATOR TLW / CD
 ZERO POINT GAGE READING (on deflector plate) 1.229 TEST # ARS-P3-JET-25-OMC2
 PRELIMINARY HEAD SETTING (IN.) 60 POINT GAGE RDG @ NOZZLE 1.262
 NOZZLE DIAMETER (IN.) 0.25 INITIAL NOZZLE HEIGHT (FT) 0.136

SCOUR DEPTH READINGS			
TIME (MIN)	DIFF TIME (MIN)	PT GAGE READING (FT)	MAXIMUM DEPTH OF SCOUR (FT)
0		1.126	0.000
1	1	1.125	0.001
2	1	1.125	0.001
4	2	1.125	0.001
8	4	1.125	0.001
16	8	1.124	0.002
30	14	1.123	0.003
70	40	1.113	0.013
130	60	1.107	0.019

HEAD SETTING	
TIME (MIN)	HEAD (IN.)
0	59.25
1	59.25
2	59.25
4	59.25
8	59.25
16	59.25
30	59.25
70	59.25
130	59.25

Compaction Properties
 Method Standard Proctor
 Compaction Energy 12375 ft-lb/ft³
 Optimum Moisture 14.20%
 $\gamma_{d,max}$ 113.44 lb/ft³

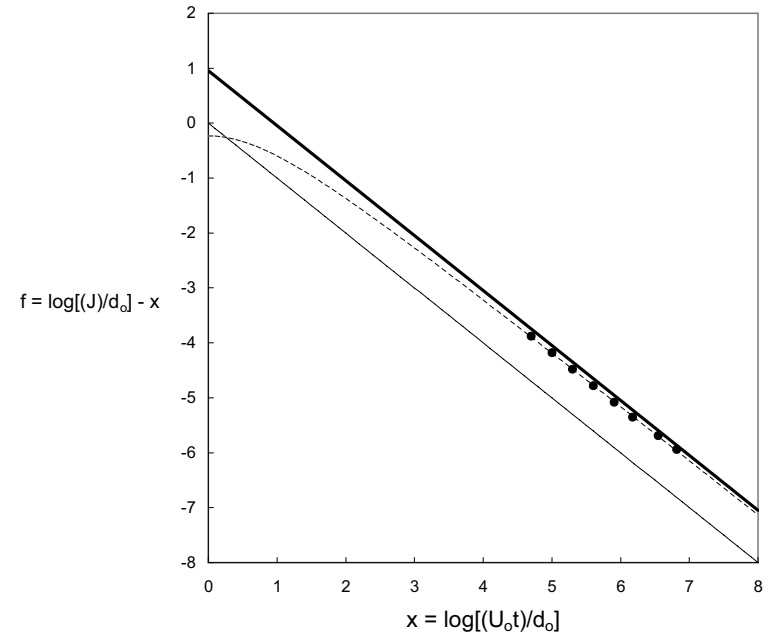
Moisture Content Determination
 Tare Container CL-154
 Tare Mass 172.4
 Tare+Wet Mass 642.1
 Tare+Dry Mass 584.2
 Moisture Content 14.06%
 % Dry (/ Wet +)
 -0.14%

Dry Density Determination
 Mold ID 4.236
 Mold Height in.
 Mold Diam. in.
 Mold Volume 0.0333 ft³
 Mold Weight 4.236 lb
 Soil+mold weight 8.738 lb
 γ_{wet} 135.06 lb/ft³
 γ_{dry} 118.41 lb/ft³
 Relative compaction 104.38%

COMMENTS

D:\BREACH\erodibility\ARS Soils\JET Phase 2\2008-08-04-ARS-P3-Jet-25-OMC2.xls\Data

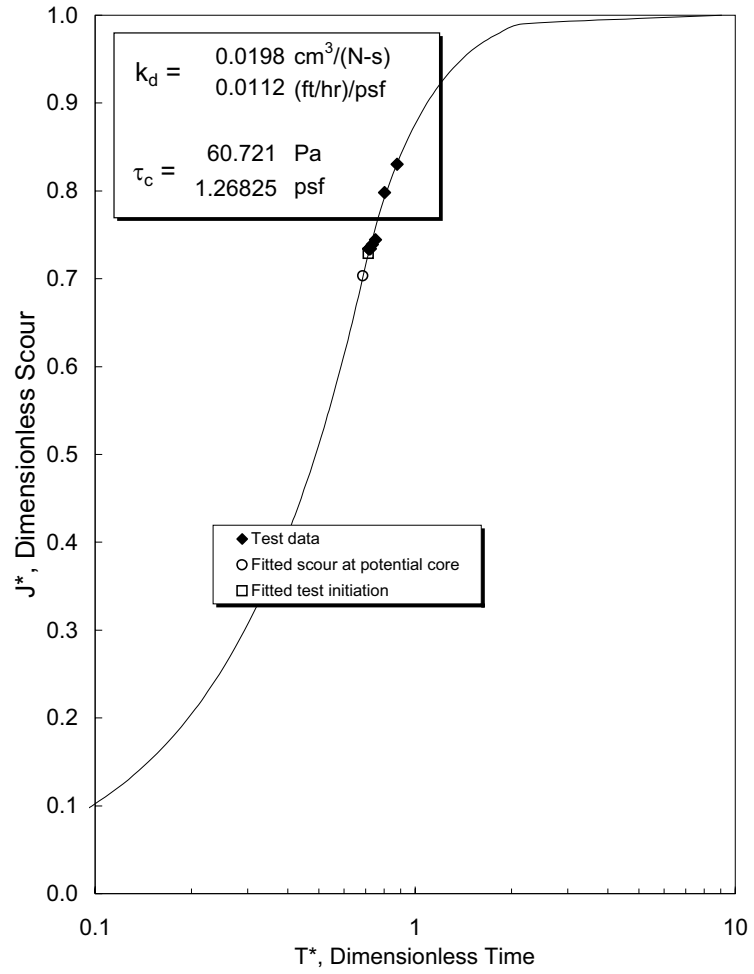
Asymptote Plot to Predict Equilibrium Scour



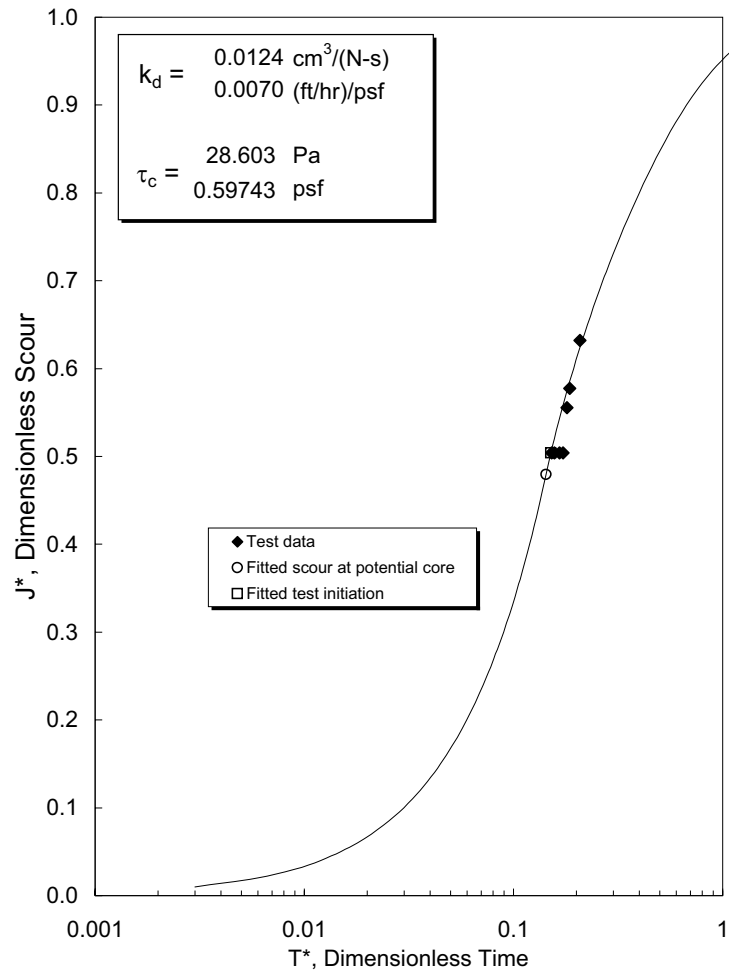
Hyperbola parameters

A = 1.184
 f_0 = 0.952
 Initial jet distance, J_i (in.) = 1.63
 Equilibrium jet distance, J_e (in.) = 2.2

Dimensionless Scour-Time Plot (Blaisdell Method)



Dimensionless Scour-Time Plot (Blaisdell Method)



SUBMERGED JET TEST DATA

PROJECT _____ DATE 8/7/2008
 SAMPLE / LOCATION P3_25 blows, 2% wet (16%) OPERATOR cd
 ZERO POINT GAGE READING (on deflector plate) 1.229 TEST # 3S-P3-Jet-25,+2
 PRELIMINARY HEAD SETTING (IN.) 60 POINT GAGE RDG @ NOZZLE 1.262
 NOZZLE DIAMETER (IN.) 0.25 INITIAL NOZZLE HEIGHT (FT) 0.136

SCOUR DEPTH READINGS			
TIME (MIN)	DIFF TIME (MIN)	PT GAGE READING (FT)	MAXIMUM DEPTH OF SCOUR (FT)
0		1.126	0.000
1	1	1.125	0.001
2	1	1.124	0.002
4	2	1.124	0.002
8	4	1.124	0.002
15	7	1.121	0.005
32	17	1.117	0.009
57	25	1.113	0.013
85	28	1.099	0.027
117	32	1.085	0.041
153	36	1.070	0.056

HEAD SETTING	
TIME (MIN)	HEAD (IN.)
0	60.00
1	60.00
2	60.00
4	60.00
8	60.00
15	60.00
32	60.00
57	60.00
85	60.00
117	60.00
153	60.00

Compaction Properties

Method Standard Proctor $\gamma_{d,max}$ 113.44 lb/ft³
 Compaction Energy 12375 ft-lb/ft³ Optimum Moisture 14.20 %

Moisture Content Determination

Tare Container CL-324 Tare Mass 206.5 Moisture Content 15.67 %
 Tare+Wet Mass 704.7 % Dry(-) / Wet(+)
 Tare+Dry Mass 637.2 +1.47 %

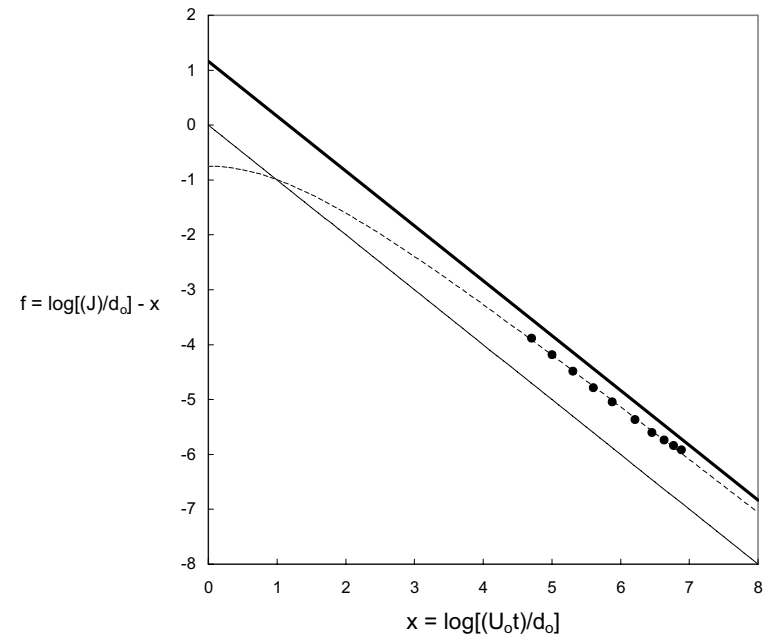
Dry Density Determination

Mold ID 4.236 Mold Weight 4.236 lb
 Mold Height in. Soil+mold weight 8.662 lb
 Mold Diam. in. γ_{wet} 132.78 lb/ft³
 γ_{dry} 114.79 lb/ft³
 Mold Volume 0.0333 ft³ Relative compaction 101.19 %

COMMENTS

D:\BREACH\Erodibility\ARS Soils\JET Phase 2\ARS-P3-Jet-25,+2.xls\Data

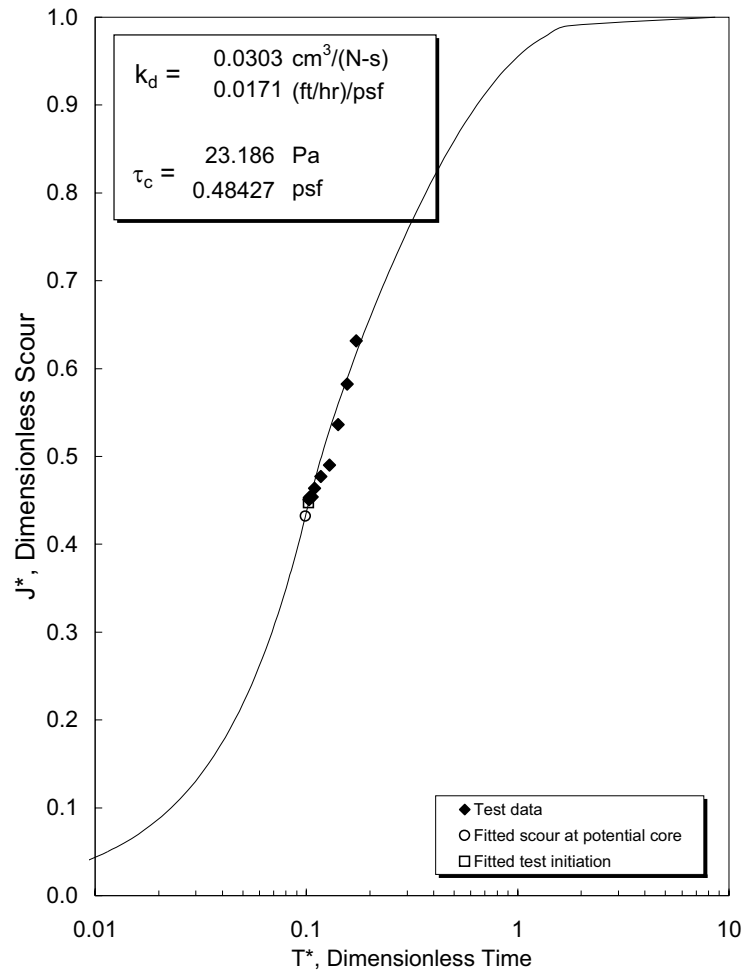
Asymptote Plot to Predict Equilibrium Scour



Hyperbola parameters

A = 1.915
 f_0 = 1.164
 Initial jet distance, J_i (in.) = 1.63
 Equilibrium jet distance, J_e (in.) = 3.6

Dimensionless Scour-Time Plot (Blaisdell Method)



Dimensionless Scour-Time Plot (Blaisdell Method)

